UNCLASSIFIED

AD 405 629

DEFENSE DOCUMENTATION CENTER

FOR

SCIENTIFIC AND TECHNICAL INFORMATION

CAMERON STATION, ALEXANDRIA, VIRGINIA

UNCLASSIFIED

NOTICE: When government or other drawings, specifications or other data are used for any purpose other than in connection with a definitely related government procurement operation, the U. S. Government thereby incurs no responsibility, nor any obligation whatsoever; and the fact that the Government may have formulated, furnished, or in any way supplied the said drawings, specifications, or other data is not to be regarded by implication or otherwise as in any manner licensing the holder or any other person or corporation, or conveying any rights or permission to manufacture, use or sell any patented invention that may in any way be related thereto.

63-3-5

405629

405629

Technical Report No. AF-103

THE DETECTION OF MULTIPLE UNKNOWN SIGNALS BY ADAPTIVE FILTERS

by

J. W. Smith

THE JOHNS HOPKINS UNIVERSITY
CARLYLE BARTON LABORATORY
BALTIMORE, MD.

CONTRACT NO. AF 33(657)-11029
[FORMERLY AF 33(616)-6753]

MAY 1963

JUN 4 1963
TISIA B

Copy No.

THE JOHNS HOPKINS UNIVERSITY
CARLYLE BARTON LABORATORY
BALTIMORE, MARYLAND

Technical Report No. AF-103

THE DETECTION OF MULTIPLE UNKNOWN SIGNALS BY ADAPTIVE FILTERS

by

J. W. Smith

Program Element Code: 62405454
Technical Area: 760D
Task: 403601

Project Engineer:

1/Lt W. F. H. Ring, Extension 33222
Aeronautical Systems Division
Wright-Patterson Air Force Base, Ohio

AF 33(657)-11029
[Formerly AF 33(616)-6753]

May 1963

ACKNOWLEDGMENT

The author wishes to express his gratitude to Professor Willis C. Gore and Dr. Frank C. Ogg, Jr., for their guidance and to Dr. John M. Kopper for reviewing the manuscript. Special thanks are extended to Mr. Paul Tittel for gathering the analog data; to Mr. Wayne A. Ray for programming the digital computer simulation; to Mrs. Marguerite Denburg for performing the computations; to Mr. C. Millard LaPorte for drafting services; and to Miss Carole M. Tennant for her careful typing of the paper.

TABLE OF CONTENTS

LIST OF ILLUSTRATIONS

ABSTRACT

Filters which modify their structures in order to recognize initially unknown waveforms in Gaussian noise are investigated experimentally. The class of filters discussed include two types previously described in the literature and one new type designed explicitly for operating in a multiple waveform environment. The new structure processes the data in a nonlinear fashion and effectively sets up a narrow decision region about the estimate of the waveform. The parallel operation of adaptive systems for detecting and estimating the signal parameters of multiple signals simultaneously is also discussed.

Throughout the discussion, the emphasis is on the effects of time of arrival errors and incorrect decision errors such as false alarms and incorrect signal identification. Low signal-to-noise ratios, 5 to 20 (7 db to 13 db), are studied.

The results clearly demonstrate the possibility of using filters of the new type for automatic data processing. Results are given in the form of learning curves which show the effects of correct and incorrect decisions. Included in much of the discussion is a graphical interpretation of the filtering process.

Two unusual applications of the new filter structure are discussed in the appendices.

I. INTRODUCTION

Many areas now being investigated may be considered as examples of pattern recognition or as the extraction of the relevant information from the irrelevant. Signal detection may be viewed as such with noise being the unimportant component. Today's world is beset by masses of data which, at some time, must be examined for the relevant. If the data could be analyzed automatically, great savings in time and storage facilities could be realized. For example, pulse signals could be recorded in terms of shape and time of arrival rather than as a continuous input. At the very least, machine analysis could determine which part of the input was completely useless and which may require additional study. On the other hand, near optimum machine performance would provide greater quantities of more reliable information than are presently possible. Most of the effort in pattern recognition has dealt with patterns known by the observer beforehand (for example, check reading devices, radar detection). Emphasis is now on the recognition of partially known or poorly articulated patterns* (1-5) (for example, recognition of hand sent Morse code, handwritten letters or spoken words).

It is the purpose of this study to consider the automatic processing of pulse waveforms in noise. In particular, the paper

---

*Numbers in parentheses refer to references given on page 131.

will be concerned with an experimental investigation of systems which modify their structure in order to recognize initially unknown waveforms in additive Gaussian noise. Some systems of this type have been discussed previously under the generic name of adaptive filters (2-4). Limited experimental and mathematical studies of their properties have been carried out (2, 6-10).

A general treatment of the problem requires consideration of the following desiderata:

1. There is no guarantee that the input contains only one waveform train.
2. The signal amplitude may vary over a wide range from pulse to pulse.
3. The waveform structures are initially unknown.
4. There is no realistic way by which costs may be assigned to errors.
5. The probability of occurrence is unknown and the repetition intervals may be random.
6. The times of arrival are unknown.
7. A limited number of signal repetitions are available to the observer before they vanish.
8. The processing is to be as close to real time as possible.

The first two conditions represent the severest departure from the past. Previous work is restricted to situations where only one fixed amplitude waveform is present. Unfortunately, if the contents of the data are unknown, it can neither be assumed a priori that only one pattern will be present nor that the patterns will have fixed amplitudes. Condition 4 reflects the observer's ignorance of the precise causes of the waveforms present. The causes are presumed unknown because the waveforms are unknown. Similarly, the probability of occurrence must be unknown. Together, these statements imply that the decision thresholds must be chosen on the basis of allowable false alarm rate or other intuitive judgments. Statements 6 and 7 are obvious, but lead to basic limitations in what the observer can expect to determine from the data. Each condition is sufficient to limit the final degree of knowledge of the waveform parameters. Although in past work (2, 4) it has not been claimed that the arrival time was known, it has been implied that it could be measured exactly. Clearly, the presence of noise spreads any measurement of time of arrival. The last requirement is somewhat arbitrary, but is imposed as a limit on the processing which may be used (for example, repeat runs for detection of other waveforms after all examples of one signal have been identified are not allowed).

It should be noted that an observer is not always faced with all of the above constraints. The relaxation of any of them means that the filtering requirements can be more accurately stated. Consequently, a filter designed under reduced restrictions will perform better on the average than a completely general one. Alternatively, the more general system will operate if the a priori knowledge of conditions is poor or faulty; whereas, the special one may fail. For the analysis of unknown data, then, the most general system must be used.

To proceed, it is necessary to make some assumptions which will hold throughout the discussion. The basic assumption, central to any scheme which utilizes past information, is that this information must be useful in the future. In other words, a system improves its performance only if future situations are similar to those of the past. In terms of the waveform filter, the signals are required to be repetitive. This is necessary from the point of view of reliably determining waveform structure and continually improving system performance. It is also presumed that the pulses do not overlap in time (that is, the pulse trains are interleaved). Further, it is assumed that the noise is stationary, additive, and Gaussian with a known variance and zero mean. Any realizable data is bandwidth limited by sensors or prefiltering and it is supposed that this limit (W) is known. The duration of any pulse is also limited ($< T$).

Thus the input can be represented by 2WT measurements. The choice of T is left to the discretion of the observer but must be large enought to include any waveforms of interest.

Proceeding from these conditions and assumptions, the study includes the derivation of a new type of filter by means of statistical decision theory. This filter, which is designed for multiple waveform environments, is described along with other adaptive systems in Section II. The inherent difficulties in transferring the equations to practice are discussed in Section III. The principal problems involve measurement bias and readout time errors. Some mathematical analysis of the adaptive filters is carried out in Section IV. A number of different filter types in various environments are studied experimentally in Section V. Special emphasis is placed on low signal to noise ratios and the effects of decision errors. Included in much of the discussion is a graphical interpretation of the filtering process.

II. THE DETECTION PROBLEM

A. MATHEMATICAL TREATMENT

The usual problem of signal detection is approached from the point of view of hypothesis testing (11). Under a number of different criteria which minimize the cost of the decisions to the observer this leads to the use of the likelihood ratio $\Lambda(V)$ for comparing hypotheses.

$$\Lambda(V) = \frac{\langle F_N(V|S_\alpha)\rangle_{S_\alpha}}{\langle F_N(V|S_\beta)\rangle_{S_\beta}} \tag{1}$$

$$\langle F_N(V|S_\alpha)\rangle_{S_\alpha} = \int W(S_\alpha)\, F_N(V|S_\alpha)\, dS_\alpha \quad . \tag{2}$$

The function $\langle F_N(V|S_\alpha)\rangle_{S_\alpha}$ is the N-dimensional conditional probability of the waveform S_α causing the data V averaged over the unknown parameters of the waveform. The function $W(S_\alpha)$ represents the distribution of the true signal parameters about the values S_α^* known to the observer.

The hypothesis H_α that signal S_α rather than S_β is present where only these two are considered, is chosen if

$$\Lambda(V) > \Lambda_{\alpha\beta} \tag{3}$$

where the threshold $\Lambda_{\alpha\beta}$ depends upon the costs assigned to the errors or the error rates allowed. The problem of detecting and

separating multiple signals in noise generally involves the construction of likelihood ratios for each pair of signals, including noise. This yields a signal space which is broken into various decision regions. The technique is useful only if no waveforms other than those previously identified are present. This assumption cannot be justified in the design of a system which is to look at incoming data with no knowledge of its contents.

It is obvious that the situations which will be of most interest in solving the overall problem will be those of detecting a waveform in noise and detecting a waveform in an environment of other signals, the characteristics of which may not be known. Some of the cases to be discussed here have been previously treated elsewhere (Cases I-III) (2), but are included for completeness and later use.

In the discussion to follow, it is assumed that

$$v(t) = \sum_{m=1}^{N} v_m f_m(t) \qquad 0 \le t \le T \qquad (4)$$

$$v(t) = s(t) + n(t)$$

$$v_m = s_m + n_m \qquad (5)$$

where the set $\{f_m(t)\}$ is a complete orthonormal basis over the interval $0 \le t \le T$. For the purposes of this paper, it is convenient

to consider the expansion to be in terms of sample values spaced $\frac{1}{2W}$ seconds apart. This representation yields noise coefficients n_m which are independent Gaussian variables with zero means and equal variances σ^2.

Case I Detection of a Completely Known Signal in Noise

If the waveform is completely known and can be specified by N = 2WT independent measurements, then

$$W(S_\alpha) = \prod_{m=1}^{N} \delta(s_{m\alpha} - s_{m\alpha}^*) \quad , \quad W(S_\beta) = \prod_{m=1}^{N} \delta(s_{m\beta}) \tag{6}$$

$$\Lambda(V) = \frac{\left(\frac{1}{2\pi\sigma^2}\right)^{N/2} \exp\left[-\frac{1}{2\sigma^2} \sum_{m=1}^{N} (v_m - s_{m\alpha}^*)^2\right]}{\left(\frac{1}{2\pi\sigma^2}\right)^{N/2} \exp\left[-\frac{1}{2\sigma^2} \sum_{m=1}^{N} v_m^2\right]}$$

$$= \exp\left[-\frac{1}{2\sigma^2} \sum_{m=1}^{N} (s_{m\alpha}^{*2} - 2 s_{m\alpha}^* v_m)\right] \quad . \tag{7}$$

H_α is selected if Equation (7) exceeds Λ_α. The decision can also be made if

$$\sum_{m=1}^{N} v_m s_{m\alpha}^* > \Lambda_{\alpha_1} \quad . \tag{8}$$

The correlation between the input and the signal provides the optimum measure for making the decision.

Case II Detection of a Completely Unknown Signal in Noise

In this situation, it is necessary to assume some form of signal parameter distribution and it is usual to assume that the parameters are equally likely to occur at any point in the signal space. Therefore, a uniform distribution is assumed for $W(S_a)$. It is also assumed that only the region

$$|s_{ma}| < d \qquad d >> \sigma \tag{9}$$

is examined for practical reasons. Then

$$\Lambda(V) = \frac{\int_{-d}^{d} \cdots \int_{-d}^{d} \left(\frac{1}{2d}\right)^{N} \left(\frac{1}{2\pi\sigma^2}\right)^{N/2} \exp\left[-\frac{1}{2\sigma^2} \sum_{m=1}^{N} (v_m - s_{ma})^2\right] ds_{ma}}{\left(\frac{1}{2\pi\sigma^2}\right)^{N/2} \exp\left[-\frac{1}{2\sigma^2} \sum_{m=1}^{N} v_m^2\right]}$$

$$\approx \left(\frac{2\pi\sigma^2}{4d^2}\right)^{N/2} \exp\left[\frac{1}{2\sigma^2} \sum_{m=1}^{N} v_m^2\right] . \tag{10}$$

Comparison of Equation (10) with a threshold is equivalent to comparing $\sum_{m=1}^{N} v_m^2$ with a different threshold. The decision is made that a signal is present on the basis of the energy measure

$$\sum_{m=1}^{N} v_m^2 > \Lambda_{a_2} . \tag{11}$$

Case III Detection of a Partially Known Signal in Noise

The basic assumption here is that the parameter values known to the observer have a Gaussian distribution about the true parameters with variance k^2.

$$W(S_a) = \left(\frac{1}{2\pi k^2}\right)^{N/2} \prod_{m=1}^{N} \exp\left[-\frac{1}{2k^2}\left(s_{ma} - s_{ma}^*\right)^2\right] \qquad (12)$$

$$\Lambda(V) = \frac{\left[\frac{1}{2\pi(k^2+\sigma^2)}\right]^{N/2} \exp\left[-\frac{1}{2(k^2+\sigma^2)} \sum_{m=1}^{N} \left(v_m - s_{ma}^*\right)^2\right]}{\left[\frac{1}{2\pi\sigma^2}\right]^{N/2} \exp\left[-\frac{1}{2\pi\sigma^2} \sum_{m=1}^{N} v_m^2\right]}$$

$$= \left[\frac{\sigma^2}{\sigma^2+k^2}\right]^{N/2} \exp\left[-\frac{1}{2(k^2+\sigma^2)}\left\{-\frac{k^2}{\sigma^2}\sum_{m=1}^{N} v_m^2 - 2\sum_{m=1}^{N} v_m s_{ma}^* + \sum_{m=1}^{N} s_{ma}^{*2}\right\}\right] \qquad (13)$$

H_a is chosen if

$$\frac{1}{k^2+\sigma^2}\left\{\frac{k^2}{\sigma^2}\sum_{m=1}^{N} v_m^2 + 2\sum_{m=1}^{N} v_m s_{ma}^*\right\} > \Lambda_{a_3} \qquad . \qquad (14)$$

The value of k is a measure of the uncertainty in the observer's knowledge of the parameters. If k = 0 the signal is known exactly and the detection process reduces to Case I. If k is very large, little is known of the parameters and the process reduces to that of Case II.

It would be possible at this point to determine the optimum detection method for separating two waveforms, each of which are partially known, but this will not be a significant case in the development. Middleton (9) has discussed this situation in detail. What will be of interest is the separation of a partially known waveform from other unknown signals.

Case IV Separation of a Partially Known Waveform from All Others

In this situation the distribution of parameters of unknown signals is again assumed to be uniform throughout the space in a manner identical to Case II. The partially known signal is again assumed to have a Gaussian distribution about the true parameters.

$$\Lambda(V) = \frac{\left[\frac{1}{2\pi(k^2+\sigma^2)}\right]^{N/2} \exp\left[-\frac{1}{2(k^2+\sigma^2)} \sum_{m=1}^{N} (v_m - s_{m\alpha}^*)^2\right]}{\int_{-d}^{d}\cdots\int_{-d}^{d} \left(\frac{1}{2d}\right)^N \left(\frac{1}{2\pi\sigma^2}\right)^{N/2} \prod_{m=1}^{N} \exp\left[-\frac{1}{2\sigma^2}(v_m - s_{m\beta})^2\right] ds_{m\beta}}$$

$$\approx \left[\frac{4d^2}{2\pi(k^2+\sigma^2)}\right]^{N/2} \exp\left[-\frac{1}{2(k^2+\sigma^2)} \sum_{m=1}^{N} (v_m - s_{m\alpha}^*)^2\right] . \qquad (15)$$

This is equivalent to saying that H_α is chosen if

$$\sum_{m=1}^{N} v_m^2 - 2\sum_{m=1}^{N} v_m s_{m\alpha}^* + \sum_{m=1}^{N} s_{m\alpha}^{*2} < \Lambda_{\alpha_4} . \qquad (16)$$

Equation (16) is simply a squared error criterion. If the above measure exceeds the threshold, it is decided that a waveform other than S_α is present. The waveform may be another signal or merely noise.

One feature to be noted is that the filter will fail to detect a signal of the same shape as S_a but with a different amplitude. The problem would occur if there should be a change in transmission characteristics that is not reflected in a change of parameter estimates. It therefore becomes important to investigate the type of filter that would be necessary for variable amplitude waveforms.

Case V Separation of a Known Signal with Variable Amplitude from All Other Waveforms

Once again a uniform distribution of unknown signal parameters is assumed. For the known signal it is assumed that the amplitude has a Gaussian distribution of mean A_0 and variance a^2. The values of the known parameters are given in normalized form with $\sum_{m=1}^{N} s_{ma}^{*2} = 1$. Under these conditions the likelihood ratio becomes

$$\Lambda(V) = \left(\frac{1}{2\pi a^2}\right)^{1/2} \left(\frac{1}{2\pi\sigma^2}\right)^{N/2}$$

$$\frac{\int_{-\infty}^{\infty}\cdots\int_{-\infty}^{\infty} \prod_{m=1}^{N} \exp\left[-\frac{1}{2\sigma^2}(v_m - s_{ma})^2\right] \delta(s_{ma} - A s_{ma}^*)\, ds_{ma} \exp\left[-\frac{1}{2a^2}(A - A_0)^2\right] dA}{\int_{-d}^{d}\cdots\int_{-d}^{d} \left(\frac{1}{2d}\right)^N \left(\frac{1}{2\pi\sigma^2}\right)^{N/2} \prod_{m=1}^{N} \exp\left[-\frac{1}{2\sigma^2}(v_m - s_{m\beta})^2\right] ds_{m\beta}}$$

$$\Lambda(V) \approx \frac{(2d)^N}{(2\pi a^2)^{1/2}(2\pi\sigma^2)^{N/2}} \int_{-\infty}^{\infty} \exp\left[-\frac{1}{2\sigma^2}\sum_{m=1}^{N}(v_m - A s_{m\alpha}^*)^2\right] \exp\left[-\frac{1}{2a^2}(A-A_0)^2\right] dA$$

$$\approx \frac{(2d)^N}{(2\pi a^2)^{1/2}(2\pi\sigma^2)^{N/2}} \int_{-\infty}^{\infty} \exp\left[-\frac{1}{2\sigma^2}\sum_{m=1}^{N}(v_m^2 - 2A v_m s_{m\alpha}^* + A^2 s_{m\alpha}^{*2})\right] \exp\left[-\frac{1}{2a^2}(A-A_0)^2\right] dA$$

$$\approx \frac{(2d)^N}{(2\pi a^2)^{1/2}(2\pi\sigma^2)^{N/2}} \exp\left[-\frac{1}{2\sigma^2}\left\{\sum_{m=1}^{N} v_m^2 - \left(\sum_{m=1}^{N} v_m s_{m\alpha}^*\right)^2\right\}\right]$$

$$\int_{-\infty}^{\infty} \exp\left[-\frac{1}{2\sigma^2}\left\{\left(\sum_{m=1}^{N} v_m s_{m\alpha}^*\right)^2 - 2A\sum_{m=1}^{N} v_m s_{m\alpha}^* + A^2\sum_{m=1}^{N} s_{m\alpha}^{*2}\right\}\right] \exp\left[-\frac{1}{2a^2}(A-A_0)^2\right] dA$$

but $\sum_{m=1}^{N} s_{m\alpha}^{*2} = 1$

$$\Lambda(V) \approx \frac{(2d)^N}{(2\pi a^2)^{1/2}(2\pi\sigma^2)^{N/2}} \exp\left[+\frac{1}{2\sigma^2}\left\{\left(\sum_{m=1}^{N} v_m s_{m\alpha}^*\right)^2 - \sum_{m=1}^{N} v_m^2\right\}\right]$$

$$\int_{-\infty}^{\infty} \exp\left[-\frac{1}{2\sigma^2}\left\{\sum_{m=1}^{N} v_m s_{m\alpha}^* A\right\}^2\right] \exp\left[-\frac{1}{2a^2}(A-A_0)^2\right] dA$$

$$\Lambda(V) \approx \frac{(2d)^N}{(2\pi a^2)^{1/2}(2\pi\sigma^2)^{N/2}} \left(\frac{2\pi a^2\sigma^2}{\sigma^2+a^2}\right)^{1/2} \exp\left[-\frac{1}{2\sigma^2}\left\{\sum_{m=1}^{N} v_m^2 - \left(\sum_{m=1}^{N} v_m s_{m\alpha}^*\right)^2\right\}\right]$$

$$\exp\left[-\frac{1}{2(a^2+\sigma^2)}\left\{\sum_{m=1}^{N} v_m s_{m\alpha}^* - A_0\right\}^2\right]$$

$$\approx \left(\frac{4d^2}{2\pi\sigma^2}\right)^{N/2} \left(\frac{\sigma^2}{\sigma^2+a^2}\right)^{1/2} \exp\left[-\frac{1}{2\sigma^2}\sum_{m=1}^{N} v_m^2 + \frac{a^2}{2\sigma^2(a^2+\sigma^2)}\left(\sum_{m=1}^{N} v_m s_{m\alpha}^*\right)^2\right.$$

$$\left. + \frac{2A_0}{2(a^2+\sigma^2)}\sum_{m=1}^{N} v_m s_{m\alpha}^* - \frac{A_0^2}{2(a^2+\sigma^2)}\right] \quad . \tag{17}$$

Thus, H_α is chosen if

$$-\sum_{m=1}^{N} v_m^2 + \frac{a^2}{a^2+\sigma^2}\left(\sum_{m=1}^{N} v_m s_{m\alpha}^*\right)^2 + \frac{2A_0\sigma^2}{a^2+\sigma^2}\sum_{m=1}^{N} v_m s_{m\alpha}^* - \frac{A_0^2\sigma^2}{a^2+\sigma^2} > \Lambda_{\alpha_5} \quad . \tag{18}$$

Notice that the variable amplitude has introduced a new term of the form $\left(\sum_{m=1}^{N} v_m s_{m\alpha}^*\right)^2$. This term will also arise in the last case to be considered.

Case VI Separation of a Partially Known Waveform of Varying Amplitude from All Other Signals

A number of assumptions are required to produce any results in this case. Their justification will be considered more completely later. The signal parameters known to the observer are once again presented in normalized form, that is

$$\sum_{m=1}^{N} s_{ma}^{*2} = 1 \quad .$$

The true normalized parameters have a Gaussian distribution about the estimates, and once more a Gaussian amplitude distribution is assumed. The characteristics of the other waveforms remain the same as in the two previous cases.

$$\Lambda(V) = \left(\frac{1}{2\pi\sigma^2}\right)^{N/2} \left(\frac{1}{2\pi k^2}\right)^{N/2} \left(\frac{1}{2\pi a^2}\right)^{1/2}$$

$$\frac{\int_{-\infty}^{\infty}\cdots\int_{-\infty}^{\infty} \prod_{m=1}^{N} \exp\left[-\frac{1}{2\sigma^2}(v_m - s_{ma})^2\right] \exp\left[-\frac{1}{2k^2}(s_{ma} - A s_{ma}^{*})^2\right] ds_{ma} \exp\left[-\frac{1}{2a^2}(A - A_0)^2\right] dA}{\int_{-d}^{d}\cdots\int_{-d}^{d} \left(\frac{1}{2d}\right)^{N} \left(\frac{1}{2\pi\sigma^2}\right)^{N/2} \prod_{m=1}^{N} \exp\left[-\frac{1}{2\sigma^2}(v_m - s_{m\beta})^2\right] ds_{m\beta}}$$

$$\Lambda(V) \approx \left(\frac{1}{2\pi\sigma^2}\right)^{N/2} \left(\frac{1}{2\pi k^2}\right)^{N/2} \left(\frac{1}{2\pi a^2}\right)^{1/2} (2d)^N \left[\frac{2\pi k^2\sigma^2}{k^2+\sigma^2}\right]^{N/2}$$

$$\int_{-\infty}^{\infty} \exp\left[-\frac{1}{2(k^2+\sigma^2)} \sum_{m=1}^{N} (v_m - A s_{m\alpha}^*)^2\right] \exp\left[-\frac{1}{2a^2}(A-A_0)^2\right] dA \ .$$

Proceeding as in Case V the likelihood ratio becomes

$$\Lambda(V) \approx \left[\frac{4d^2}{2\pi(k^2+\sigma^2)}\right]^{N/2} \left[\frac{\sigma^2+k^2}{\sigma^2+k^2+a^2}\right]^{1/2} \exp\left[-\frac{1}{2(k^2+\sigma^2)} \sum_{m=1}^{N} v_m^2\right.$$

$$\left. + \frac{a^2}{2(k^2+\sigma^2)(k^2+\sigma^2+a^2)} \left(\sum_{m=1}^{N} v_m s_{m\alpha}^*\right)^2 + \frac{2A_0}{2(k^2+\sigma^2+a^2)} \sum_{m=1}^{N} v_m s_{m\alpha}^* - \frac{A_0^2}{2(k^2+\sigma^2+a^2)}\right] \tag{19}$$

The optimum detector chooses H_a if

$$-\sum_{m=1}^{N} v_m^2 + \frac{a^2}{k^2+\sigma^2+a^2} \left(\sum_{m=1}^{N} v_m s_{m\alpha}^*\right)^2 + \frac{2A_0(k^2+\sigma^2)}{k^2+\sigma^2+a^2} \sum_{m=1}^{N} v_m s_{m\alpha}^*$$

$$- \frac{(k^2+\sigma^2)A_0^2}{k^2+a^2+\sigma^2} > \Lambda_{a_6} \tag{20}$$

The detector, as did the last one, measures the input energy, the correlation of the input with the estimate, and the square of the correlator output.

An interpretation and extension of the previous results will be presented in Part B but some superficial discussion of the assumptions involved is in order. It is unlikely that some of the suppositions will ever be met in practice. A Gaussian amplitude distribution is quite improbable, particularly since it implies a definite probability of the amplitude's shifting signs. Such a distribution also implies an a priori knowledge of the input. Case VI is also suspect since a true Gaussian distribution about the normalized estimate seems unlikely when the amplitude is variable. However, Case VI can be somewhat justified by noting that it reduces to the other problems in the limit of $a \to 0$ and/or $k \to 0$. It will also be partially justified in the discussion of a graphical approach to the problem. Therefore, the results of this section seem valid in indicating the measurements which are required for the detection problem. The coefficients of these measurements remain the weak part of the discussion.

B. GRAPHICAL INTERPRETATION OF THE DETECTION PROBLEM

In the mathematical approach to detection it was seen that a signal was represented by N numbers. These numbers are independent and can thus be pictured as components of a vector in an N dimensional vector space. The detection process becomes one in which the N dimensional signal vector (some components

may be zero) is compared to the N dimensional input vector. Detection occurs when the data vector appears in a specific region of the space about the reference signal. These ideas will become clearer as the previous six detection cases are re-examined.

In the discussion to follow, only two of the N dimensions will be shown. These two will be defined by the plane formed by the data vector and the signal estimate vector.

Case I Detection of a Completely Known Signal in Noise

The problem is shown graphically in Figure 1 with the signal and noise classes represented as circles. Although the areas are shown as non-overlapping, there is a finite probability that the signals and noise will be outside the boundaries and will indeed overlap. The radius of the circle is large enough to include some arbitrarily large probability that the occurrence of S_a will be within the boundary.

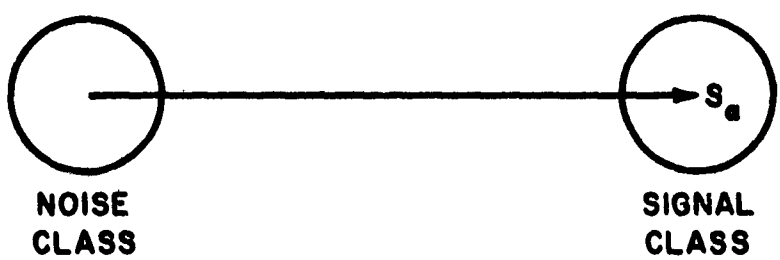

FIGURE 1 BASIC DETECTION SITUATION

The optimum filter was of the form

$$\sum_{m=1}^{N} v_m s_{ma}^* > \Lambda_{a_1} \tag{8}$$

which is seen to require a calculation of the projection of the data vector onto the signal vector

$$\sum_{m=1}^{N} v_m s_{ma}^* = |V| \, |S_a| \cos\theta \quad .$$

Detection takes place when

$$|V| \cos\theta > \frac{\Lambda_{a_1}}{|S_a|} \quad .$$

However,

$$|V| \cos\theta = \frac{\Lambda_{a_1}}{|S_a|}$$

is the equation of a straight line perpendicular to S_a, so the optimum filter can be represented by the region shown in Figure 2. The choice of Λ_{a_1} depends upon the criterion chosen. The data V would be detected as an example of S_a. Notice that this filter will detect a very large signal which may be almost orthogonal to S_a; thus, the filter is not good for separating waveforms.

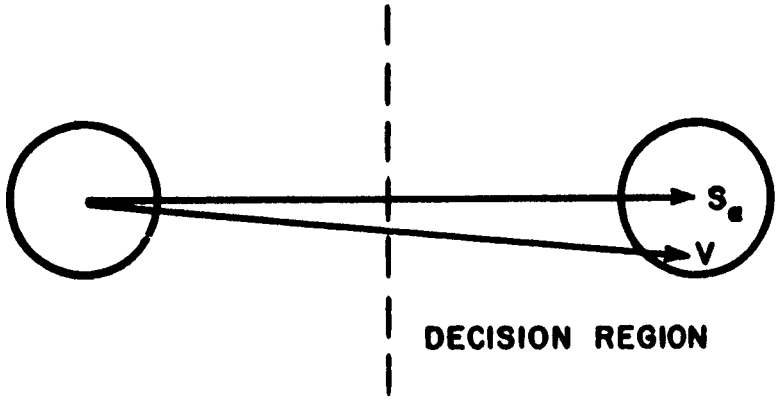

FIGURE 2 DETECTION OF A KNOWN SIGNAL

Case II Detection of a Completely Unknown Signal in Noise

Here detection is based upon

$$\sum_{m=1}^{N} v_m^2 > \Lambda_{a_2} \quad . \tag{11}$$

Graphically this is shown in Figure 3. It satisfies the intuitive feeling that if nothing is known of signal parameters, one must search in all directions equally to determine the presence of a signal.

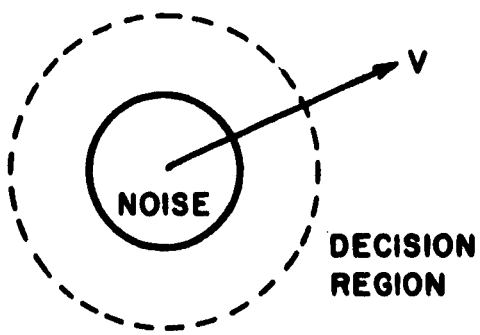

FIGURE 3 ENERGY DETECTION

Case III Detection of a Partially Known Signal in Noise

The optimum measure for this problem is

$$\frac{1}{k^2+\sigma^2}\left\{\frac{k^2}{\sigma^2}\sum_{m=1}^{N} v_m^2 + 2\sum_{m=1}^{N} v_m s_{ma}^*\right\} > \Lambda_{a_3} \qquad (14)$$

which can be written

$$\frac{k^2}{\sigma^2}|V|^2 + 2|V||S_a^*|\cos\theta > \Lambda_{a_3}(k^2+\sigma^2) \quad .$$

If the S_a^* direction is called the x direction, the filter becomes

$$\frac{k^2}{\sigma^2}(x^2+y^2) + 2|S_a^*|x > \Lambda_{a_3}(k^2+\sigma^2)$$

otherwise written

$$\left\{x + \frac{\sigma^2|S_a^*|}{k^2}\right\}^2 + y^2 > \frac{\sigma^2}{k^2}\Lambda_{a_3}(k^2+\sigma^2) + \frac{\sigma^4}{k^4}|S_a^*|^2 \qquad (21)$$

which is the equation of a circular decision region. The graphical representation of the filter as a function of $\ell = \sigma^2/k^2$ is shown in Figure 4.

The filter has been proposed as an adaptive filter (2), in which, after each detection, the value of k decreases and the weights of the various terms are automatically changed. When this is done and each detection is perfect $k^2 = \sigma^2/\ell$ where ℓ represents the number of previous detections.

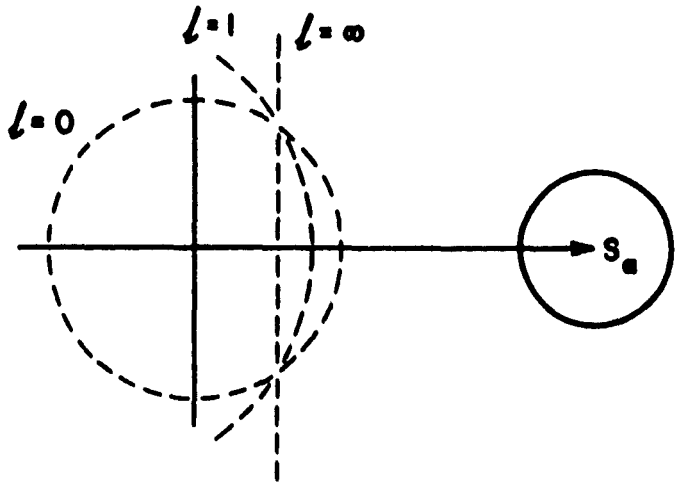

FIGURE 4 CASE III ADAPTIVE FILTER

In operation the filter has no estimate of the signal initially, $l = 0$, so detection is based upon vector length as shown in Case II. As l increases, the estimates of the signal parameters improve and the filter approaches the matched filter of Case I.

Case IV Separation of a Partially Known Signal from All Others

In this case it was shown that H_a was chosen if

$$\sum_{m=1}^{N} v_m^2 - 2 \sum_{m=1}^{N} v_m s_{ma}^* + \sum_{m=1}^{N} s_{ma}^{*2} < \Lambda_{a_4} \tag{16}$$

or, with S_a^* chosen in the x direction

$$(x^2 + y^2) - 2|S_a^*|x + |S_a^*|^2 < \Lambda_{a_4} \tag{22}$$

which is the equation of a circle centered at $x = |S_a^*|$ as shown in Figure 5. A vector lying inside the decision circle would be detected as S_a.

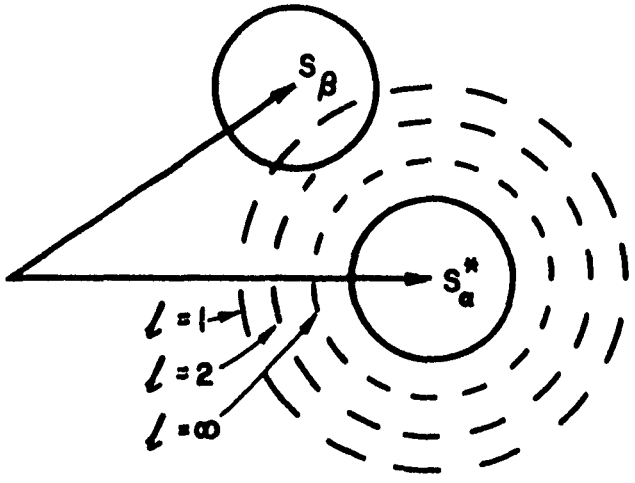

FIGURE 5 DETECTION OF A PARTIALLY KNOWN SIGNAL IN AN UNKNOWN ENVIRONMENT

In operation this type of filter would initially detect the presence of S_a by means of energy and form an estimate S_a^* of the parameters. A rather large decision region ($\ell = 1$ circle) would then be formed which would insure that with some larger probability the next example of S_a would be properly detected. As the number of detections and the quality of the estimate increase, the radius of the circle can be diminished without decreasing the probability of detection.

The filter poses two apparent problems. As was noted before, the filter will fail to detect variable amplitude waveforms which are not reflected in the estimate. Secondly, if another signal S_β is located in the vicinity of S_α, it is likely to be detected as S_α by this filter during the beginning of the process when the radius of detection is large. Figure 5 also demonstrates another point. If the repetition frequency of S_β is much larger than that of S_α, it may become quite likely that S_β will be detected at $\ell = 1$. At higher values of ℓ, this becomes unlikely, but, if it does occur early, the entire future operation may fail, because the estimate stored in the filter will be a linear combination of S_α^* and S_β^* and may never converge to either signal. These difficulties will be reduced in the next two situations.

Case V Separation of a Known Signal with Variable Amplitude from All Other Waveforms

Detection of S_α is based upon

$$-\sum_{m=1}^{N} v_m^2 + \frac{a^2}{a^2+\sigma^2}\left(\sum_{m=1}^{N} v_m s_{m\alpha}^*\right)^2 + \frac{2A_0\sigma^2}{a^2+\sigma^2}\sum_{m=1}^{N} v_m s_{m\alpha}^* - \frac{A_0^2\sigma^2}{a^2+\sigma^2} > \Lambda_{\alpha_5} \qquad (18)$$

where

$$\sum_{m=1}^{N} s_{m\alpha}^{*2} = 1 \quad .$$

With S_a^* chosen to be a unit vector in the x direction the filter becomes

$$-(x^2+y^2) + \frac{a^2}{a^2+\sigma^2}\, x^2 + \frac{2A_0\sigma^2}{a^2+\sigma^2}\, x - \frac{A_0^2\sigma^2}{a^2+\sigma^2} > \Lambda_{a_5}$$

$$-y^2 - \frac{\sigma^2}{a^2+\sigma^2}\,(x - A_0)^2 > \Lambda_{a_5}$$

or

$$\frac{\sigma^2}{\sigma^2+a^2}\,(x - A_0)^2 + y^2 < -\Lambda_{a_5} \tag{23}$$

which is the equation of an ellipse centered at A_0. The filter is shown in Figure 6.

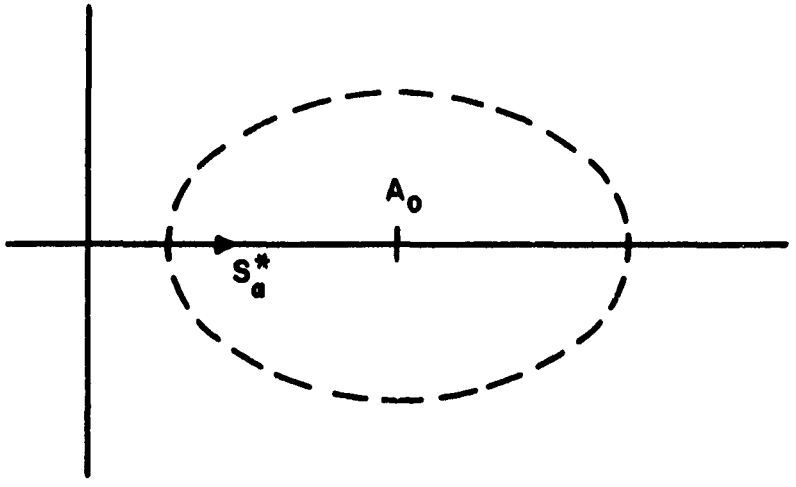

FIGURE 6 DETECTION OF A VARIABLE AMPLITUDE KNOWN SIGNAL IN AN UNKNOWN ENVIRONMENT

The filter can be interpreted in two ways. If the amplitude of the signal truly has a Gaussian distribution, then the filter is a fixed one as shown. If the amplitude is fixed and unknown initially, the filter becomes an adaptive one in which the A_0 in the equations is actually an estimate, and a^2 decreases as the estimate improves. Finally, the filter would reduce to a circle centered at the true value of A_0.

Case VI Separation of a Partially Known Waveform of Varying Amplitude from All Other Waveforms

This is the most general case and reduces to all other cases in the limit. Detection of the partially known signal S_a^* is based upon

$$-\sum_{m=1}^{N} v_m^2 + \frac{a^2}{k^2+\sigma^2+a^2}\left(\sum_{m=1}^{N} v_m s_{ma}^*\right)^2 + \frac{2A_0(k^2+\sigma^2)}{k^2+\sigma^2+a^2}\sum_{m=1}^{N} v_m s_{ma}^*$$

$$-\frac{(k^2+\sigma^2)A_0^2}{k^2+\sigma^2+a^2} > \Lambda_{a_6} \qquad (20)$$

where

$$\sum_{m=1}^{N} s_{ma}^{*2} = 1 \quad .$$

With S_a^* chosen as a unit vector in the x direction the filter becomes

$$-y^2 - \frac{k^2+\sigma^2}{k^2+\sigma^2+a^2}(x - A_0)^2 > \Lambda_a{}_6$$

or

$$y^2 + \frac{k^2+\sigma^2}{k^2+\sigma^2+a^2}(x - A_0)^2 < -\Lambda_a{}_6 \qquad (24)$$

which once again is an ellipse centered at A_0. The filter is shown in Figure 7.

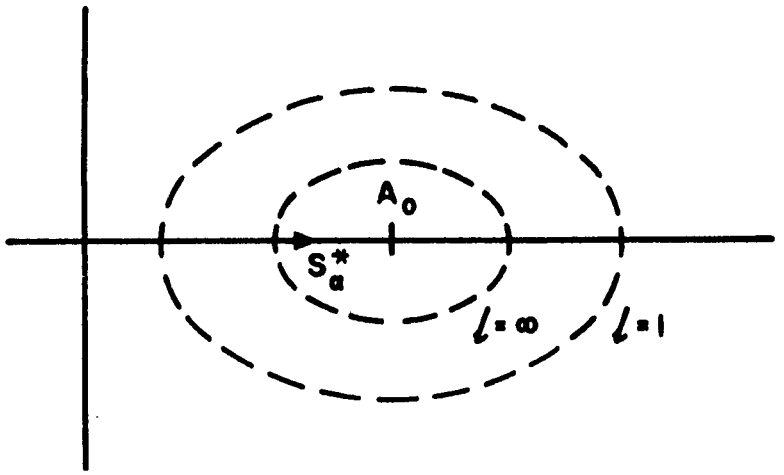

FIGURE 7 DETECTION OF A VARIABLE AMPLITUDE UNKNOWN SIGNAL

It is seen that the optimum decision region under the given assumptions is an ellipse whose size decreases as the number of detections increase. A more thorough discussion of these results will be presented in the next section.

C. EXTENSION TO UNIFORM AMPLITUDE DISTRIBUTION

Unfortunately, little of the discussion which has gone before is of specific help in the problem being discussed. It is, however, useful in that it agrees with intuitive notions and thus, to some degree, justifies the extension of these notions. An extension of the theory from Cases III and IV will be undertaken here.

As stated before, one of the main difficulties with the derivation springs from an unrealistic amplitude assumption. The Gaussian distribution will now be dropped in favor of a uniform amplitude from A_{min} to A_{max}, which will be considered the worst case. A mathematical derivation of this filter is difficult, but it is felt that Figure 8 is a good representation of a filter which separates a known waveform of variable amplitude from any other waveform. It can be arrived at by arguing that if the distribution is uniform, all amplitudes should be examined equally. However, each amplitude is examined by means of a circle centered at that amplitude and this leads to Figure 8.

If the above reasoning is extended to the case of a partially known waveform with uniform amplitude distribution, the filter should be as shown in Figure 9. The same argument applies here except that the radii of the circles depend upon the degree of uncertainty in the signal parameters.

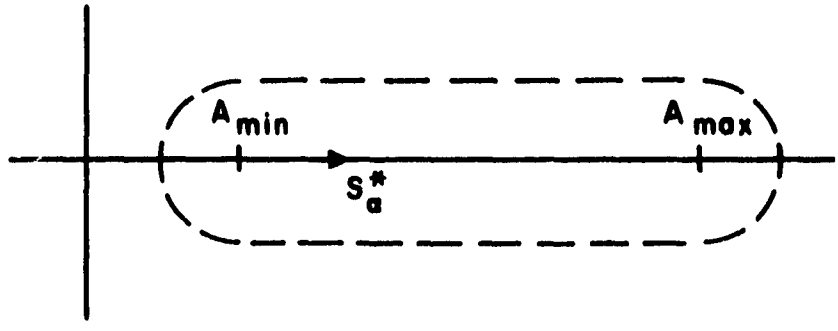

FIGURE 8 UNIFORM AMPLITUDE DISTRIBUTION FILTER FOR KNOWN SIGNALS

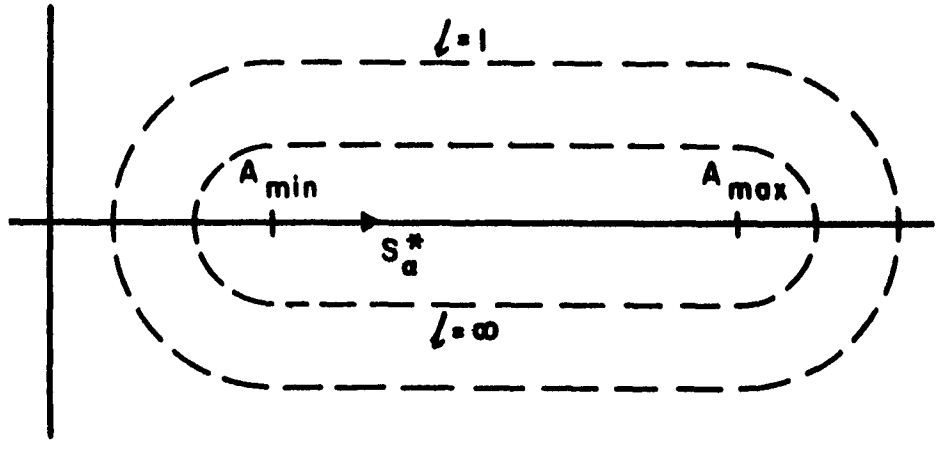

FIGURE 9 UNIFORM AMPLITUDE DISTRIBUTION FILTER FOR PARTIALLY KNOWN SIGNALS

If it is now stated that the final filter must separate a partially known waveform of variable amplitude from noise and other possible signals, the solution will be a combination of Figures 9 and 4, and is shown in Figure 10. The dimensions will depend upon the decision criterion used.

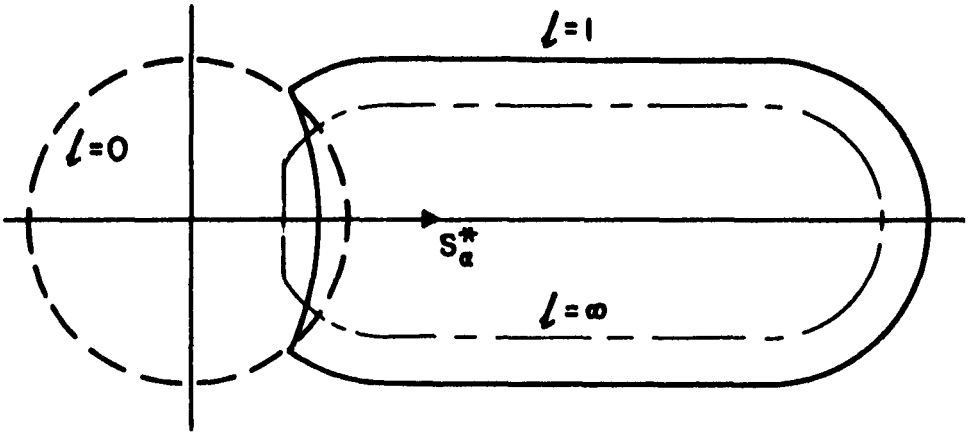

FIGURE 10 FINAL ADAPTIVE FILTER

The filter is not easy to instrument because it would require powers of $\sum_{m=1}^{N} v_m s_{ma}^*$ greater than two for its implementation. Various conic sections can be considered as approximations to these filters. An ellipse is an obvious approximation. A parabola also could be considered even though it is open ended. This merely means that the filter will pass very large waveforms and is identical to assuming $A_{max} \rightarrow \infty$.

A hyperbola can also be used with the center at a large negative value of x so that the right half of the hyperbola is the only one of importance in the detection operation.

Any of these conic sections can be represented by an equation of the form

$$Ax^2 + Bx + Cy^2 = K \tag{25}$$

which in terms of the measurements to be used becomes

$$A\left(\sum_{m=1}^{N} v_m s_{m\alpha}^*\right)^2 + B\left(\sum_{m=1}^{N} v_m s_{m\alpha}^*\right) + C\left[\sum_{m=1}^{N} v_m^2 - \left(\sum_{m=1}^{N} v_m s_{m\alpha}^*\right)^2\right] = K$$

$$(A-C)\left(\sum_{m=1}^{N} v_m s_{m\alpha}^*\right)^2 + B\sum_{m=1}^{N} v_m s_{m\alpha}^* + C\sum_{m=1}^{N} v_m^2 = K \tag{26}$$

where

$$\sum_{m=1}^{N} s_{m\alpha}^{*2} = 1 \quad .$$

For an ellipse	$C < 0$	$B > 0$	$A < 0$
For a parabola	$C < 0$	$B > 0$	$A = 0$
For a hyperbola	$C < 0$	$B > 0$	$A > 0$

Thus, one sees an indication of how the desired filter can be implemented by using the measurements required for Cases V and VI. Notice also that one of the approximations is just the ellipse which was derived in those situations; however, there is no specific rule for the values of the coefficients as a function of the noise and uncertainty in the parameters.

It is easy to visualize approximate values for A, B, and C and reasonable rules for their variation throughout the detection process, but the validity of these rules is not known. The experimental investigation of filters with decision boundaries given by

$$a(\ell)\left(\sum_{m=1}^{N} v_m s_{m\alpha}^*\right)^2 + b(\ell)\sum_{m=1}^{N} v_m s_{m\alpha}^* + c(\ell)\sum_{m=1}^{N} v_m^2 = F(\ell) \qquad (27)$$

$$\sum_{m=1}^{N} s_{m\alpha}^{*2} = 1 \quad ,$$

where ℓ represents the number of past detections, will be presented in Section V. The above form includes all six cases previously discussed.

D. THE LINEAR ADAPTIVE FILTER

One other filter which has been widely discussed in the literature (3, 6, 7, 8) will be investigated in modified form. This filter determines the presence of a waveform by measuring continuously the correlation between the input and the memory. When

the threshold is exceeded, the output of the filter is weighted and added to the previously existing memory to obtain a new estimate. Initially the threshold is set very low and noise is stored in the memory. When a signal appears at the input, there is a certain probability that the correlation will exceed the threshold. Once this occurs, the threshold is increased and a signal estimate is obtained. The memory has decay so that, in theory, initial incorrect detections will not continue to prevent true detections. The detection process is shown in Figure 11.

Several features of the graphical representation should be discussed. The M_ℓ vectors represent the stored waveform in the memory before the $(\ell+1)^{th}$ detection. The figure also is presented with the assumption that each detection represents an improvement in M, but this is not necessarily true. Also the M's are shown in one plane when in reality they are in different planes of a hyperspace. The initial detection requires at least some component of the memory to be in the S direction or the convergence process will not begin. With no component in this direction, it seems likely that the filter will continue to detect noise with a corresponding wander of the memory vector until some component lies in the signal direction. The filter then may begin to operate properly.

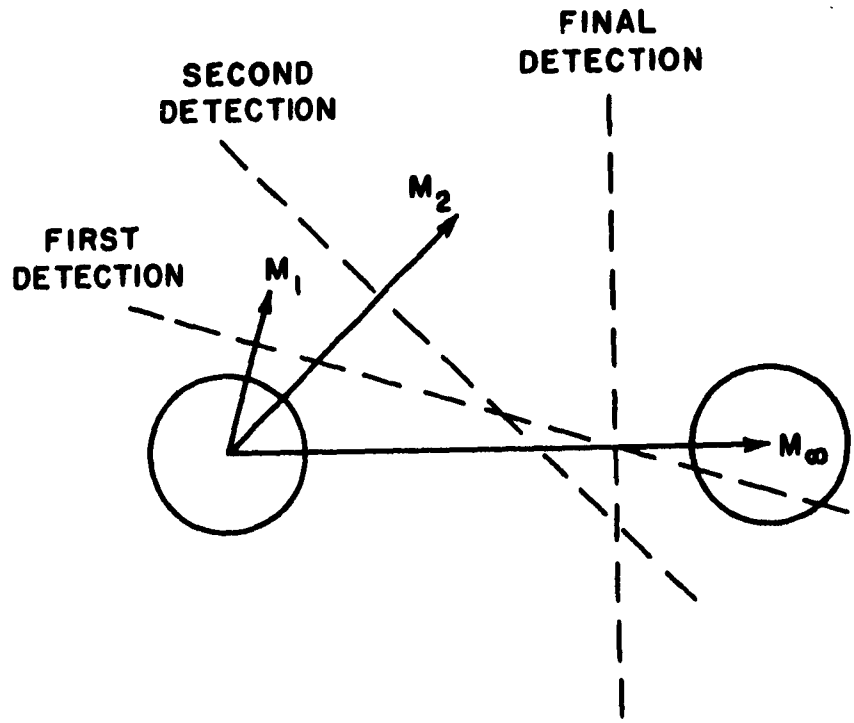

FIGURE 11 INTERPRETATION OF THE LINEAR ADAPTIVE FILTER

The version of the above filter which will be studied here has the following modifications:

1. The initial detection will be on the basis of energy rather than correlation with noise.
2. The threshold will no longer depend upon the previous correlation peak.
3. The threshold will not change between detections.
4. All data will be weighted equally in forming the estimates.

These modifications lead to a filter with a decision boundary given by

$$\sum_{m=1}^{N} v_m s_{m\alpha}^{*} = \Lambda \quad . \tag{28}$$

Notice that the filter is just an approximation to Case III for large ℓ. The observer uses the estimate as if it were exact rather than having a degree of uncertainty. It may also be viewed as a filter matched to the estimate instead of to the true signal.

III. THE COMPLETE FILTER SYSTEM - A DISCUSSION

A. LIMITATIONS ON ESTIMATE QUALITY

The equations of the previous section provide the guide for the analysis of unknown data by adaptive filters. A complete system may be separated into three distinct operations:

1. Determining that a signal is present (detection)
2. Determining the relevant parameters of the waveform (estimation)
3. Utilization of the new parameters for future improvement (adaptation).

The process of estimation and the use of the estimates will be discussed here. In studying the estimation and adaptive operations, the assumptions of Section II will be re-examined. The assumptions are found to be poor at low signal to noise ratios; however, no alternatives will be offered.

Glaser (2) has discussed the problem of estimation under the assumptions of Case II and Case III. The optimum estimate, under a variety of criteria, with no previous knowledge of the signal is the input at the time of detection. Assuming a Guassian distribution of the estimates, the estimate of the m^{th} coefficient following the ℓ^{th} detection is

$$s_m^*[\ell] = \frac{k^2[\ell-1]\, v_m[\ell] + \sigma^2 s_m^*[\ell-1]}{\sigma^2 + k^2[\ell-1]} \qquad (29)$$

where

$v_m[\ell]$ = value of v_m at the ℓ^{th} detection

$k^2[\ell-1]$ = variance of the estimate after the $(\ell-1)^{th}$ detection

$$E\left\{s_m^*[\ell]\right\} = s_m$$

$$\text{Var}\left\{s_m^*[\ell]\right\} = k^2[\ell] = \frac{\sigma^2 k^2[\ell-1]}{\sigma^2 + k^2[\ell-1]} \quad .$$

Since the first estimate was merely the data

$$s_m^*[1] = v_m[1]$$

$$k^2[1] = \sigma^2 \qquad k^2[2] = \sigma^2/2$$

$$k^2[\ell] = \sigma^2/\ell \quad . \tag{30}$$

Thus, the quality of the estimate does improve as the number of detections increase. The estimate can then be written

$$s_m^*[\ell] = \frac{1}{\ell} v_m[\ell] + \frac{\ell-1}{\ell}\left\{\frac{1}{\ell-1} v_m[\ell-1] + \frac{\ell-2}{\ell-1}(\cdots)\right\}$$

$$= \frac{1}{\ell}\left\{v_m[\ell] + v_m[\ell-1] + \cdots\cdots v_m[1]\right\} \quad . \tag{31}$$

The optimum estimate is then the average of all data samples. In other words, all estimates are weighted equally in determining the final estimate. In the analysis, it is implied that the time of arrival of the signal is known exactly and that the process of making a decision does not affect the post-estimate distribution. Unfortunately, neither of these conditions is correct.

The quantity v_m is a measured value and, as such, is subject to certain errors. One error arises because the measurement must be made at a precise time

$$v(t) = \sum_{m=1}^{N} v_m f_m(t) \qquad s(t) = \sum_{m=1}^{N} s_m f_{in}(t)$$

$$s_m = \int_0^T s(t) f_m(t)\, dt \tag{32}$$

but s_m can be obtained by passing the signal through a filter with an impulse response

$$f_m(T - t) \qquad 0 \le t \le T$$

$$r(t) = \int_0^T s(t-\tau) f_m(T-\tau)\, d\tau$$

Letting

$$u = T - \tau$$

$$r(t) = \int_0^T s(t-T+u) f_m(u)\, du \tag{33}$$

it can be seen that $r(T) = s_m$.

However, the decision that the coefficients should be read out is based upon some measure of the data. At the time chosen, the outputs of the orthogonal filters are v_m by definition. Because of the presence of noise, the readout time t_R is not, in general, equal to T and the expected value of v_m is not s_m. There will be some distribution of readout time error y, and

$$E\left\{s_m^*\right\} = \int_0^T \int_{-\infty}^{\infty} D(y)\, s(y+u)\, f_m(u)\, dy\, du \quad . \tag{34}$$

The final estimate (after an infinite number of detections) is

$$s^*(u) = \int_{-\infty}^{\infty} D(y)\, s(y+u)\, dy \quad . \tag{35}$$

The final result is not s(t), but it is the convolution of s(t) and the readout density function D(y) [see also (6)]. In terms of sample values (where the sampling rate is synchronous with the repetition rate)

$$E\left\{s_m^*\left[\ell\right]\right\} = \frac{1}{I}\left[N_0\, s_m + N_1\, s_{m+1} + \cdots + N_{-1}\, s_{m-1} + \cdots\right]$$

$$E\left\{s_m^*\left[\ell\right]\right\} = \sum_{j=-N}^{N} D_j\, s_{m+j}, \qquad \sum_{j=-N}^{N} D_j = 1 \quad . \tag{36}$$

In review, the assumption that v_m has a mean of s_m holds at one time t_R only. The expected value of v_m is s_m only if all detections occur at the proper time which leads to $D(y) = \delta(y)$ or $D_0 = 1$. Thus, there is a limit to the accuracy of the estimate which depends upon the ability to determine the proper readout time.

It appears obvious that the optimum $D(y)$ or D_j for use in parameter estimation is the one with the sharpest distribution about the true time. The problem becomes one of maximizing the probability of detection at the correct time. Figure 12 illustrates how the problem may be approached. Figure 12(a) represents a signal and Figures 12(b-f) represent the various parameter estimates which are obtained for different choices of t_R. It is apparent that what is really desired in readout determination is the separation of signal - Figure 12(d) - from the other four. Thus, readout can be considered as a multiple detection problem where it is to be decided which of 2N-1 waveforms (2N, if the null signal is included) is present.

Using the elements of decision theory leads to the construction of decision rules of the form

$$\Lambda(V) = \frac{\langle F_N(V|S_\alpha)\rangle_{S_\alpha}}{\langle F_N(V|S_\beta)\rangle_{S_\beta}} > \Lambda_{\alpha\beta} \quad , \qquad (1),(3)$$

where S_β represents time displaced versions of S_α.

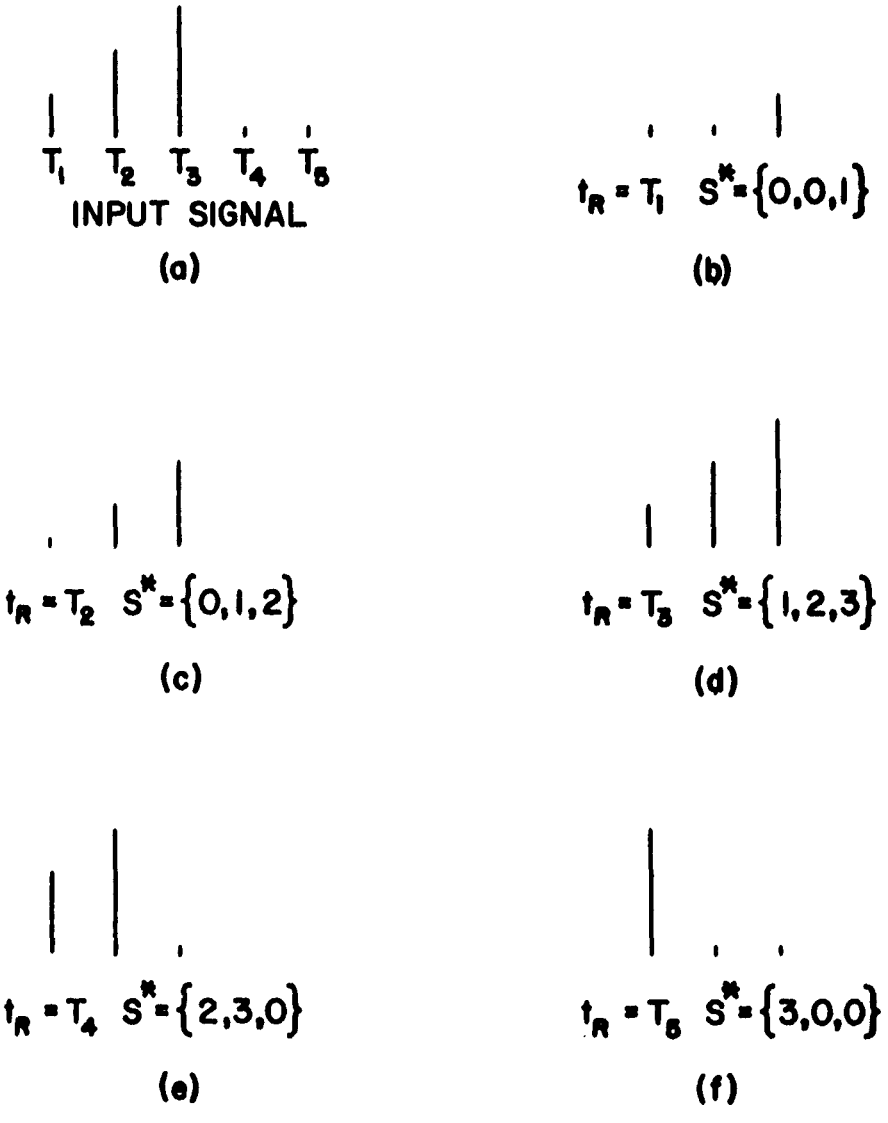

FIGURE 12 ESTIMATE VARIATION WITH READOUT TIME

By making the same assumptions as for Case III, Section II, H_a is chosen if

$$\Lambda(V) = \frac{\left[\frac{1}{2\pi(k^2+\sigma^2)}\right]^{N/2} \exp\left[-\frac{1}{2(k^2+\sigma^2)} \sum_{m=1}^{N} (v_m - s_m^*)^2\right]}{\left[\frac{1}{2\pi(k^2+\sigma^2)}\right]^{N/2} \exp\left[-\frac{1}{2(k^2+\sigma^2)} \sum_{m=1}^{N} (v_m - s_{m+j}^*)^2\right]} > \Lambda_j \qquad (37)$$

or

$$2\sum_{m=1}^{N} v_m s_m^* - 2\sum_{m=1}^{N} v_m s_{m+j}^* > 2(k^2+\sigma^2) \ln \Lambda_j + \sum_{m=1}^{N} (s_m^{*2} - s_{m+j}^{*2}) . \qquad (38)$$

The values of Λ_j, depend only upon the costs assigned to the errors since the probability of occurrence of all signals is the same. A graphical representation of this situation is shown in Figure 13.

It should be realized that while this type of measurement provides the optimum timing measurement, it is difficult to instrument for moderately high dimension signals. A reasonable approximation to the decision region of Figure 13 would be a parabola centered about the estimate. Thus, the filter developed for detecting waveforms in an unknown environment can also be used to provide good timing information.

The costs of more accurate identification of t_R are two-fold. The probability of detection is lowered because of the decrease in the acceptance region. The more important effect is the increased reliance upon the quality of the first detection. By narrowing the

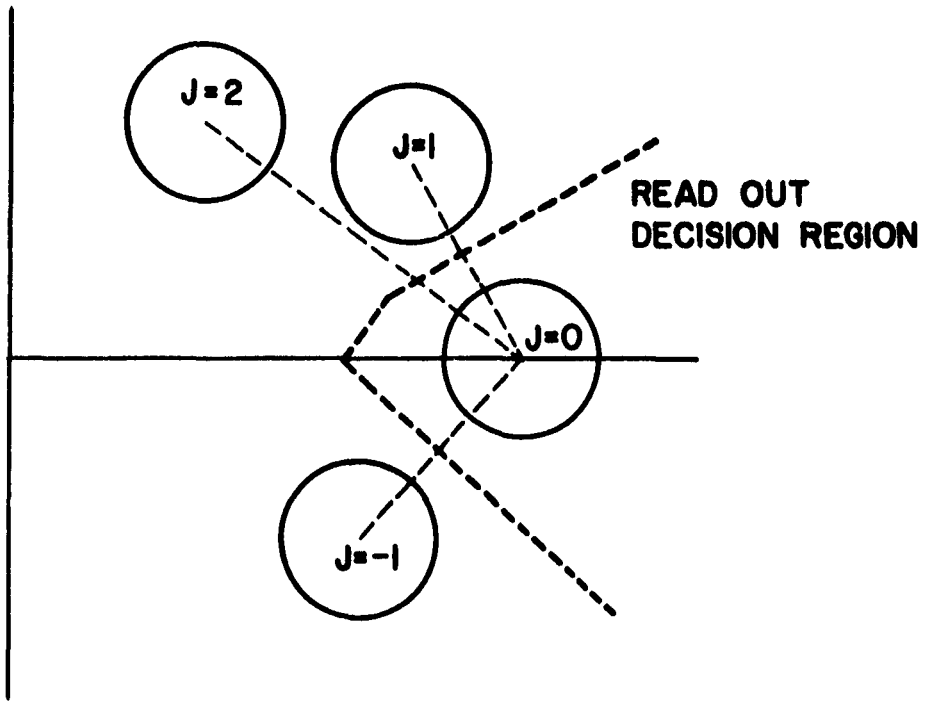

FIGURE 13 READOUT AS A DETECTION PROBLEM

decision region, succeeding detections are going to depend greatly on the first estimate. All detections will occur with about the same time error as the first.

The fact that decisions precede the estimation process leads to another basic difficulty with the problem formulation. The estimation procedure is accurate (neglecting now the readout error) if it is known with certainty that a signal is present. If the presence is not known, then a detection decision does two things; it eliminates some examples needed for an accurate estimate and, secondly, it allows false alarms to be accepted as signal examples.

As an example, consider that a linear filter is used for detection. A detection decision is made when

$$\sum_{m=1}^{N} v_m s_m^* > \Lambda \tag{39}$$

and at the same time a new estimate is made

$$\text{new} \quad s_m^* = v_m \quad .$$

Assuming a signal is present

$$v_m = s_m + n_m$$

$$\sum_{m=1}^{N} v_m s_m^* = \sum_{m=1}^{N} (s_m + n_m) s_m^* > \Lambda$$

$$\sum_{m=1}^{N} n_m s_m^* > \Lambda - \sum_{m=1}^{N} s_m s_m^* \quad . \tag{40}$$

Letting

$$x = \sum_{m=1}^{N} n_m s_m^* \quad ,$$

we have before detection

$$p(x) = \frac{1}{\sqrt{2\pi\sigma^2 \sum_{m=1}^{N} s_m^{*2}}} \exp\left[-\frac{x^2}{2\sigma^2 \sum_{m=1}^{N} s_m^{*2}}\right] \quad , \qquad (41)$$

and after detection

$$p_d(x) = \frac{\exp\left[-\frac{x^2}{2\sigma^2 \sum_{m=1}^{N} s_m^{*2}}\right]}{\int_{\Lambda - \sum_{m=1}^{N} s_m^* s_m}^{\infty} \exp\left[-\frac{x^2}{2\sigma^2 \sum_{m=1}^{N} s_m^{*2}}\right] dx}, \quad x > \Lambda - \sum_{m=1}^{N} s_m s_m^*$$

$$= 0 \qquad x < \Lambda - \sum_{m=1}^{N} s_m s_m^* \qquad (42)$$

But

$$\frac{1}{\sqrt{2\pi\sigma^2 \sum_{m=1}^{N} s_m^{*2}}} \int_{\Lambda - \sum_{m=1}^{N} s_m^* s_m}^{\infty} \exp\left[-\frac{x^2}{2\sigma^2 \sum_{m=1}^{N} s_m^{*2}}\right] dx = P_d(s) \qquad (43)$$

$P_d(s)$ = the probability of detecting S .

The expected value of x after detection

$$E\{x\} = \frac{1}{P_d(2\pi\sigma^2 \sum_{m=1}^{N} s_m^{*2})^{1/2}} \int_{\Lambda - \sum_{m=1}^{N} s_m s_m^*}^{\infty} x \exp\left[-\frac{x^2}{2\sigma^2 \sum_{1}^{N} s_m^{*2}}\right] dx$$

$$= \frac{1}{P_d}\left(\frac{\sigma^2 \sum_{1}^{N} s_m^{*2}}{2\pi}\right)^{1/2} \exp\left[-\frac{(\Lambda - \sum_{1}^{N} s_m s_m^*)^2}{2\sigma^2 \sum_{1}^{N} s_m^{*2}}\right] \quad . \qquad (44)$$

Equation (44) is the bias of $\sum_{1}^{N} n_m s_m^*$. Thus, after detection, the noise has a bias with a component in the direction of the old estimate. As $\sum_{1}^{N} s_m s_m^*$ increases, P_d increases, and the magnitude of the bias decreases. Therefore, at high values of signal-to-noise ratio the bias is unimportant. Two cases are shown graphically in Figure 14. Figure 14(a) shows the expected value of the estimate for a correct detection and Figure 14(b), for a false alarm.

The question now arises as to what effect the estimate bias has upon the operation of an adaptive filter. The expected value of the data (at correct time) is no longer the signal, but

$$E\{V\} = S + qS^* \quad . \qquad (45)$$

If estimates of equal value are desired, new data must be weighted more heavily than old data due to the occurrence of the bias term.

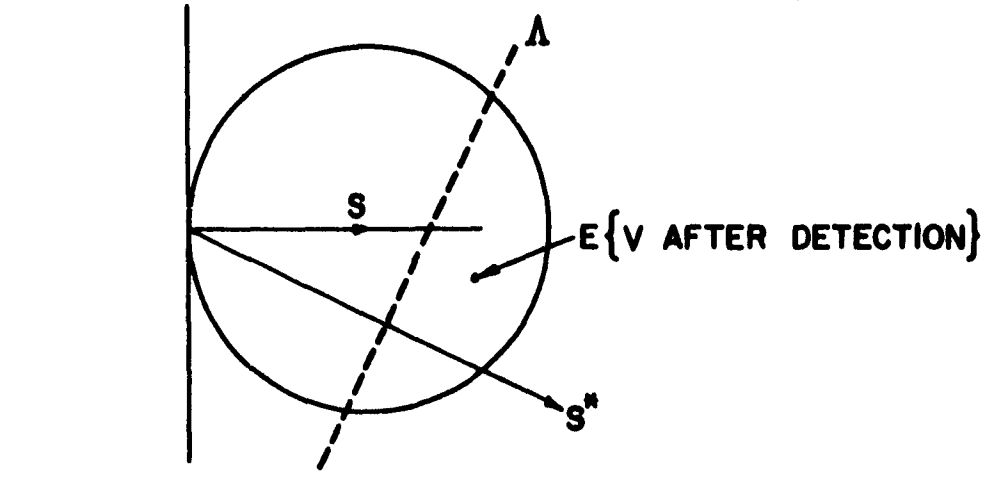

(a) BIAS IN TRUE SIGNAL DETECTION

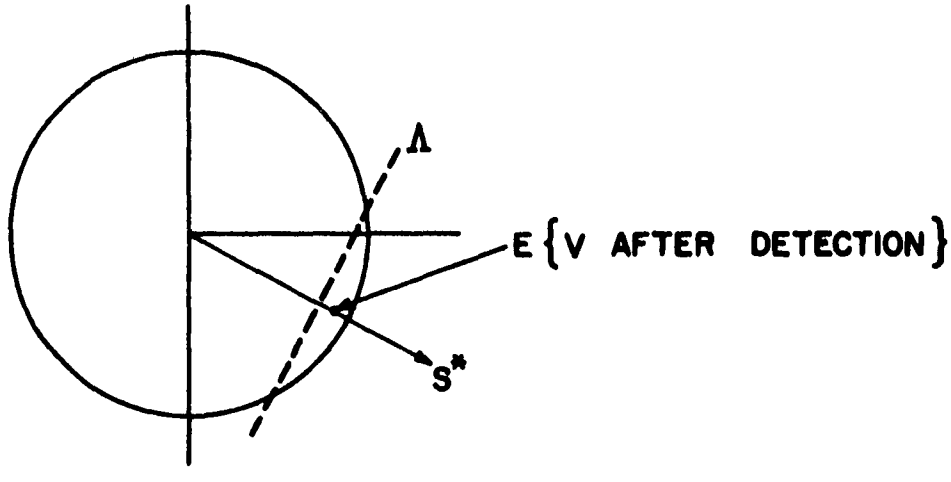

(b) BIAS IN FALSE ALARM DETECTION

FIGURE 14 GRAPHIC INTERPRETATION OF DETECTION BIAS

The argument against weighting new data more heavily is that it may be the result of a false detection. Notice that in the case of a false alarm, the bias actually has some merit. For a false alarm

$$E\{V\} = rS^* \tag{46}$$

and the new data do not affect the total estimate drastically. If the post-detection noise were truly random, the deterioration of filter estimate could be severe. Similarly, if another waveform were identified as S, the bias would make the decision less harmful to the estimate. On the other hand, true detections show less improvement. Overall, it appears that equal weighting of the data is still the best procedure.

The preceding discussion illustrates that the assumption of Gaussian estimate distribution is unrealistic at low signal-to-noise ratios. However, the results obtained appear useful. The use of more precise distributions W(S) does not appear feasible.

B. EXTENSION TO MULTIPLE SIGNALS

Some work has been done on separating partially known waveforms (9), but it is necessary to retreat one step and determine how the observer can obtain even partial knowledge of the second signal. The main difficulty in multiple signal detection arises from the fact that the detection process is not stationary as the equations imply. The problem may be illustrated by Figure 15.

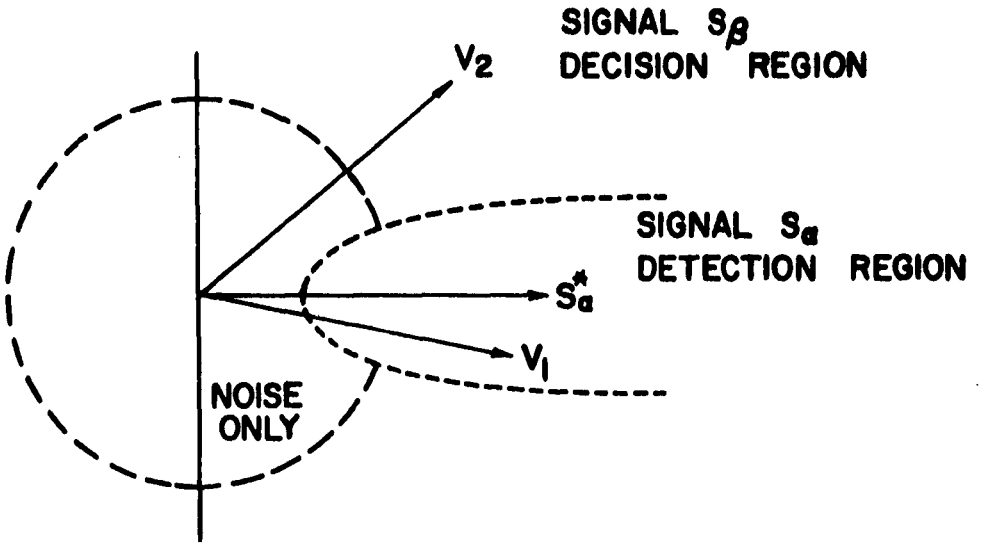

FIGURE 15 DIFFICULTIES IN INITIATING SECOND FILTER

Here, it is assumed that S_a has been detected and a decision region has been defined about the estimate. Any new waveform present in the input would be optimally detected by means of energy if it did not fall within the S_a region. Data vectors V_1 and V_2, which are slight time displacements of the same pulse, may be used to show that the problem is not stationary. The data may be an example of S_a in which case it would be detected properly at one time. At a slightly different time it would be detected as a new waveform. If the data were S_β, the same situation might arise. In other words, the observer might decide two waveforms were present when, in fact, only one was. If V_1 and V_2 both lie outside the S_a region, a new detection is unambiguous.

In view of the above discussion, a rather arbitrary criterion has been chosen for determining the presence of a second waveform (only two will be considered). The criterion is based upon the assumption that the S_α filter provides more information than the energy alone. Consequently, a new signal is detected if and only if there is no detection from the S_α filter during the interval that the energy threshold is exceeded. As a result, a new waveform will not be recognized if it is incorrectly detected by the first filter. After the first detection of S_β, the two filters operate independently.

It is of interest to examine graphically the expected operation of a number of filters in an environment of two waveforms. Figure 16 shows three basic configurations which will be studied experimentally. In each case, the filters are tuned to S_α and the effect of another waveform S_β is of interest. Generally, it would be expected that the parabolic filter would be affected least while the Case III filter would be affected most by the presence of S_β. Both the linear filter and the Case III filter may exhibit a tendency to switch to S_β if the rate of occurrence of S_β is high. In the absence of S_β, however, they should be superior to the parabolic filter. These intuitive results will be verified by the experiments.

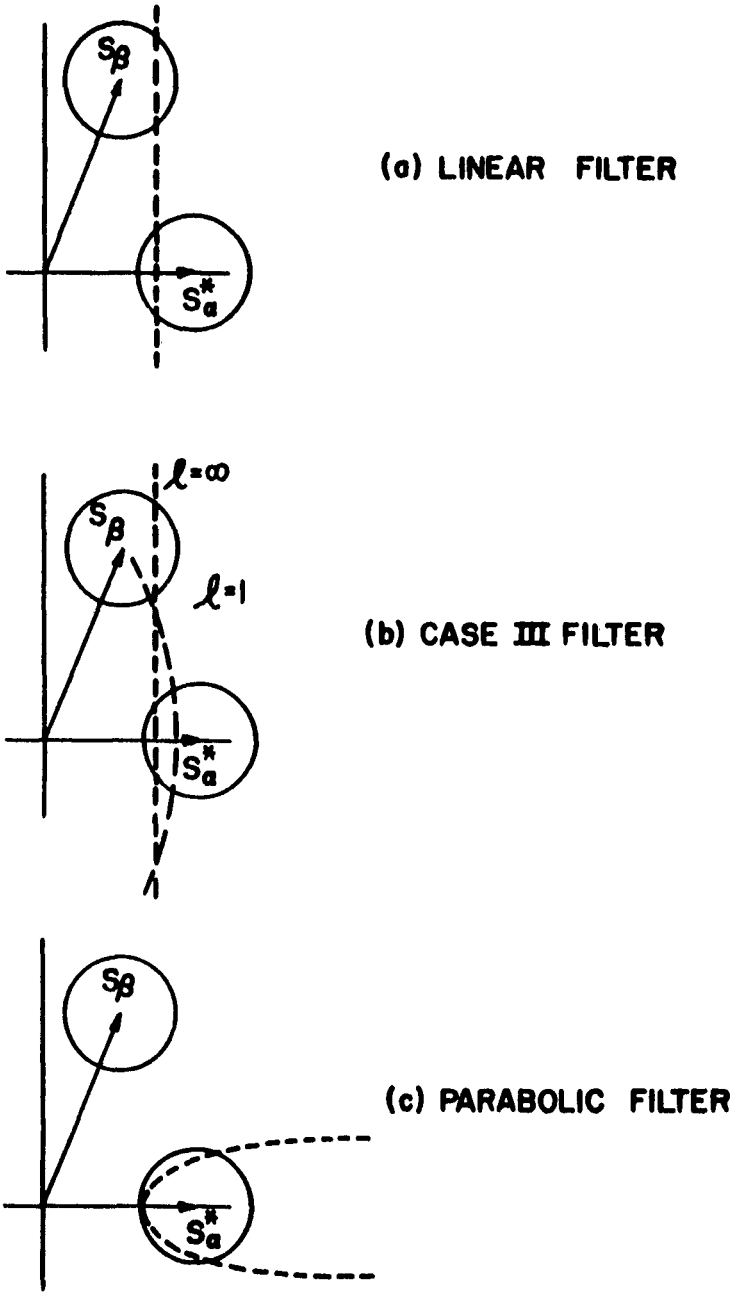

FIGURE 16 COMPARISON OF BASIC STRUCTURES

IV. NUMERICAL ANALYSIS OF SOME ADAPTIVE FILTERS

The present section will attempt to assess the operation of some adaptive filters in numerical terms. The discussion is limited to high dimensional signals and to two of the filters previously described. Similar treatment of the conic section filter is quite difficult and is not included. The section is included for three reasons:

1. It demonstrates the expected operation for N large (cases which will not be studied experimentally).
2. It demonstrates parameter effects which are expected to hold for low values of N, thus providing a guide for examining the experimental results.
3. It includes derivations of some of the parameter values used in the experiments.

The analysis is based upon the ideal assumptions of Section II. It should also be noted that the probability of detection calculations are carried out only at the correct readout time. There is also the possibility of detecting the pulse at a slightly different time while missing it at the correct time. Thus, true detection probabilities are somewhat higher than those given.

The initial step of the filter procedure is the detection of the first signal. Under the conditions of Section I, the threshold must be determined on the basis of allowable false alarm rate α. The

dimension of the filter, N, must be chosen on the basis of some intuitive judgment. Once N is selected, the threshold is chosen by assuming that

$$\sum_{m=1}^{N} v_m^2 = \sum_{m=1}^{N} (s_m + n_m)^2$$

has a Gaussian distribution. For $N > 100$ the assumption is fairly accurate (10). All n_m are independent with a mean of zero and a variance σ^2. In all calculations to follow $\sum_{m=1}^{N}$ will be written as Σ

$$E\left\{\Sigma v_m^2\right\} = \Sigma s_m^2 + N\sigma^2 \tag{47}$$

$$\text{Var}\left\{\Sigma v_m^2\right\} = 4\sigma^2 \Sigma s_m^2 + 2N\sigma^4 \quad . \tag{48}$$

Then, the probability of a false alarm is

$$\alpha = \frac{1}{\sqrt{4\pi N\sigma^4}} \int_{\Lambda}^{\infty} \exp\left[-\frac{(x - N\sigma^2)^2}{4N\sigma^4}\right] dx$$

$$= \frac{1}{\sqrt{\pi}} \int_{\frac{\Lambda - N\sigma^2}{\sqrt{4N\sigma^4}} = A}^{\infty} \exp\left[-y^2\right] dy \quad . \tag{49}$$

The observer can determine the value of A which yields the desired false alarm rate α.

The threshold Λ becomes

$$\Lambda = 2\sigma^2 A \sqrt{N} + N\sigma^2 \tag{50}$$

which depends upon σ^2, a known value, and upon A and N, chosen values.

With the threshold chosen, the probability of detection becomes

$$P_d = \frac{1}{\sqrt{2\pi(4\sigma^2 \Sigma s_m^2 + 2N\sigma^4)}} \int_{\Lambda}^{\infty} \exp\left[-\frac{\left\{x - (\Sigma s_m^2 + N\sigma^2)\right\}^2}{(8\sigma^2 \Sigma s_m^2 + 4N\sigma^4)}\right] dx$$

$$= \frac{1}{\sqrt{\pi}} \int_{\frac{A2\sigma^2\sqrt{N} - \Sigma s_m^2}{\sqrt{8\sigma^2 \Sigma s_m^2 + 4N\sigma^4}}}^{\infty} \exp\left[-y^2\right] dy \quad . \tag{51}$$

Now, the signal-to-noise ratio R is defined as the signal energy divided by the noise power per cycle ($-W < f < W$) or

$$R = \frac{\int_0^T s^2(t)\, dt}{\sigma^2/2W} \tag{52}$$

or in terms of sample values

$$R = \frac{\Sigma s_m^2 \Delta t}{\sigma^2/2W}$$

where $\Delta t = 1/2W$ is the sample interval

$$R = \frac{\Sigma s_m^2}{\sigma^2} \quad . \tag{53}$$

Equation (51) becomes

$$P_d = \frac{1}{\sqrt{\pi}} \int_{\frac{A\sqrt{N}-R/2}{\sqrt{2R+N}}}^{\infty} \exp\left[-y^2\right] dy \quad . \tag{54}$$

Equation (54) illustrates the obvious result that an increase in R produces an increase in the probability of detection. For a fixed R, an increase in N lowers the value of P_d. Figure 17 demonstrates the effect of N on the detection probability. The implications of Figure 17 are several:

1. For the same energy, high dimensional waveforms are more difficult to detect (by energy means) than low
2. A poor choice of N (N >> signal dimension) may reduce severely the observer's chances of detecting the waveform
3. If more were known about the signal class (for example, signal bandwidth less than noise bandwidth), better results could be obtained with fewer measurements.

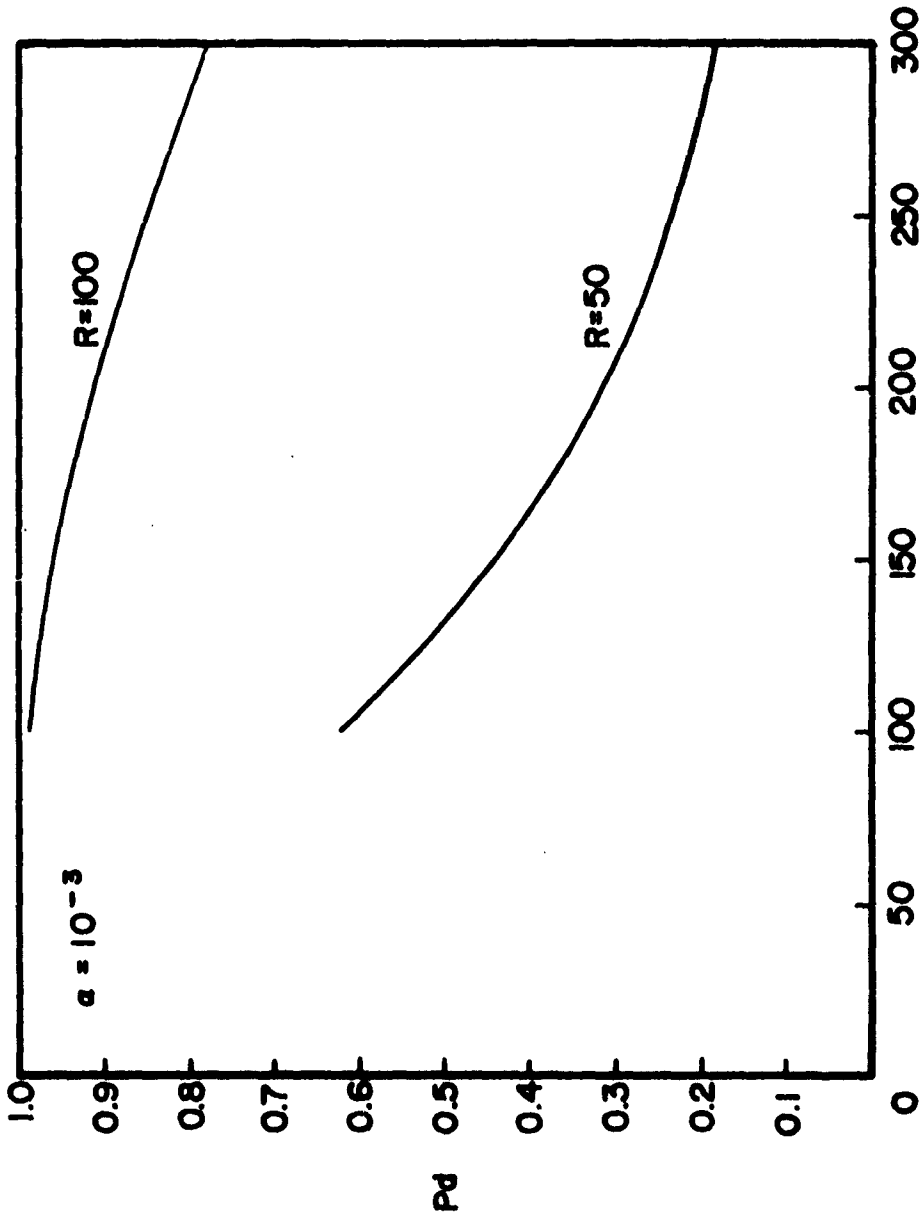

FIGURE 17 PROBABILITY OF DETECTION OF FIRST SIGNAL BY ENERGY

Another technique for determining the presence of a waveform has been proposed (3). It is based upon the correlation of the input and a random waveform exceeding a threshold. A threshold may be chosen by assuming

$$\Sigma M_m v_m = \Sigma M_m (s_m + n_m)$$

has a Gaussian distribution which again only holds for N large (12). M_m is a Gaussian random variable of zero mean and variance k^2.

$$E\left\{\Sigma M_m v_m\right\} = 0 \tag{55}$$

$$\text{Var}\left\{\Sigma M_m v_m\right\} = N\sigma^2 k^2 + k^2 \Sigma s_m^2 \quad . \tag{56}$$

The probability of a false alarm is

$$\alpha = \frac{1}{\sqrt{2\pi N\sigma^2 k^2}} \int_{\Lambda}^{\infty} \exp\left[-\frac{x^2}{2N\sigma^2 k^2}\right] dx$$

$$= \frac{1}{\sqrt{\pi}} \int_{\frac{\Lambda}{\sqrt{2N\sigma^2 k^2}}}^{\infty} \exp\left[-y^2\right] dy \tag{57}$$

and the probability of detection is

$$P_d = \frac{1}{\sqrt{2\pi(N\sigma^2k^2 + k^2\Sigma s_m^2)}} \int_{\Lambda}^{\infty} \exp \frac{-x^2}{2(N\sigma^2k^2+k^2\Sigma s_m^2)}\, dx$$

$$= \frac{1}{\sqrt{\pi}} \int_{\frac{A}{\sqrt{1+R/N}}}^{\infty} \exp\left[-y^2\right] dy \quad . \tag{58}$$

Figure 18 illustrates the characteristics of the correlation detection. A comparison of Figures 17 and 18 clearly demonstrates the superiority of the energy detection. In use, however, much higher values of α are used until a signal is found. In other words, false alarms are not considered a problem until a reasonable waveform estimate is obtained. The correlation approach also eliminates the need of much squaring circuitry.

Each of the above approaches chooses the readout time at the peak of the filter output. The peak corresponds to the maximum likelihood ratio for the detection decision. At the readout time, the first estimates are recorded.

Once the first estimate has been made, the general filter to be studied in this section takes the form

$$c(\ell)\, \Sigma\, v_m^2 + b_1(\ell)\, \Sigma\, v_m s_m^* = F(\ell) \tag{59}$$

$$v_m = s_m + n_m \quad , \qquad s_m^* = e_m + k_m$$

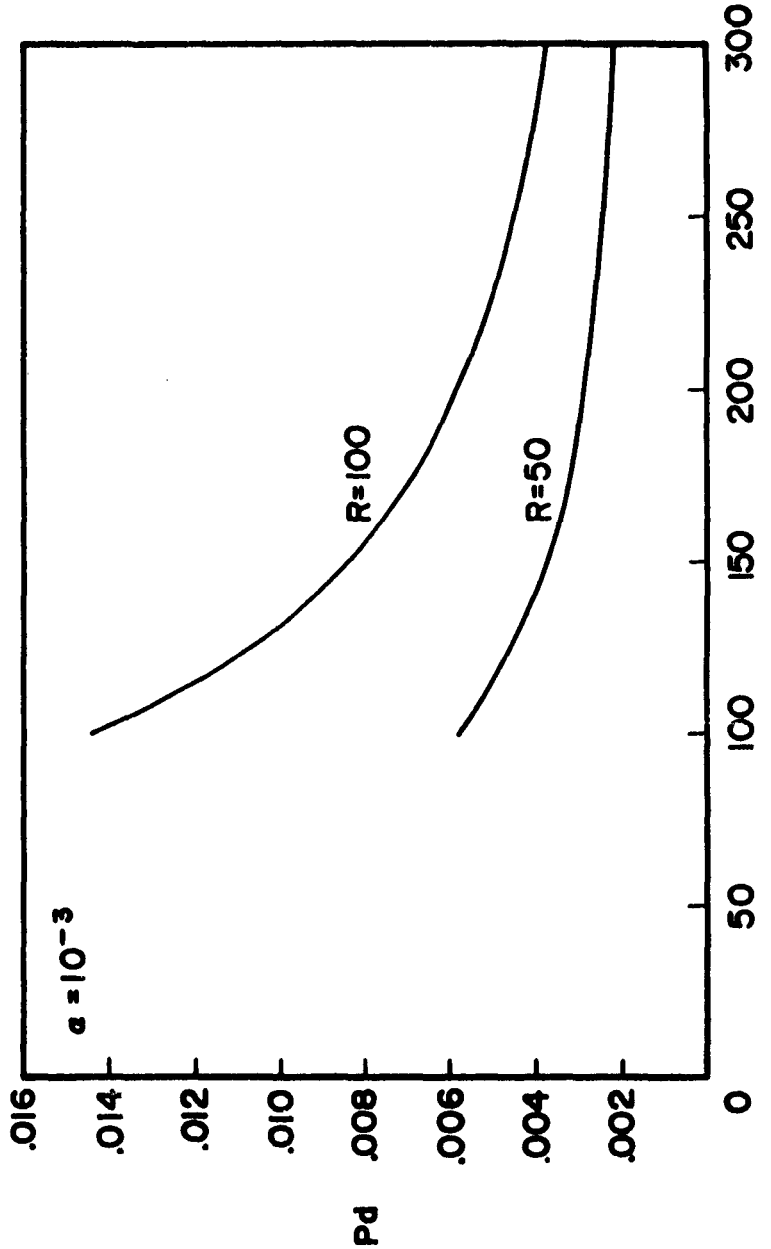

FIGURE 18 PROBABILITY OF DETECTION OF FIRST SIGNAL BY NOISE CORRELATION

where n_m and k_m are independent random variables of zero mean and variance σ^2 and k^2 respectively. Again, assuming N large, $F(\ell)$ approximates a Gaussian distribution (10), (12).

$$E\left\{F(\ell)\right\} = c(\Sigma s_m^2 + N\sigma^2) + b_1 \Sigma s_m e_m \tag{60}$$

$$\mathrm{Var}\left\{F(\ell)\right\} = c^2(4\sigma^2 \Sigma s_m^2 + 2N\sigma^4) + b_1 c\, 4\sigma^2 \Sigma s_m e_m$$

$$+ b_1^2(\sigma^2 \Sigma e_m^2 + k^2 \Sigma s_m^2 + N\sigma^2 k^2) \quad . \tag{61}$$

The probability of false alarm is

$$\alpha = \frac{1}{\sqrt{2\pi\left\{c^2 2N\sigma^4 + b_1^2(\sigma^2 \Sigma e_m^2 + N\sigma^2 k^2)\right\}}}$$

$$\int_{\Lambda}^{\infty} \exp\left[\frac{-(x - cN\sigma^4)}{2\left\{c^2 2N\sigma^4 + b_1^2(\sigma^2 \Sigma e_m^2 + N\sigma^2 k^2)\right\}}\right] dx$$

$$= \frac{1}{\sqrt{\pi}} \int_{A=\frac{\Lambda - cN\sigma^2}{\sqrt{2\left\{c^2 2N\sigma^4 + b_1^2(\sigma^2 \Sigma e_m^2 + N\sigma^2 k^2)\right\}}}}^{\infty} \exp\left[-y^2\right] dy \tag{62}$$

and the probability of detection is

$$P_d=\frac{1}{\sqrt{\pi}}\int_{\frac{A\sqrt{2\left[c^2 2N\sigma^4+b_1^2(\sigma^2\Sigma e_m^2+N\sigma^2k^2)\right]}-c\Sigma s_m^2-b_1\Sigma s_m e_m}{\sqrt{2\left[c^2(4\sigma^2\Sigma s_m^2+2N\sigma^4)+4b_1c\sigma^2\Sigma s_m e_m+b_1^2(\sigma^2\Sigma e_m^2+k^2\Sigma s_m^2+N\sigma^2k^2)\right]}}}^{\infty}\exp\left[-y^2\right]dy \tag{63}$$

There are now two situations which are of interest and can be examined by means of Equation (63). The first is the linear adaptive filter in which $c = 0$ and $b_1 = 1$. Then

$$P_d=\frac{1}{\sqrt{\pi}}\int_{\frac{A\sqrt{2(\sigma^2\Sigma e_m^2+N\sigma^2k^2)}-\Sigma s_m e_m}{\sqrt{2(\sigma^2\Sigma e_m^2+N\sigma^2k^2+k^2\Sigma s_m^2)}}}^{\infty}\exp\left[-y^2\right]dy \quad . \tag{64}$$

If the estimate mean is the signal, $s_m = e_m$, and $k^2 = \sigma^2/\ell$

$$P_d = \frac{1}{\sqrt{\pi}}\int_{\frac{A\sqrt{N+R\ell}-R\sqrt{\ell/2}}{\sqrt{N+R(\ell+1)}}}^{\infty}\exp\left[-y^2\right]dy \tag{65}$$

Turning now to the Case III filter and letting $c = 1$ and $b_1 = 2\ell$

$$P_d=\frac{1}{\sqrt{\pi}}\int_{\frac{A\sqrt{4N\sigma^2+8\ell^2(\sigma^2\Sigma e_m^2+N\sigma^2k^2)}-\Sigma s_m^2-2\ell\Sigma s_m e_m}{\sqrt{2(4\sigma^2\Sigma s_m^2+2N\sigma^2+8\ell\sigma^2\Sigma s_m e_m+4\ell^2\left[\sigma^2\Sigma e_m^2+k^2\Sigma s_m^2+N\sigma^2k^2\right])}}}^{\infty}\exp\left[-y^2\right]dy \tag{66}$$

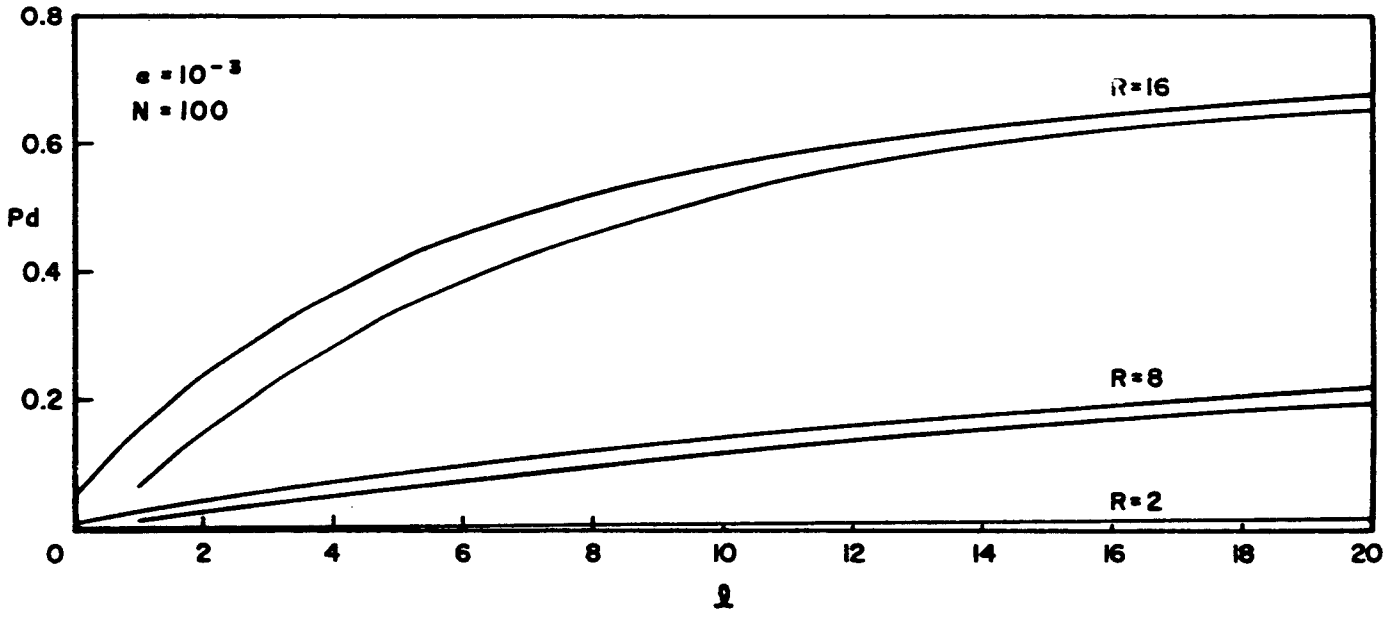

FIGURE 19 PROBABILITY OF DETECTION FOR ADAPTIVE FILTERS (TOP CURVES - CASE III FILTER, BOTTOM CURVES - LINEAR FILTER)

Figure 20 shows the probability of detecting the second waveform as a function of ℓ and the correlation between the signals. The curves are plotted under the assumption that the expected value of the estimate is S_a. The optimum filter, Case III, is the best at detecting S_a, but, unfortunately, it is also the one which is most likely to incorrectly identify other pulses. If the new waveform had a larger energy, there would be an even greater probability of incorrect identification.

The previous discussion was concerned with the performance of filters on the average. Here, it is of interest to examine the filters in terms of the measurable quantities $\{s_m^*\}$. In the following discussion s_m^* is a constant between detections.

$$F(\ell) = c(\ell) \Sigma v_m^2 + b_1(\ell) \Sigma v_m s_m^* \quad . \tag{59}$$

Again $F(\ell)$ is assumed to be a Gaussian distribution for N large.

$$E\{F\} = c(\Sigma s_m^2 + N\sigma^2) + b_1 \Sigma s_m s_m^* \tag{69}$$

$$Var\{F\} = c^2(4\sigma^2 \Sigma s_m^2 + 2N\sigma^4) + 4b_1 c \Sigma s_m s_m^* + b_1^2 \sigma^2 \Sigma s_m^{*2} . \tag{70}$$

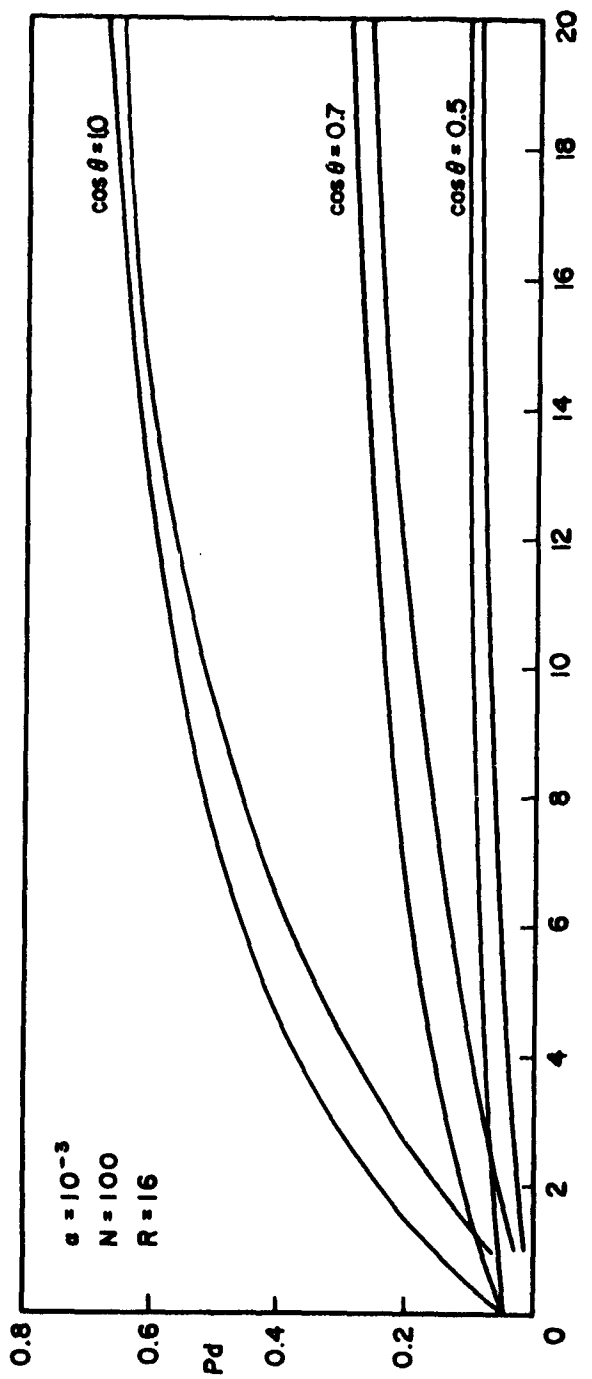

FIGURE 20 PROBABILITY OF DETECTION OF OTHER SIGNALS BY ADAPTIVE FILTERS (TOP CURVES - CASE III FILTER, BOTTOM CURVES - LINEAR FILTER)

The probability of false alarm is

$$\alpha = \frac{1}{\sqrt{2\pi(c^2 2N\sigma^4 + b_1^2\sigma^2 \Sigma s^{*2})}} \int_{\Lambda}^{\infty} \exp\left[\frac{-(x - cN\sigma^2)^2}{2(c^2 2N\sigma^4 + b_1^2\sigma^2 \Sigma s^{*2})}\right] dx$$

$$= \frac{1}{\sqrt{\pi}} \int_{\frac{\Lambda - cN\sigma^2}{\sqrt{4c^2 N\sigma^4 + 2b_1^2\sigma^2 \Sigma s^{*2}}}}^{\infty} \exp\left[-y^2\right] dy \qquad (71)$$

$$\Lambda = A \sqrt{2(c^2 2N\sigma^4 + b_1^2\sigma^2 \Sigma s_m^{*2})} + cN\sigma^2 \quad . \qquad (72)$$

Equation (72) provides a means of calculating threshold setting in terms of arbitrarily chosen constants A, N, b_1, c, a known constant σ^2, and the measured value Σs_m^{*2}.

For $c = 0$ $\qquad b_1 = 1$

$$\Lambda = A \sqrt{2\sigma^2 \Sigma s_m^{*2}} \qquad (73)$$

For $c = 1$ $\qquad b_1 = 2\ell$

$$\Lambda = A \sqrt{4N\sigma^4 + 8\sigma^2 \ell^2 \Sigma s_m^{*2}} + N\sigma^2 \quad . \qquad (74)$$

The ℓ term in Equation (74) represents the number of past detections. The above choice of ℓ is predicated upon perfect operation of the filter. Therefore, any error of commission on the part of the filter will result in an incorrect threshold level and a deterioration of the optimum performance will result. The probability of detection becomes

$$P_d = \frac{1}{\sqrt{\pi}} \int_{\frac{A\sqrt{2(c^2 2N\sigma^4 + b_1^2\sigma^2\Sigma s_m^{*2}) - c\Sigma s_m^2 - b_1\Sigma s_m s_m^*}}{\sqrt{2\left[c^2(4\sigma^2\Sigma s_m^2 + 2N\sigma^4) + 4b_1 c\Sigma s_m s_m^* + b_1^2\sigma^2\Sigma s_m^{*2}\right]}}}^{\infty} \exp\left[-y^2\right] dy \quad . \tag{75}$$

Equation (75) illustrates that for fixed waveforms and estimate (between detections), the important factor in determining P_d is

$$\Sigma s_m s_m^* = \sqrt{\Sigma s_m^2}\ \sqrt{\Sigma s_m^{*2}}\ \cos\theta \quad .$$

The significance of the $\cos\theta$ term makes it a good measure of quality for the filter.

For c = 0, Equation (75) is exact for any value of N. In this case the probability of detection is

$$P_d = \frac{1}{\sqrt{\pi}} \int_{A - \frac{\Sigma s_m s_m^*}{\sqrt{2\sigma^2 \Sigma s_m^{*2}}}}^{\infty} \exp\left[-y^2\right] dy$$

$$= \frac{1}{\sqrt{\pi}} \int_{A - \sqrt{\frac{R}{2}} \cos\theta}^{\infty} \exp\left[-y^2\right] dy \qquad (76)$$

Thus, for the linear filter, P_d depends only upon R and the correlation measure, cos θ. Curves of P_d versus cos θ for various values of R are given in Figure 21.

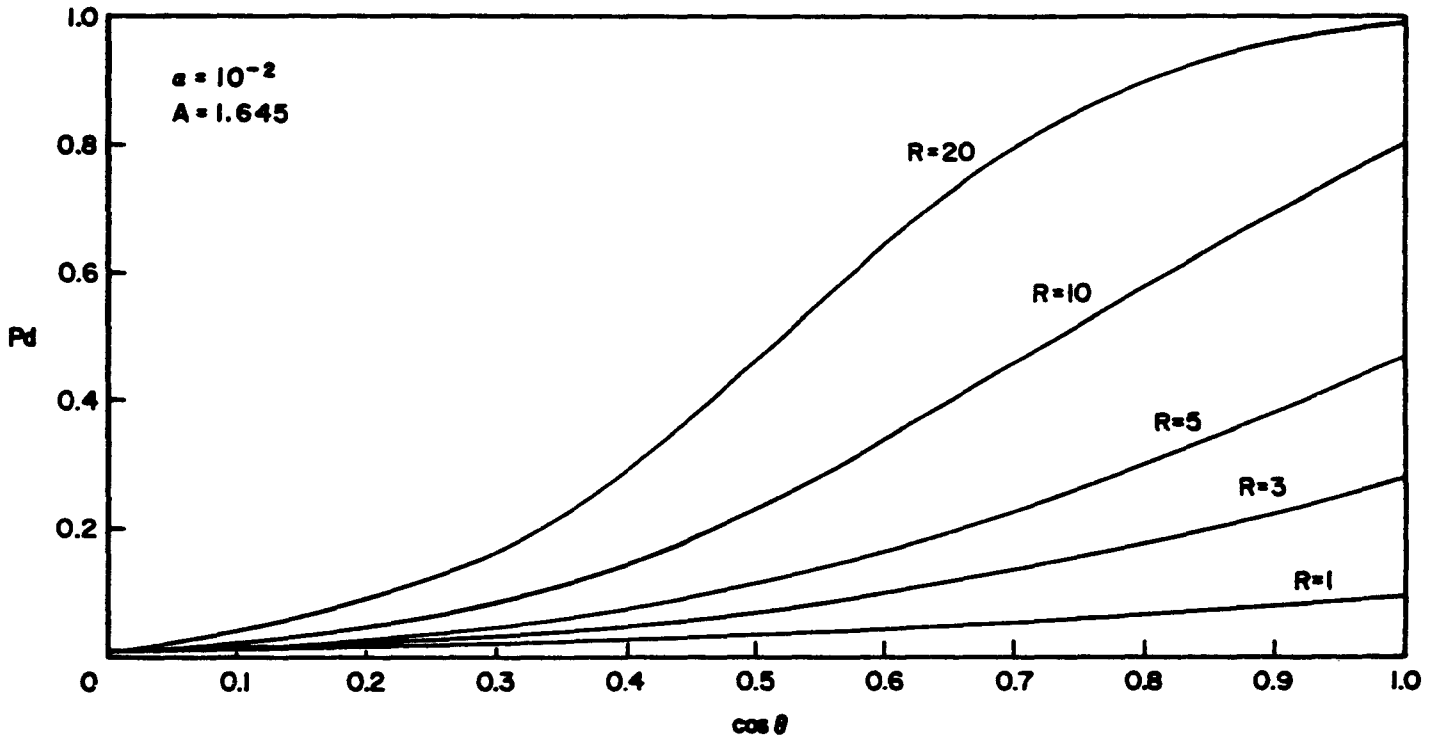

FIGURE 21 P_d VERSUS CORRELATION WITH ESTIMATE - LINEAR FILTER

V. EXPERIMENTAL RESULTS

The main purpose of the paper is the experimental study of the use of adaptive filters for examining unknown data. To this end, an extensive analog and digital computer investigation was undertaken to determine the characteristics and limitations of several systems. Prelminary tests were made with analog equipment to obtain qualitative indications of performance. The large amount of equipment involved and the approximations necessary, limit the usefulness of the analog results. Consequently, they contribute little quantitative insight into the filter operation. All data presented here are the result of the digital computer simulation.

For purposes of simplicity and time saving, the computer performed all operations including the generation of the waveforms and noise. For the most part, the experiments were performed with two waveforms S_α and S_β present. Figure 22 illustrates the two waveforms which have slightly different lengths. The waveform lengths were selected to be close to the filter length which was chosen to be $N = 10$. To illustrate the effect of a poor choice of N, a few trials were made with other waveforms of varying dimensions which are also illustrated in Figure 22. The waveforms used were invariant in shape, throughout the trials, corresponding to the sampling of analog data with a sampling frequency which is synchronized with the repetition rate. Appendix B provides some results for true samplings of analog data. Another simulation has been

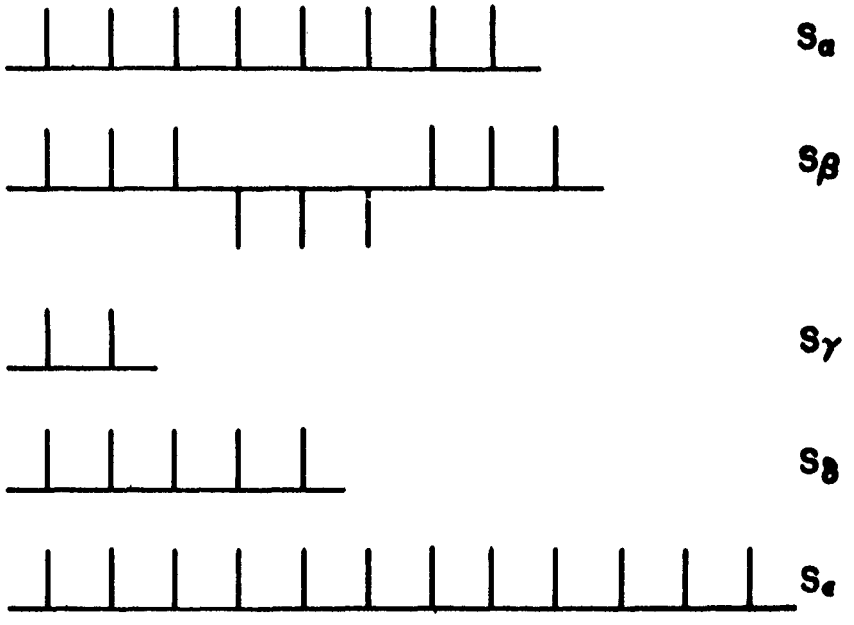

FIGURE 22 SIGNALS USED IN EXPERIMENTS

carried out on one type of filter (8) in which the results from sampled analog data were quite similar to those from computer generated samples. The amplitudes of the waveforms were usually chosen to provide signal-to-noise ratios of 5, 10, and 20. The noise samples are numbers from a computer table of random numbers. The table approximates a Gaussian distribution and the samples are independent with zero mean and unit variance. An example of the data processed by the computer is given in Figure 23. Although the data are really represented by sample points, lines have been drawn between the points for clarity.

The waveforms occurred with fixed intervals for convenience. In general, S_α occurred every 50 intervals, S_β every 100 intervals. Most trials were limited to an examination of 1000 sample points although a few had a duration of 1500 or 2000 intervals.

At each sample point p the computer was programmed to calculate $F_p(\ell)$.

$$F_p(\ell) = a(\ell)\left[\frac{\sum_{m=1}^{10} v_{p+m-10} s_m^*}{\sqrt{\sum_{m=1}^{10} s_m^{*2}}}\right]^2 + b(\ell)\frac{\sum_{m=1}^{10} v_{p+m-10} s_m^*}{\sqrt{\sum_{m=1}^{10} s_m^{*2}}} + c(\ell)\sum_{m=1}^{10} v_{p+m-10}^2 \qquad (77)$$

where ℓ is again the number of past detections. In other words, at every point, the last 10 data samples form the vector which is examined. The processing is analogous to using a tapped delay line.

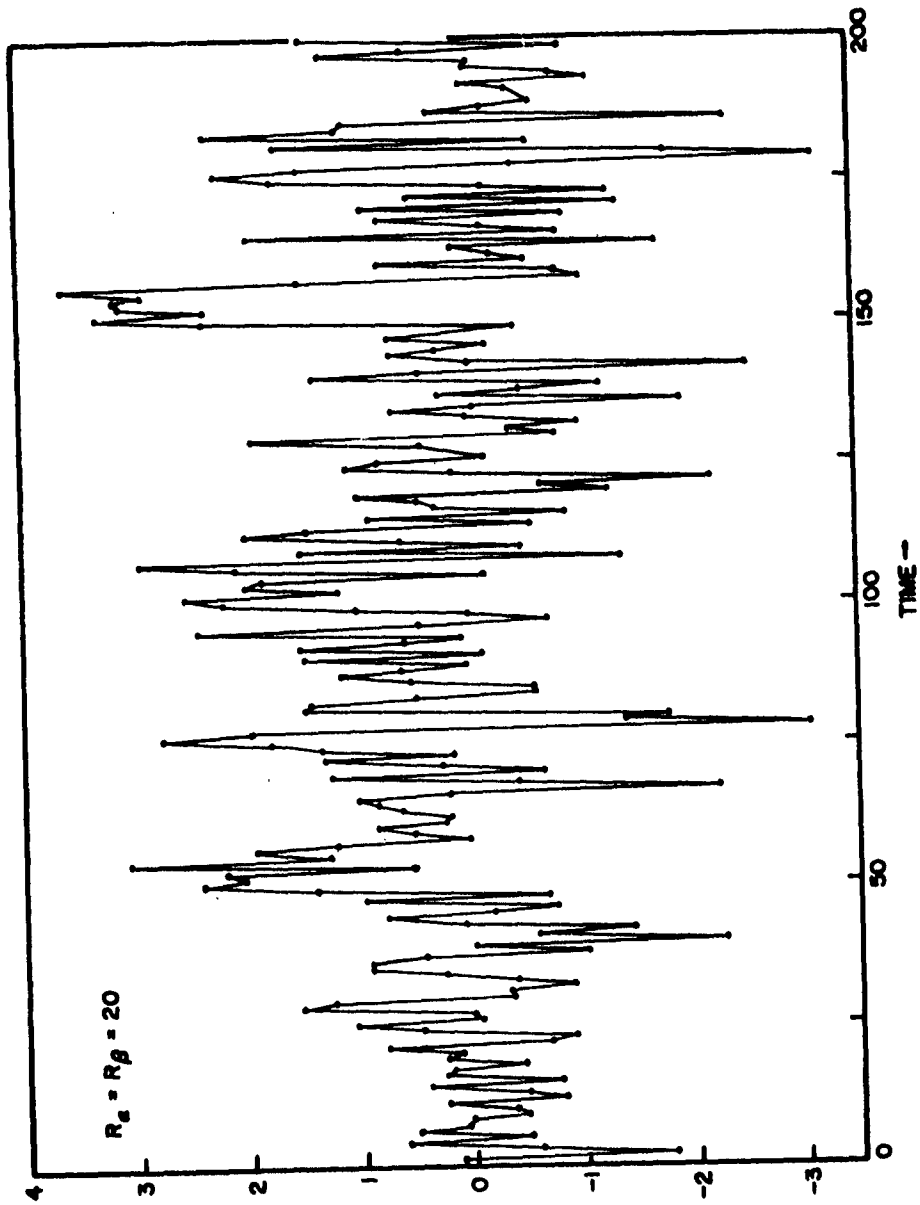

FIGURE 23 SAMPLE OF INPUT DATA CONTAINING TWO DIFFERENT WAVEFORMS

The normalized estimates of Equation (27) are made explicit in Equation (77). The number F_p is compared with a threshold and, if it is below the threshold, F_{p+1} is calculated. At some time the point p' will be reached where

$$F_{p'} > \Lambda \qquad \text{and} \qquad F_{p'-1} < \Lambda \quad . \tag{78}$$

Then, the computer goes to a subroutine which sequentially examines the interval $p' \leq p \leq p' + 12$. At time p' the data values $\{v_{p'}, v_{p'-1}, \cdots v_{p'-9}\}$ are stored. Each successive F_p is calculated until

$$F_{p'+j} > F_{p'} \qquad j \leq 12 \quad . \tag{79}$$

If this occurs, the memory is replaced by $\{v_{p'+j}, v_{p'+j-1}, \cdots v_{p'+j-9}\}$. If another value occurs,

$$F_{p'+j+i} > F_{p'+j} \qquad j + i \leq 12 \tag{80}$$

the memory is again replaced by the appropriate data. At the end of the twelfth interval, the time of the largest F_p is recorded, ℓ is increased by one, and the data $\{v_p, v_{p-1} \cdots v_{p-9}\}$ are added to the old unnormalized estimate $\{s^*_{10}, s^*_9, \cdots s^*_1\}$. At p'+13 the computer returns to the routine of determining F_p and comparing it with the threshold. The interval of twelve was chosen to prevent more than one detection of any pulse. At each time of detection, the data and the new estimates are printed out.

In the case of parallel systems and $F_{p\alpha}$ and an $F_{p\beta}$ are calculated using S_α^*, ℓ_α, and S_β^*, ℓ_β, respectively. In other words, each system uses the basic equation with different estimates and, in general, with different numbers of past detections. The one new feature arises in determining the first detection and estimate of S_β. The problem was discussed in Section III-B. The solution used here involves calculation $F_{p\alpha}$ and $\sum_{m=1}^{10} v_{p+m-10}^2$ at each point after an initial detection of S_α. At a time when

$$\left.\begin{aligned} &\sum_{m=1}^{10} v_{p''+m-10}^2 > \Lambda \\ &\sum_{m=1}^{10} v_{p''-1+m-10}^2 < \Lambda \end{aligned}\right\} \qquad (81)$$

and

$$F_{p''\alpha} < \Lambda_\alpha$$

The computer goes to another subroutine which sequentially examines the interval $p'' \le p \le p'' + 16$. If, at any time during this interval,

$$F_{p'\alpha} > \Lambda_\alpha \qquad (82)$$

the computer returns to the main routine. If, however, at each point of the interval

$$F_{p\alpha} < \Lambda_\alpha \quad , \qquad (83)$$

the energy peak is determined and the data at that time are used as the first estimate of S_β. The computer then returns to the main routine and calculates $F_{p\alpha}$ and $F_{p\beta}$.

The general form of Equation (77) allows all filters previously discussed to be studied by a change of coefficients. It was convenient, because of the time involved in compiling the program and data, to process the same data with several filters. Use of the same input is also helpful in comparing the systems. A subroutine was, therefore, employed to change the parameters after each pass through the data.

Some of the parameter values are obtained from previous equations, some are the result of guesses based on early analog and digital work. The basic structures which will be examined are:

1. Case II filter ($\ell = 0$, a = 0, b = 0, c = 1)

   All systems to be studied have this structure for $\ell = 0$. The approximate value of the threshold (N large) is

$$\Lambda_{II} \cong \sigma^2(2A\sqrt{N} + N) \quad . \tag{50}$$

   Choosing a false alarm rate $\alpha = 10^{-2}$ leads to A = 1.645.

$$\Lambda_{II} \cong 20.5 \quad . \tag{84}$$

   Equation (84) is approximate, but Turner (6) supplies a table with the true threshold which will be used in the experiments

$$\Lambda_{II} = 23.2 \quad . \tag{85}$$

2. Linear filter ($\ell \geq 1$, a = 0, b = 1, c = 0)

Detection is now based upon

$$\frac{\sum_{m=1}^{N} v_m s_m^*}{\sqrt{\sum_{m=1}^{N} s_m^{*2}}} > \Lambda_L \qquad (86)$$

or

$$\sum_{m=1}^{N} v_m s_m^* > \Lambda_L \sqrt{\sum_{m=1}^{N} s_m^{*2}} = \Lambda \ . \qquad (87)$$

From Equation (73)

$$\Lambda = A\sqrt{2\sigma^2 \sum_{m=1}^{N} s_m^{*2}} \ , \qquad (73)$$

or

$$\Lambda_L = A\sqrt{2\sigma^2} \ . \qquad (88)$$

Choosing

$$\alpha = 10^{-2}$$

gives

$$\Lambda_L = 2.33 \ . \qquad (89)$$

3. Case III filter ($\ell \geq 1$, a = 0, $b = 2\sqrt{\sum_{m=1}^{N} s_m^{*2}}$, c = 1)

Detection is based upon

$$\sum_{m=1}^{N} v_m^2 + 2 \sum_{m=1}^{N} v_m s_m^* > \Lambda_{III} \ . \qquad (90)$$

The filter takes the form of Equation (90) because the estimate in the computer simulation is merely the unnormalized sum of the past data. In other words, assuming perfect detections

$$E\left\{S_a^*\right\} = \ell S_a \quad . \tag{91}$$

From Equation (72)

$$\Lambda_{III} = A\sqrt{4N\sigma^4 + 8\sigma^2 \sum_{m=1}^{N} s_m^{*2}} + N\sigma^2$$

$$= 1.65\sqrt{40 + 8 \sum_{m=1}^{N} s_m^{*2}} + 10 \quad . \tag{92}$$

4. Parabolic filter ($\ell \geq 1$, b = 1, a = -c)

Of the conic sections, only the parabolic form was chosen for study. With no analysis of the filter, it was necessary to make intuitive judgments about the parameter value. Generally, it can be said that the larger the value of a, the narrower the decision region. Tests were made with wide, narrow, and variable width regions. In some cases, the threshold was chosen as a constant at the same level as that for the linear filter. In other situations, the threshold was reduced slightly as a function of ℓ. It was thus insured that α would be no greater than 10^{-2}.

Table I describes the parameter rules governing the six filters examined.

TABLE I

Description of Filters Examined

System	ℓ	a	b	c	Λ
1-6	0	0	0	1	23.2
1	≥1	0	1	0	2.33
2	≥1	0	$2\sqrt{\sum_{m=1}^{N} s_m^{*2}}$	1	$1.65\sqrt{40+8\sum_{m=1}^{N} s_m^{*2}}+10$
3	≥1	1/23	1	-1/23	2.33
4	≥1	1/8	1	-1/8	2.33
5	≥1	1/23	1	-1/23	$2+\frac{.33}{\ell}$
6	≥1	$(3\ell+40)10^{-3}$	1	$-(3\ell+40)10^{-3}$	$2+\frac{.33}{\ell}$

The value of a was purposely chosen to be high since the effect of false alarms on future operation has been largely ignored. By electing to observe numerous false detections, the effects can be better assessed. It should be stated here that a detection was identified as false only if all samples $\{v_p, \ldots v_{p-9}\}$ represented noise alone. Thus, if the output of the filter was, in any way, due to the presence of a signal (even one sample of signal), it was called a detection of that waveform.

The experimental results are presented in three basic forms:

1. Tables of errors and correct decisions

   The number of false alarms, correct detections, incorrect identifications (identifying S_β as S_α), and missed signals provide the gross results of a trial. Correct detections are those signals corresponding to the first signal detected.

2. Plots of estimate quality versus time of detection

   The plots represent the peak of the cross correlation of the signal with the estimate, in other words, the largest

$$r_j = \frac{\sum_{m=1}^{N} s_{m+j} s_m^*}{\sqrt{\left(\sum_{m=1}^{N} s_m^2\right)\left(\sum_{m=1}^{N} s_m^{*2}\right)}} .$$

   The correlation was seen to be a good measure of the estimate quality. These figures provide a good indication of the effects of false alarms and incorrect identifications.

3. Illustration of the estimate as a function of t

   The figures are plotted to correspond to the impulse response of a filter matched to S^*. In other words, they represent the time inverse of the signal estimate.

The experiments themselves were designed to demonstrate the tendencies and limits of the filters under a wide variety of circumstances. On the basis of preliminary tests, it was felt that filter operation deteriorated rapidly for signal-to-noise ratios below 5. The operating characteristics were determined at the preassigned limit (R = 5) by making 48 trials with each system. Each run contained 19 examples of S_α (R_α = 5) and 10 examples of S_β (R_β = 5). Table II gives one picture of the results.

TABLE II

Result of 48 Trials ($R_\alpha = R_\beta = 5$)

System	1	2	3	4	5	6
False Alarms	156	159	66	30	122	106
Correct Detections	285	310	190	75	238	207
Missed Signals	319	294	414	529	366	397
Detection Percentage	47	51	31.5	12.5	39.5	34
Incorrect Identifications	129	162	62	8	90	71
Incorrect Detection Percentage	27	34.5	13.2	1.7	19	15

Detection percentage =

$$\frac{\text{number of signals detected similar to first signal detected}}{\text{number of signals available similar to first signal detected}}$$

Incorrect detection percentage =

$$\frac{\text{number of signals detected which are not similar to first signal detected}}{\text{number of signals available which are not similar to first signal detected}}$$

As stated before, it was not possible to calculate the proper thresholds for the parabolic filters. Table II, however, offers a comparison of the relative false alarm ratio for the thresholds chosen. Systems 1, 2, 5, and 6 have fairly high rates and can be compared directly. The other two have fairly low rates and must be compared to the linear or Case III filter with higher thresholds. As expected, the first two systems in a multiple signal environment detect the most waveforms, both correctly and incorrectly. It should be noted, however, that an increase in the thresholds of the first two would decrease the number of detections, correct and incorrect. The conclusion, without experimental verification, is that it is difficult to tell the difference between Systems 1, 2, 5, 6 at low R and equal false alarm rates.

A more useful picture of the results can be obtained from Table III which illustrates the convergence tendencies of the filter estimates as a function of the first detection.

TABLE III

Convergence Tendencies of the Estimates

System	1	2	5	6
Number of Initial S_α Detections	26	26	26	26
Initial S_α Detections Converging to S_α	22	22	21	20
Initial S_α Detections Converging to S_β	0	0	0	0
Initial S_α Estimates which Improve	16	14	11	14
Number of Initial S_β Detections	11	11	11	11
Initial S_β Detections Converging to S_α	1	1	1	0
Initial S_β Detections Converging to S_β	5	5	4	4
Initial S_β Estimates which Improve	1	2	2	0
Number of Initial Noise Detections	11	11	11	11
Initial Noise Detections Converging to S_α	3	3	3	2
Initial Noise Detections Converging to S_β	0	0	0	0

It is seen that S_α was the initial detection about one half of the time, and S_β about one quarter of the time. Convergence was arbitrarily assumed if the correlation between the estimate and the signal exceeded 0.5. The estimate was said to improve if the last correlation was greater than the first.

It appears that if S_α (the predominant waveform) is detected initially, it is quite likely that the estimate will converge to S_α. An example of the convergence process is given in Figure 24. In this example, the estimate improves rapidly until a few errors are made which cause some deterioration of quality. If the initial detection is S_β (low frequency waveform), it is much less likely that it will converge. It is probable that the estimate will deteriorate completely, but there is also the possibility of convergence to S_α. The possibility also arose of a false alarm initiated estimate converging to S_α. An example of this phenomena is shown in Figure 25. It should be noted that about 40% of the filters actually improved their initial estimates and about 70% terminate detecting the same signal as the initial detection (null signal in the case of initial false alarm).

Another measurement of interest is the distribution of readout times. Three separate distributions are shown in Figure 26. Figure 26(a) represents the measured D_j for the energy detections of S_α. Figures 26(b-c) give the distribution for the same data as processed by Systems 1 and 4 respectively. The results are typical that System 1 has a wide spread of readout times while System 4 is fairly narrow. System 4, however, detects far fewer waveforms at $R = 5$.

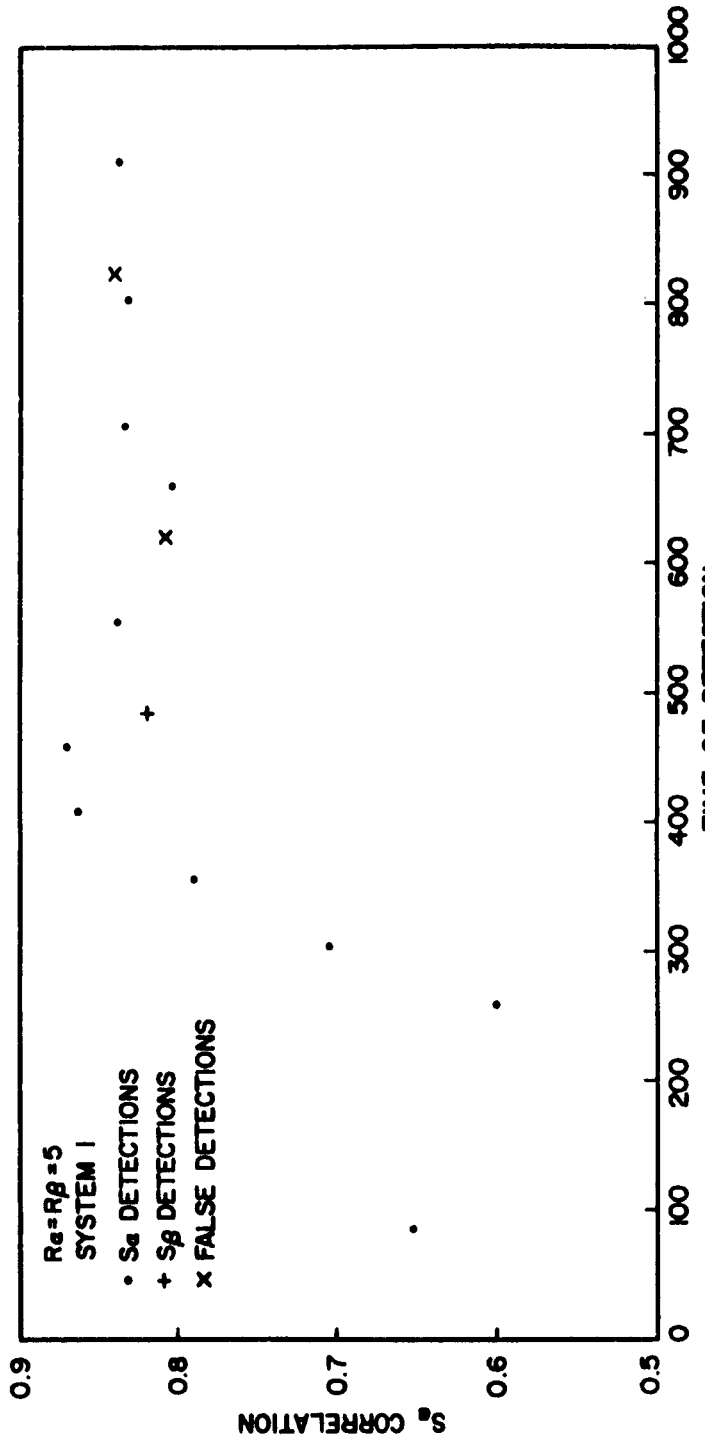

FIGURE 24 CORRELATION VERSUS TIME OF DETECTION

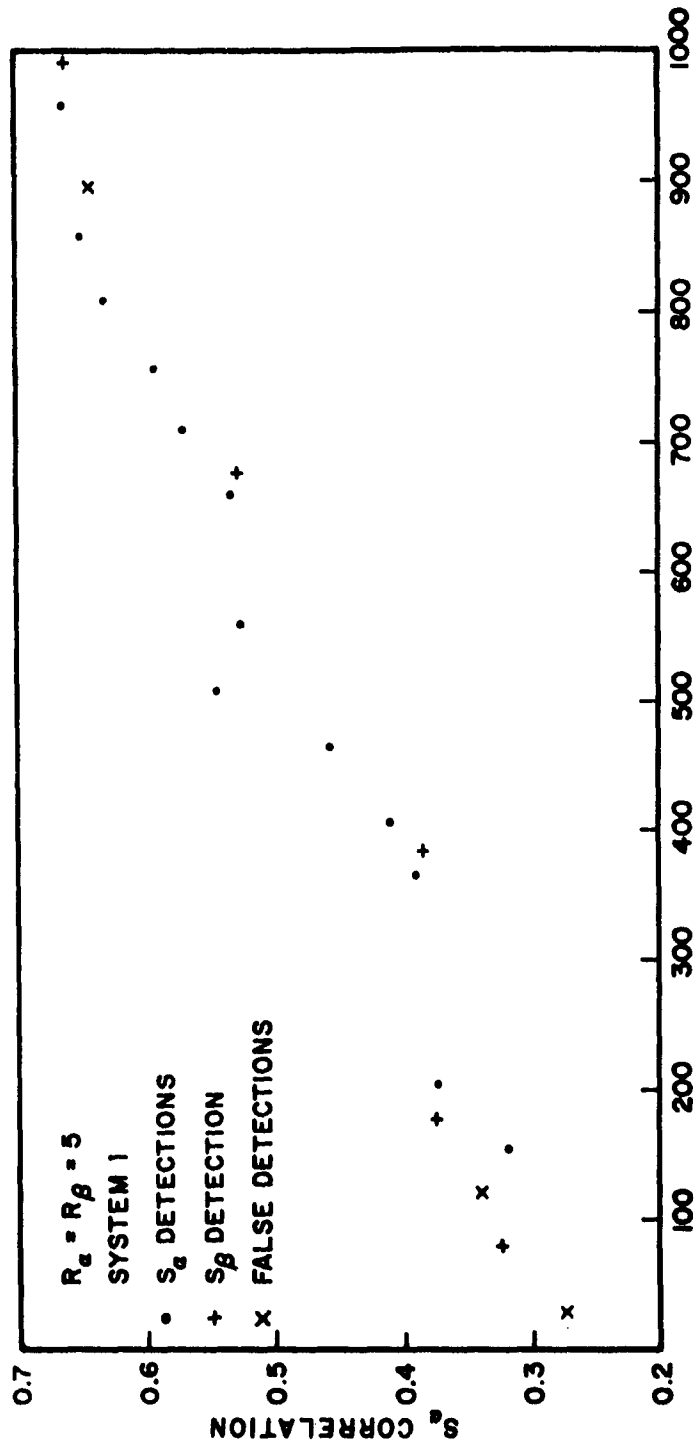

FIGURE 25 CORRELATION VERSUS TIME OF DETECTION - INITIAL FALSE ALARM

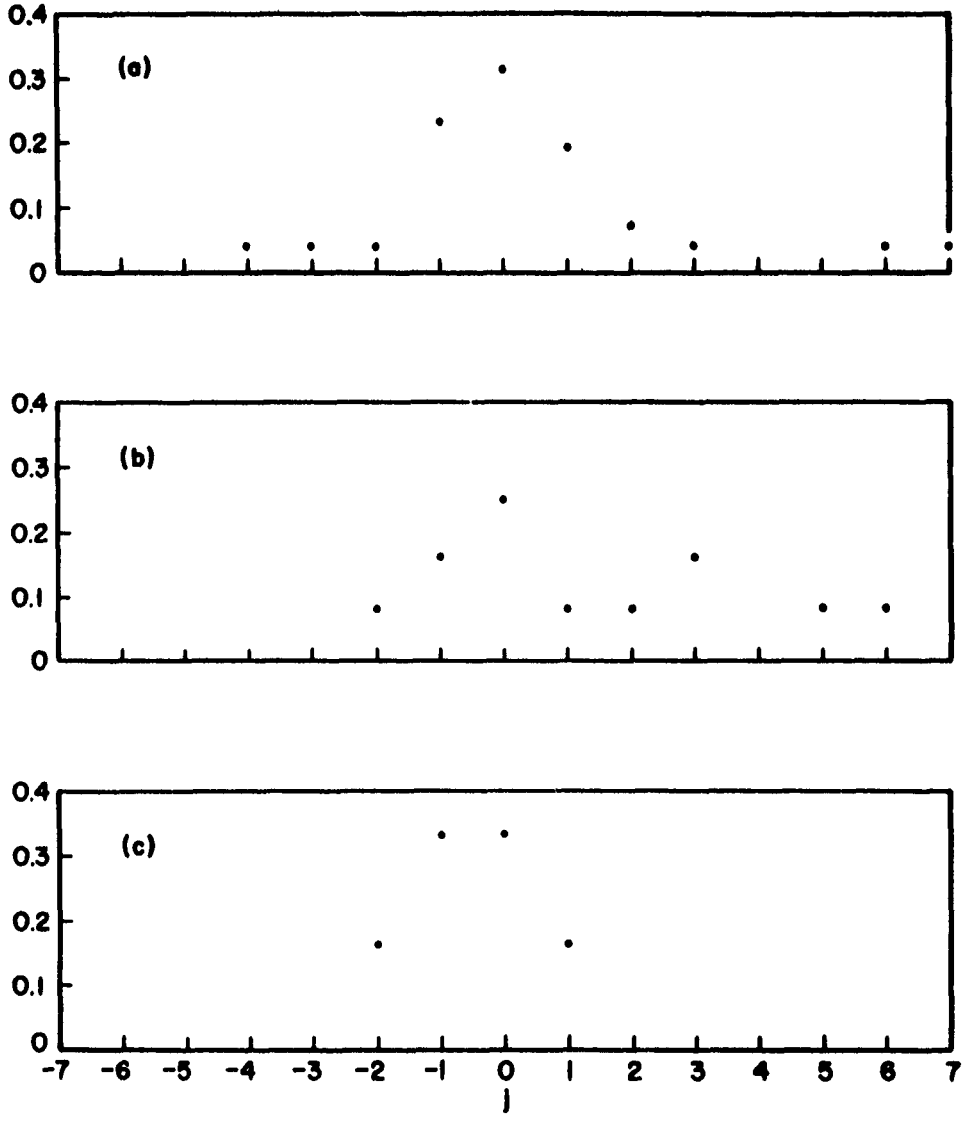

FIGURE 26 EXPERIMENTAL READOUT DISTRIBUTIONS D_j

The results of this test also verify that the time of detection of the first waveform to a large extent determines the time of detection of the rest of the pulses. Hence, if the initial detection is early, all will have a tendency to be early.

Although the general problem involves multiple waveform environments, it is of interest to examine filter operation in the presence of only one signal. Table IV gives the results of the few trials run using a single waveform. The first three tests used fixed amplitudes while the last treated the variable amplitude situation. The initial and final quality of the estimates are given and it is seen that they improve as the signal-to-noise ratio improves. System number 4 does not seem to produce good results until R = 20. In the case of variable amplitude pulses, all systems worked well missing only some of the lower level signals.

Table V illustrates the filter operation in the presence of two waveforms of higher signal-to-noise ratio. In one case, one signal varies in amplitude while the other remains fixed. The one new tendency displayed is the increase in incorrect detections by Systems 1 and 2 as R_β increases. One would expect this tendency to arise in view of past discussion. For example, a linear filter matched to S_α will detect a very large S_β even if the correlation of the two waveforms is small.

TABLE IV

Filter Operation in a Single Waveform Environment

	System	1	2	3	4	5	6
	Correct Detections	12	12	4	2	12	
$R_\alpha = 5$	Missed Signals	7	7	15	17	7	
$R_\beta = 0$	False Alarms	5	5	3	1	3	
	Initial Correlation	.71	.71	.71	.71	.71	
	Final Correlation	.69	.68	.55	.66	.64	
	Correct Detections	17	18	15	2	17	
$R_\alpha = 10$	Missed Signals	2	1	4	17	2	
$R_\beta = 0$	False Alarms	2	4	1	0	2	
	Initial Correlation	.83	.83	.83	.83	.83	
	Final Correlation	.915	.90	.91	.65	.92	
	Correct Detections	19	19	19	17	19	
$R_\alpha = 20$	Missed Signals	0	0	0	2	0	
$R_\beta = 0$	False Alarms	1	1	0	0	0	
	Initial Correlation	.905	.905	.905	.905	.905	
	Final Correlation	.978	.978	.985	.98	.985	
	Correct Detections	15	15	15	13	15	15
$R_\alpha = 5\text{-}40$	Missed Signals	4	4	4	6	4	4
$R_\beta = 0$	False Alarms	2	2	0	0	2	1
	Initial Correlation	.945	.945	.945	.945	.945	.945
	Final Correlation	.95	.95	.965	.975	.95	.96

TABLE V

Filter Operation in a Two Waveform Environment

	Systems	1	2	3	4	5	6
	Correct Detections	15	15	13	3	15	14
$R_\alpha = 10$	Missed Signals	4	4	6	16	4	5
$R_\beta = 10$	False Alarms	0	0	0	0	0	0
	Incorrect Identification	4	4	1	0	3	1
	Initial Correlation	.61	.61	.61	.61	.61	.61
	Final Correlation	.76	.77	.71	.80	.55	.79
	Correct Detections	19	19	19	17	19	19
$R_\alpha = 20$	Missed Signals	0	0	0	2	0	0
$R_\beta = 20$	False Alarms	0	1	0	0	0	0
	Incorrect Identification	7	7	2	1	4	2
	Initial Correlation	.903	.903	.903	.903	.903	.903
	Final Correlation	.948	.963	.921	.979	.948	.921
$R_\alpha = 5\text{-}40$	Correct Detections	18	17	17	14	18	16
$R_\beta = 20$	Missed Signals	1	2	2	5	1	3
	False Alarms	0	2	1	0	2	1
	Incorrect Identification	4	6	2	1	4	3
	Initial Correlation	.905	.905	.905	.905	.905	.905
	Final Correlation	.92	.93	.90	.975	.895	.91

To demonstrate the discrimination superiority of the parabolic filter over Systems 1 and 2 (linear and Case III), it is necessary to focus on large signals. If S_β is made so large that

$$\sum_{m=1}^{N} s_{m\beta}\, s_{m\alpha}^{*} \approx \sum_{m=1}^{N} s_{m\alpha}\, s_{m\alpha}^{*} \quad , \tag{93}$$

then no change in the threshold will affect the discrimination properties of the first two systems. An experiment of ten trials was performed with $R_\alpha = 20$ and $R_\beta = 56$, and the results are given in Table VI.

TABLE VI

Operation with Large S_β

Systems	1	2	3	4	5	6
Initial Detection S_α						
Per Cent S_α Detected	99		99	89	99	99
Per Cent S_β Detected	100		51	16	61	34
Initial Detection S_β						
Per Cent S_α Detected	84		40	8	46	40
Per Cent S_β Detected	100		100	100	100	100
Initial Detection Noise						
Per Cent S_α Detected	94		60	0	79	60
Per Cent S_β Detected	100		100	0	100	100

Due to an error, no data was obtained for System 2. It would have been almost identical to that obtained for System 1. System 1 performs very poorly and detects nearly all waveforms, while the parabolic structures show varying degrees of discrimination. It is also noted that System 4 is quite narrow and detects little that is not similar to the first detection. The fact that it did not detect either S_α or S_β after an original false alarm also verifies the discrimination characteristics.

As one last test on this point two very large waveforms ($R_\alpha = 200$, $R_\beta = 900$) were used and Table VII illustrates the results.

TABLE VII

Operation with Large S_α and S_β

Systems	1	2	3	4	5	6
Initial Detection S_α						
Per Cent S_α Detections	100	100	100	100	100	100
Per Cent S_β Detections	100	100	50	0	50	0

As expected, the first two systems detected everything while the others showed varying degrees of discrimination. System 4 completely eliminated S_β.

A comparison of Tables VI and VII is interesting because it reveals that the parabolic filters actually perform better in the presence of large unwanted signals. This may be explained by noting that detection is based upon

$$F = -a\left[\sum_{m=1}^{10} v_{p+m-10}^2 - \left(\frac{\sum_{m=1}^{10} v_{m+p-10} s_m^*}{\sqrt{\sum_{1}^{10} s_m^{*2}}}\right)^2\right] + b\,\frac{\sum_{m=1}^{10} v_{p+m-10} s_m^*}{\sqrt{\sum_{1}^{10} s_m^{*2}}} \quad . (94)$$

But

$$\frac{\sum_{1}^{10} v_{m+p-10} s_m^*}{\sqrt{\sum_{1}^{10} s_m^{*2}}} = |V| \cos\theta \qquad (95)$$

so Equation (94) becomes

$$-a\, V^2 \sin^2\theta + b|V| \cos\theta = F \quad . \qquad (96)$$

At a fixed angle, the first term becomes more important at higher energy, thus lowering F below the detection threshold. In other words, the larger the magnitude of the data, the more closely it must match the estimate to be detected. This particular feature is of advantage in filters where the data is used to form an estimate. A very large incorrect detection would deteriorate the future performance greatly.

To study detection and estimation of more than one signal at a time, a second filter (B) was constructed under the criterion discussed in Section III. In all cases filters A and B followed the same parameter rules. Since filter B had no effect on filter A, the results of A are similar to what has already been presented. The performance of the second filter will be summarized. At low values of R, the second system does not detect an initial signal until quite late and, consequently, accomplishes little. Even at $R_\alpha = R_\beta = 10$ the second filter behaves poorly. In several cases, the initial detection was S_β, but the final estimate was S_α. Thus, in many cases, both estimates converged to S_α. Figure 27 illustrates one complete system and the difficulties involved. It is noted that filter B did not begin operating until late because some early examples of S_β were being detected by filter A. Examples of S_β which were not detected by filter A did not have enough energy to trigger the second system until quite late in the run. At higher signal-to-noise ratios, the problem of incorrect detections by filter A blocking initiations of filter B became more pronounced. Thus, the linear and Case III structures worked very poorly in parallel arrangement. The parabolic structures operated with varying degrees of success, but for the most part worked very well and in some cases perfectly. Figure 28 shows the correlation versus time for one successful parallel arrangement. Figures 29 and 30 illustrate the build-up of the two estimates for the trial shown in Figure 28.

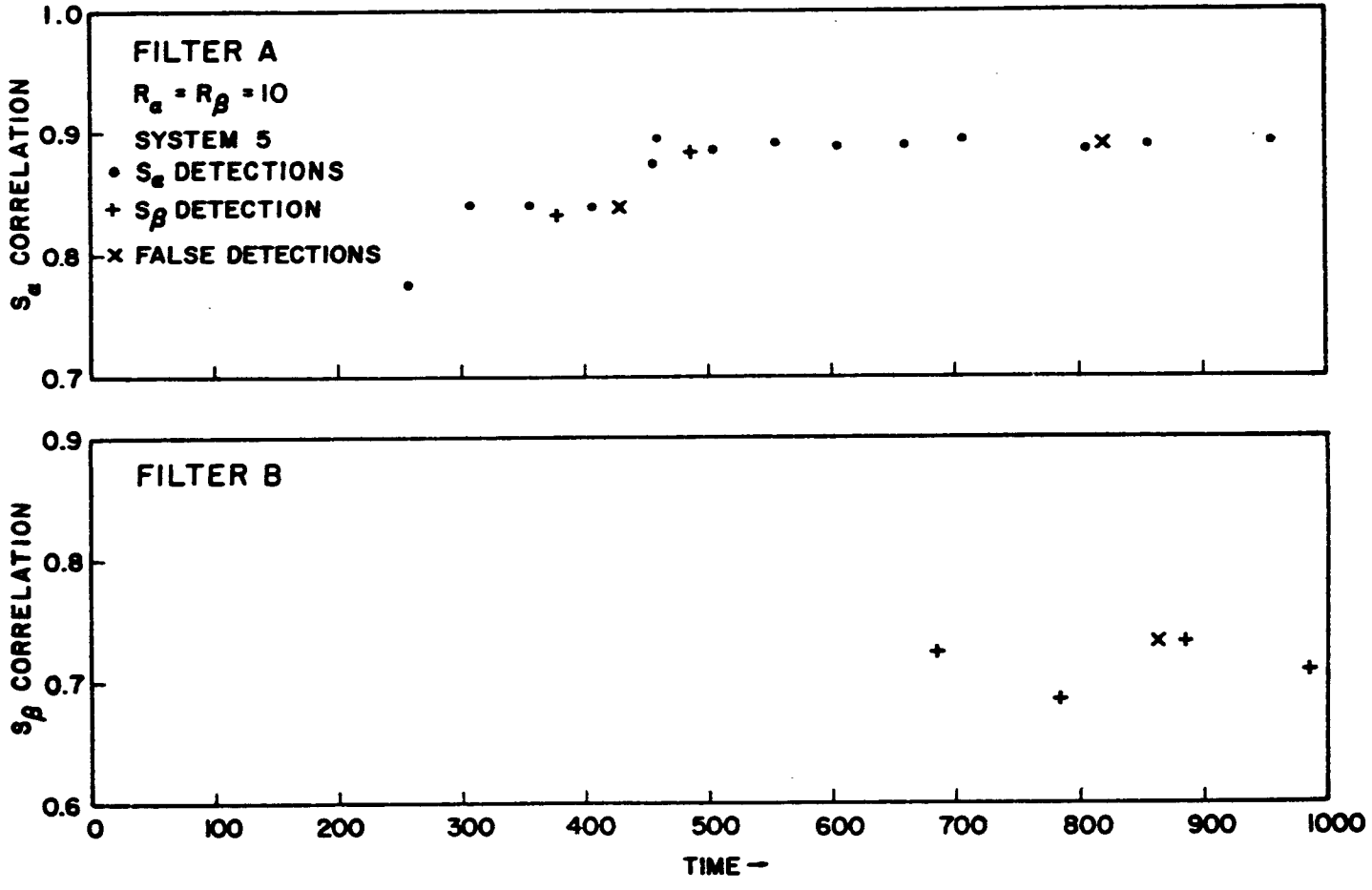

FIGURE 27 CORRELATION VERSUS TIME OF DETECTION FOR DOUBLE FILTER

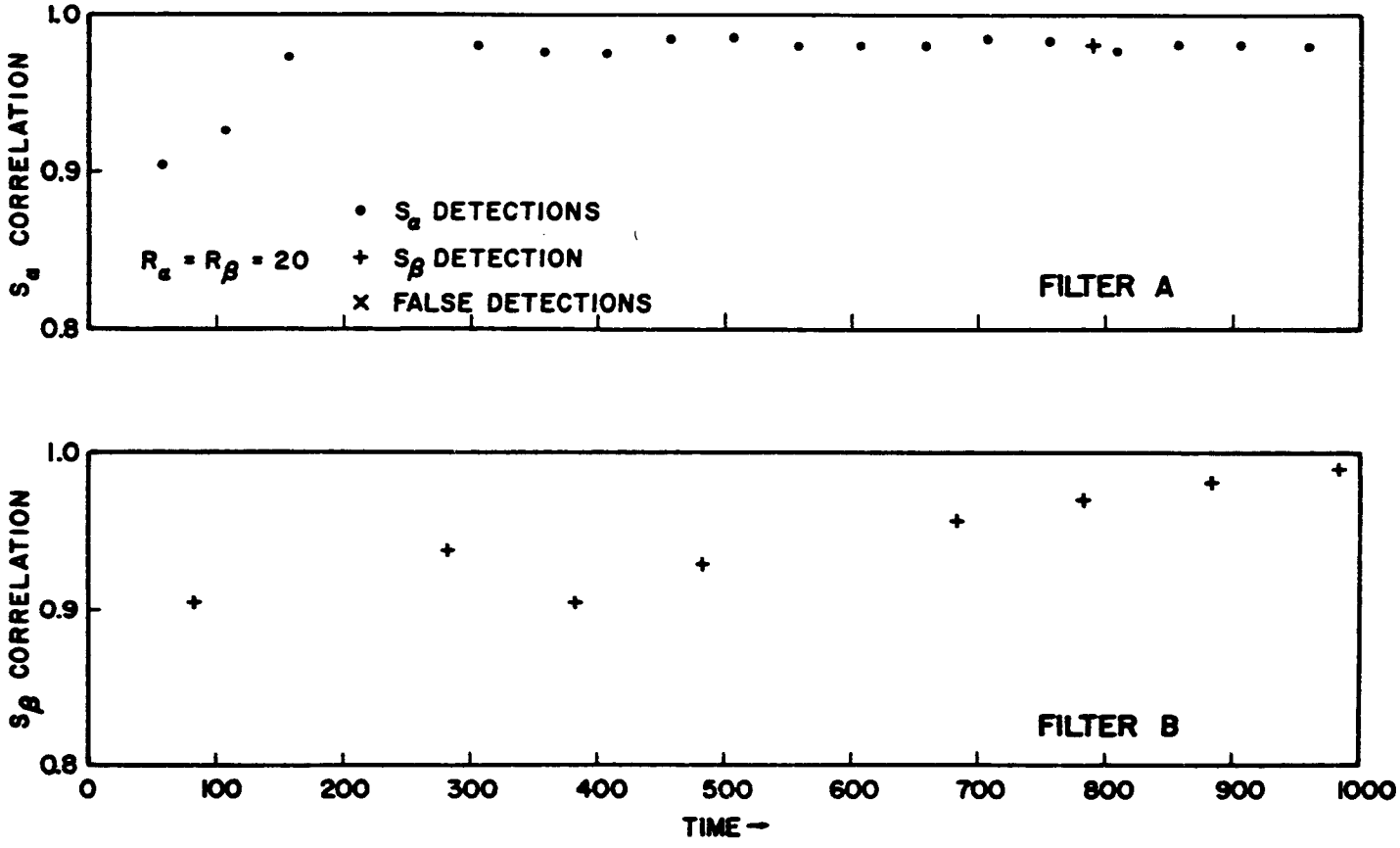

FIGURE 28 CORRELATION VERSUS TIME OF DETECTION FOR DOUBLE FILTER

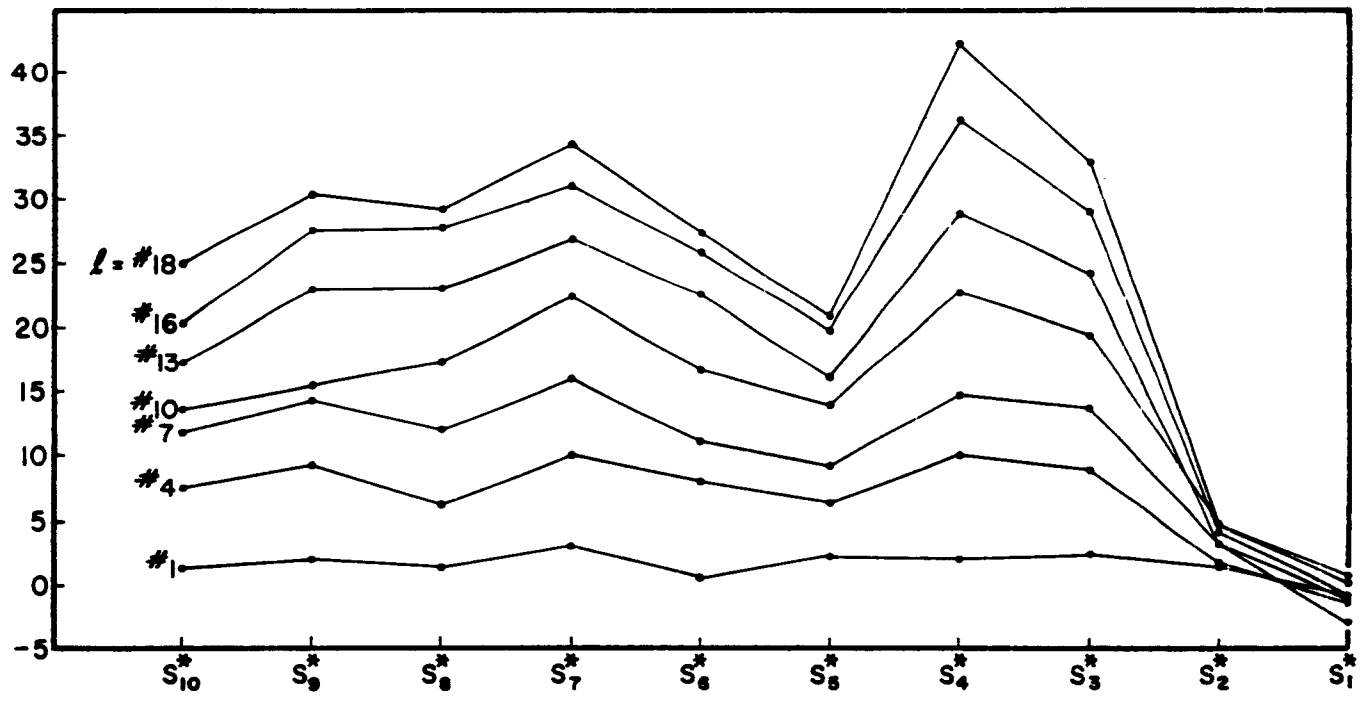

FIGURE 29 BUILD-UP OF ESTIMATE AS A FUNCTION OF NUMBER OF DETECTIONS ℓ - FILTER A

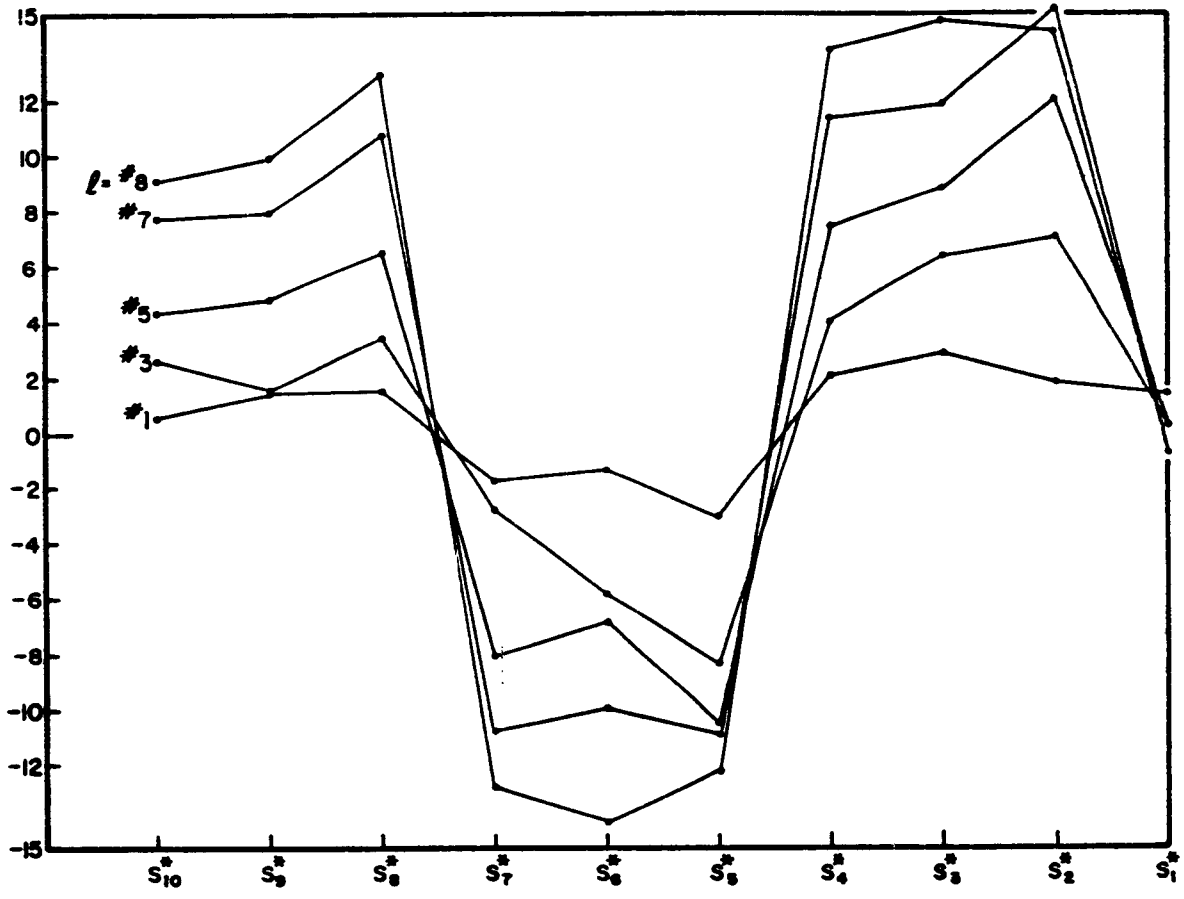

FIGURE 30 BUILD-UP OF ESTIMATE AS A FUNCTION OF NUMBER OF DETECTIONS
ℓ - FILTER B

The only new feature here is in obtaining the initial estimate. Once it is obtained, the filter B has the same characteristics as the ones previously discussed. However, to insure a good initial detection, it is necessary to have a structure with good discrimination properties.

A few other tests were also run to demonstrate certain points. One set of runs was made to determine the effects of different dimension signals upon operation. In other words, the effect of a poor choice of N or T was observed. It was found that for signal dimension greater than N (S_ϵ of Figure 22), the estimates converged to a part of the waveform. For very low dimension waveforms (S_γ and S_δ of Figure 22), poor results were obtained for R = 5, 10. There seemed to be improvement as the dimension increased, but too few trials were made to be conclusive.

One test was made to show the change over from an S_α filter to an S_β filter. The input was set up to start with an S_α detection, but the normal repetition rate of S_α was reduced by 4. Thus, S_β became the predominant waveform. Figure 31 shows the estimate correlation with each function as a function of computer time. Figure 32 shows the final estimate of the filter. It is seen that $s_3^* - s_{10}^*$ provides a good estimate of S_β and $s_1^* - s_5^*$ provides a rather poor estimate of S_α. The actual estimate was formed by detecting in S_β pulses one interval early and the S_α pulses three intervals too late. Thus, the observer obtains a somewhat ambiguous

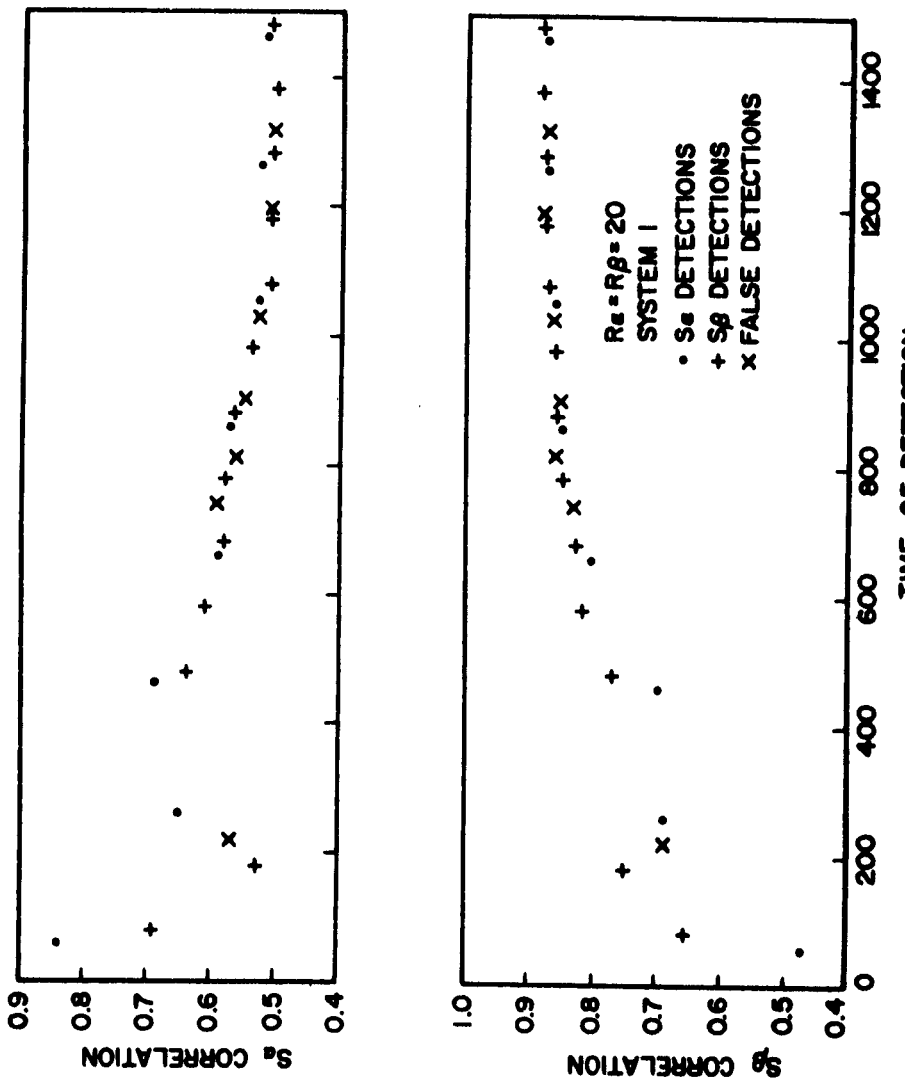

FIGURE 31 ILLUSTRATION OF AMBIGUOUS FILTER OPERATION

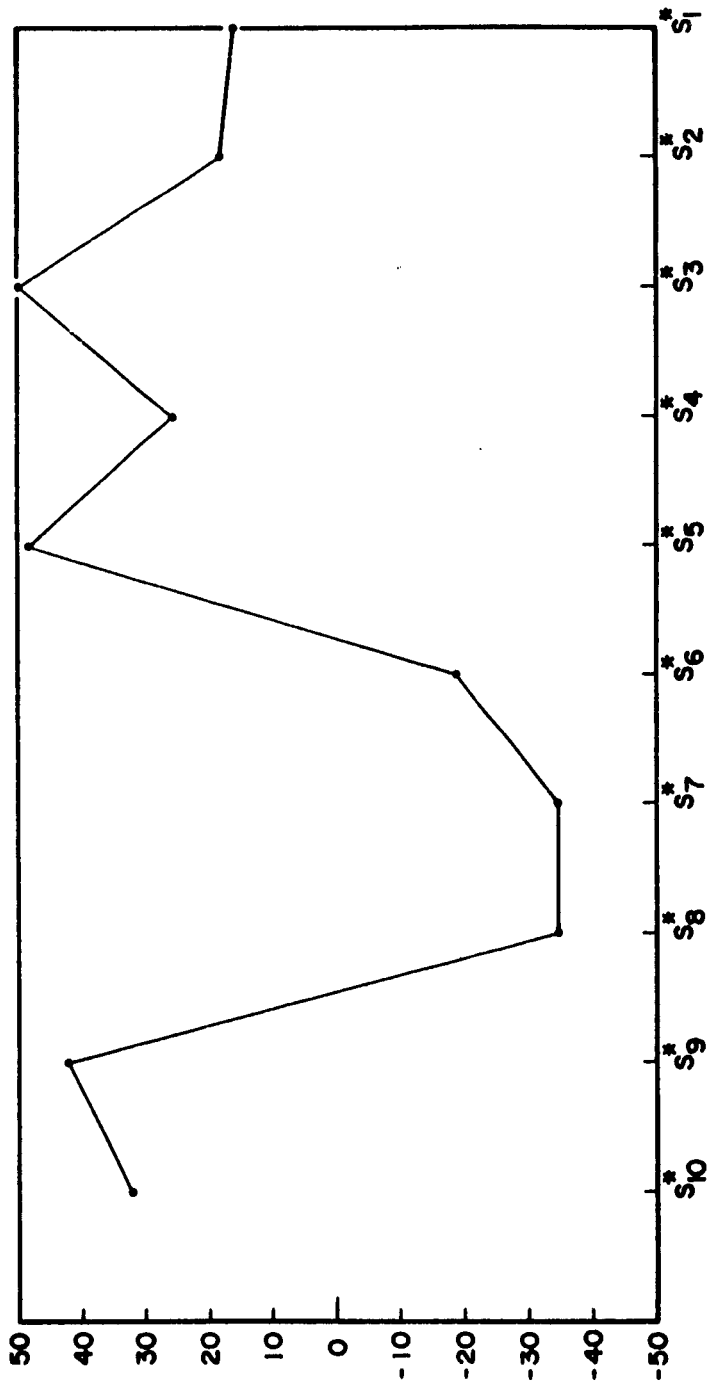

FIGURE 32 FINAL ESTIMATE FOR AMBIGUOUS OPERATION

result. Note, however, that the estimate was obtained with a filter which is not useful for multiple waveform environments. Figure 32 demonstrates the type of result the observer would obtain thinking that only one waveform was present.

To illustrate the effect of bias in the estimates, one run was made with no signals present and all detections were false. Table VIII shows the number of false alarms and the correlation of the final estimate with the initial.

TABLE VIII

Bias Effect of False Alarms

Systems	1	2	6	7
False Alarms	5	7	6	4
Correlation	.792	.887	.920	.904

The results of this short experiment show how little the estimate has changed from its initial value even though only false detections have occurred. It illustrates that a noise pattern similar to the first estimate has been found.

The effects of bias can also be well illustrated by means of Figures 33 and 34. Figure 33 shows the convergence of a filter from an initial false estimate to S_a. The relatively minor effects of false alarms and incorrect identifications are evident. Note, however, that the curve reaches a limit of approximately 0.87.

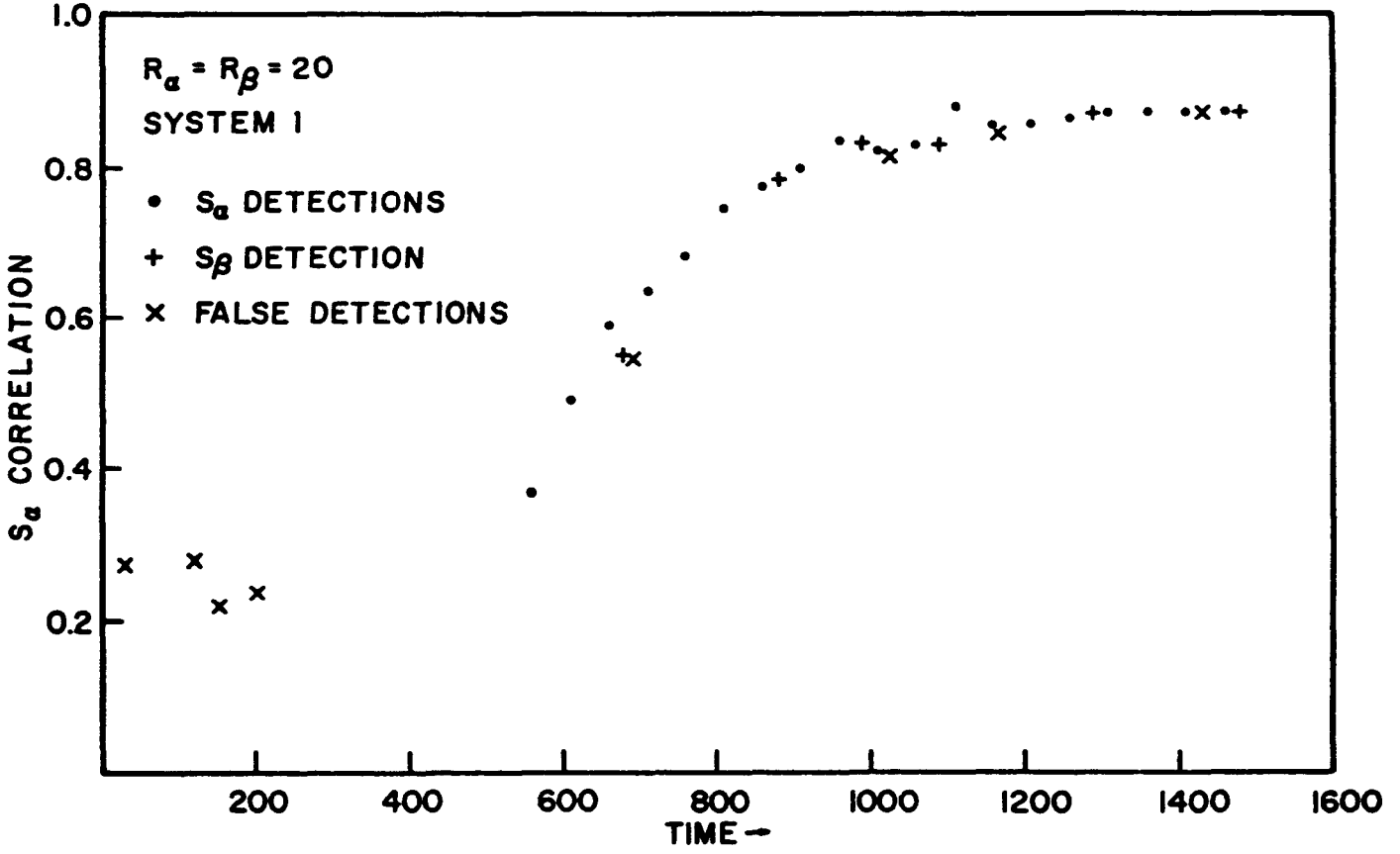

FIGURE 33 CORRELATION VERSUS TIME OF DETECTION - INITIAL FALSE ALARM

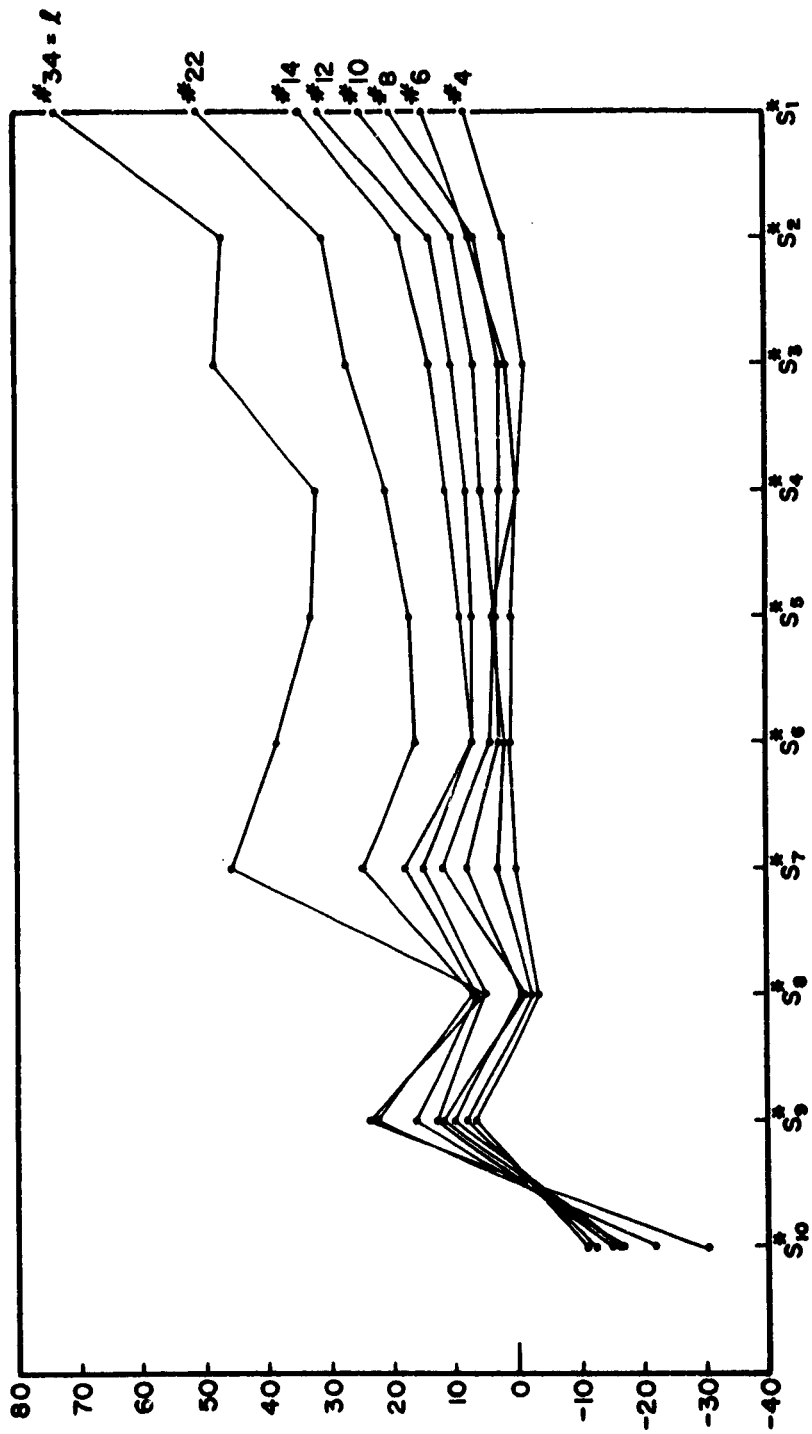

FIGURE 34 BUILD-UP OF ESTIMATE AS A FUNCTION OF ℓ - INITIAL FALSE ALARM

Figure 34 illustrates why this is so. It also shows the similarity between the initial and final estimates particularly at s^*_{10}, s^*_9, s^*_7, and s^*_1. The estimate is made up primarily of detections which are late by one interval. With this type of readout time, the limit of the convergence would be approximately 0.93.

One other way of demonstrating the bias effect consists of eliminating all previous explicit information. The elimination was accomplished by replacing the estimate completely by the most recent detection. A run was made using the last detection as the estimate. After approximately ten detections, filters 3 and 4 still had a correlation of final and initial estimate of greater than 0.5. The other correlations were lower.

A few experiments were run where the same data were passed through the filters a number of times with the estimate continually increasing. In other words, the last estimate of one pass formed the first estimate of the next pass. In all cases, very little effect was noted other than the detection of pulses which had occurred before the initial energy detection of the first pass. There was seldom any improvement in the estimate quality after the first trial.

One other result of moderate interest is the energy in the estimate after a number of detections. Table IX shows the energy in one set of estimates after 5 detections of signals with R = 0, 5, 10, 20.

TABLE IX

R	Estimate Energy
0 (false alarms)	329
5	371
10	435
20	690

Not all of the detections are necessarily correct. Thus, by measuring the estimate energy, the observer has not only an indication of the signal energy, but also an indication of whether the estimate might be due to false alarms only. On the basis of the thresholds used for the linear system in the experiments the minimum possible value of the estimate energy would be

$$\left(\sqrt{23.2} + 4 \times 2.33 \right)^2 \approx 200 \quad . \tag{97}$$

Equation (97) assumes each detection is just at the threshold.

VI. CONCLUSIONS

The experiments have demonstrated some of the capabilities and limitations of automatic data processing. An examination of the experiments and results provides an overall picture of the possibilities of adaptive filtering. It is apparent that the cross section of filter structures studied operate moderately well at a signal-to-noise ratio of 5. It is unfortunate that a lower threshold was not chosen for Systems 3 and 4 in order to obtain a better assessment of performance at low R. With lower thresholds, it is expected that both would operate, but with lower detection rates than those of Systems 1 and 2. Throughout the experiments, there is only one situation where the first two structures show to advantage; that of an initial false or poorly timed detection in a single waveform environment. Here the larger decision region offered by these filters explains the ability to correct for poor initial decisions. The parabolic filter (System 6) can be used to some extent to compensate for initial error. At low values of ℓ the decision region is large and decreases in size as ℓ increases and, hopefully, the estimate improves. One set of data did exhibit the phenomenon of going from an initial false alarm to an estimate of S_a before the filter structure became too narrow. System 6 has the advantage, however, of being able to operate in this mode in a multiple signal environment. Surprisingly, there are no apparent advantages in using the first two systems in a single waveform environment

other than to compensate for initial error. For large multiple waveforms, the parabolic filters were obviously superior as should be expected from Section II. In large signal cases where the initial detections are very accurately timed, the narrow structure performed very well.

The parallel processing of more than one estimate was very successful for R = 20, utilizing parabolic filters. To more fully investigate lower values of R, it would be necessary to provide more samples of S_β and perhaps lower the filter thresholds slightly. In any event, the automatic processing of the two waveforms produces results which could not be matched by any visual techniques. (For example, see Figure 23 which is the beginning of the data leading to Figures 28-30). There is no new difficulty in now extending the processing to as many parallel filters as desired. Each new one would be initiated if none of the established filters detected a pulse during the interval that the energy exceeded the threshold. It should also be noted that some criterion could be used to prevent ambiguous detections (for example, t = 783, Figure 28) after the initial detection of filter B. An added condition for detection in filter B could then prevent some detections of S_α and force the estimate of S_β to be more reliable. In the paper, no such restriction was used.

The experiments were run with moderately high duty ratios and a rather fortuitous choice of N. Each condition has an effect upon the preceding arguments. If the pulses occur less frequently, it would be necessary to lower the false alarm rate thus reducing the probability of detection. More signal examples would then be required to yield the same estimate qualities shown here. The relative merits of the various filters would not change. A less accurate choice of N does affect the relative merits. In dealing with unknown data, the observer will generally choose N larger than any waveform expected. As the estimate builds up, some of the components will tend to zero, effectively reducing the dimension of the estimate. But, if nothing else is done, the energy dimension will remain at N and the energy component in Equation (77) will be too large for accurate detection. If desired, the energy dimension could also be reduced by determining the number of components containing some fraction of the estimate energy and using it in Equation (77). One advantage of an energy dimension larger than signal dimension will be illustrated in Appendix B.

The one unexpected result of the experiments is the high correct detection rate of the first two systems at R = 5. Figure 21 indicates that the detection rate for the matched filter is only 0.46. However, the value assumes detection only at the correct readout time. There is also the possibility of the signal being detected at a slightly different time while being missed at the correct time.

Thus, it is possible for detection probabilities to be considerably higher than the theoretical values. An examination of 190 signals at R = 5 showed that the probability of detection with a matched filter at the correct time was 0.46, but the overall detection probability was 0.57. The fact that the signal may be detected at several different times also tends to increase the curves of Figure 21 for low values of cos θ. As an example, consider the detection of S_a (R_a = 5) by three linear filters with poor correlation.

a. Filter which examines each data sample independently

($S^* = \{1, 0, \cdots 0\}$)

Here $\cos\theta = \frac{1}{\sqrt{8}} = 0.354$

and the probability of detection is 0.063.

There are now eight independent points at which a true detection can take place. The probability of missing all eight samples is $(1 - 0.063)^8 = 0.594$

and the total probability of detection is 0.406.

b. Filter which examines two successive samples

($S^* = \{1, 1, 0, \cdots 0\}$)

Here $\cos\theta = 0.5$

and the probability of detection is 0.115.

There are now 4 independent measurements which could produce correct detections.

The total probability of detection is

$1 - (1 - 0.115)^4 = 0.387$.

c. Filter which examines four successive samples

$(S^* = \{1, 1, 1, 1, 0, \cdots 0\})$

Here $\cos \theta = 0.707$

and the probability of detection is 0.233.

There are two independent measurements which could produce detections. The total probability of detection is $1 - (1 - 0.233)^2 = 0.412$.

It should be noted that the total probability of detection is still higher for Cases b and c than the values given. There are actually more than four or two times at which detection can occur, but these measurements are not independent of the others. Thus, it can be seen that the filters can still have high detection probabilities with poor estimates.

The three cases discussed above correspond to estimates which may be caused by poor initial readout time or peaks in the estimate due to noise. An example of a poor initial estimate from the experiments is given below in normalized form.

$$S^* = \{0.32, 0.28, 0.74, 0.06, 0.31, 0.00, 0.04, 0.24, -0.16, 0.27\}$$

It is seen that most of the energy is concentrated in the first 3 terms and most of it in the 0.74 term. Although the estimate is poor, it does allow future waveforms to be detected more reliably than Figure 21 indicates, but with poor readout timing.

It is of some interest to study the effects of removing the restrictions on the problem imposed in the Introduction. For instance, if it is known with certainty that only one waveform exists either System 1 or 2 could be used to slight advantage. The relaxation of the variable amplitude restriction offers no particular advantage, but will be discussed from a different point of view in Appendix A. If the waveforms are known, matched filters are the optimum approach. However, there is still the problem of determining the times to read the outputs of the filters in the case of multiple signals. Appendix B will discuss the read-out problem of multiple known signals. If the waveforms have a fixed period, the detection and estimation process could be improved. Errors can also be found and perhaps removed if storage facilities are used. Figure 28 shows how the errors can be determined. It is obvious from the figure that both S_α and S_β have a fixed repetition rate. The repetition intervals can be determined easily by looking at the figure, or the determination could be done automatically. The filter used is narrow and the readout times are quite accurate. It is apparent that two samples of S_α have been missed (t = 208, 258) and two samples of S_β have been missed (t = 183, 583). Without using the symbols given in the figure, it is obvious that the ambiguous detection at t = 783 correctly belongs to the S_β system. If many pulses are available to the observer, it may be possible to determine the period and use

the information to lower the thresholds at future expected arrival times. Very good estimates could be obtained because of the large number of samples and the decrease in bias because of the threshold reduction. Knowledge of readout time removes almost all of the problems outlined previously. The only limitation of estimates would be the number of signals available and the bias inherent in the detection decision. If the observer removes the real time restriction, a number of types of operation are possible. These include new passes of the data through different parameter filters to perhaps refine the estimates. The few experiments of this type attempted gave no indication that the approach is useful, however.

APPENDIX A AMPLITUDE FILTERS

A special application of the basic filter structure, Equation (77), is presented here. In some of the discussion of Section II, it was assumed that two identical waveforms of different amplitudes represented entirely different signals. For example, in Case IV detection was based upon the given waveform falling within a small range of amplitudes. This feature may be used to advantage in separating pulses on the basis of amplitude. Waters (13) has discussed the separation of rectangular pulses in noise. It will be noted from the discussion of Case IV that the discrimination qualities of structures of the form of Equation (16) are independent of wave shape.

To examine the separation characteristics, a single test was run and the results are presented here because of the assumption of known waveform and amplitudes. The computer program previously described was modified to utilize a fixed, known estimate. Since pulse shape was irrelevant, a rectangular pulse was used for convenience. The input included four signals of ten interval length and R = 20, 80, 180, and 320. The noise again had unit variance and zero mean. The hypothesis H_i that a signal of amplitude A_i is present is chosen if

$$\sum_{m=1}^{N} \left(v_m - \frac{A_i s_m^*}{\sqrt{\sum_{1}^{N} s_m^{*2}}} \right)^2 < \Lambda$$

$$\sum_{m=1}^{N} v_m^2 - 2A_i \sum_{m=1}^{N} \frac{v_m s_m^*}{\sqrt{\sum_{m=1}^{N} s_m^{*2}}} + A_i^2 < \Lambda$$

or

$$2A_i \sum_{m=1}^{N} \frac{v_m s_m^*}{\sqrt{\sum_{m=1}^{N} s_m^{*2}}} - \sum_{m=1}^{N} v_m^2 > A_i^2 - \Lambda \quad . \tag{A-1}$$

Detection is based upon the error energy being less than a specified level.

No attempt was made to optimize (in any sense) the filter performance. The threshold value was selected by noting that if the hypothesis is correct

$$v_m = \frac{A_i s_m^*}{\sqrt{\sum_{1}^{N} s_m^{*2}}} + n_m$$

$$E\left\{ \sum_{m=1}^{N} \left(v_m - \frac{A_i s_m^*}{\sqrt{\sum_{1}^{N} s_m^{*2}}} \right)^2 \right\} = N\sigma^2 = 10 \quad , \tag{A-2}$$

and if the hypothesis is incorrect

$$v_m = \frac{A_j s_m^*}{\sqrt{\sum_{1}^{N} s_m^{*2}}} + n_m$$

$$E\left\{ \sum_{m=1}^{N} \left(v_m - \frac{A_j s_m^*}{\sqrt{\sum_{1}^{N} s_m^{*2}}} \right)^2 \right\} = N\sigma^2 + (A_j - A_i)^2 \quad . \tag{A-3}$$

With the values of A_i used, the minimum value of Equation (A-3) is 30. A threshold of $\Lambda = 15$ was chosen to provide fairly good separation characteristics.

Table A-I gives the results of the experiment and a comparison with the ideal performance of matched filters with dual thresholds.

TABLE A-I

Detection Characteristics of Amplitude Filters

Input Amplitude	$\sqrt{20}$	$2\sqrt{20}$	$3\sqrt{20}$	$4\sqrt{20}$	0
Number of Signals	10	10	5	4	
Error Energy Criterion					
Detections of $\sqrt{20}$ Filter	9				6
Detections of $2\sqrt{20}$ Filter	1	9			
Detections of $3\sqrt{20}$ Filter		2	4		
Detections of $4\sqrt{20}$ Filter				4	
Matched Filter					
Detections of $\sqrt{20}$ Filter	9				3
Detections of $2\sqrt{20}$ Filter	1	10			
Detections of $3\sqrt{20}$ Filter			5		
Detections of $4\sqrt{20}$ Filter				4	

The matched filter results are based upon thresholds spaced equidistant between the expected outputs from the five possible signals ($A_i = \sqrt{20},\ 2\sqrt{20},\ 3\sqrt{20},\ 4\sqrt{20}$ and 0).

The results show rather poor performance at the lowest level because of numerous false alarms, but good characteristics at other amplitudes. The fact that one signal was detected simultaneously by two filters demonstrates that the threshold chosen does not lead to mutually exclusive decision regions. The threshold could be modified to provide exclusive decision regions or slightly better overall performance.

The filter of Equation (A-1) possesses certain advantages over other types of amplitude filters. It operates equally well for all pulse shapes and does not require the use of dual thresholds. The system described also inherently discriminates against other waveforms which may be present.

APPENDIX B AUTOMATIC RECOGNITION OF HAND SENT MORSE CODE CHARACTERS

The automatic detection of Morse code signals represents an interesting application of adaptive filtering techniques (5). In hand sent messages the character lengths may vary considerably with time and variable processing could be used to track these changes. There is one difficulty in using the filter previously discussed in the decoding operation. Generally, the problem is that of separating two waveforms where one waveform is identical to a portion of the other. Figure B-1 illustrates the difficulties in deciding which of two waveforms, S_K or S_R, is present. Unless special precautions are taken, a filter which detects S_K will also detect S_R. The precautions necessary may be determined by referring to Figures B-1(b, c) which show the paths of S_R and S_K through the signal space as a function of time. The coordinates represent the last three samples observed with the most recent sample in the s_3^* direction and the oldest sample in the s_1^* direction. If the S_K decision region is chosen in either the s_1^* or the s_3^* direction, S_K would be detected properly. However, the filter would also detect S_R at $t_B + 4$ or at t_B. Notice that if the observer places a parabolic decision region in the s_2^* direction (Figure B-1(d)), S_R will be discriminated against because its path through the space does not enter the region.

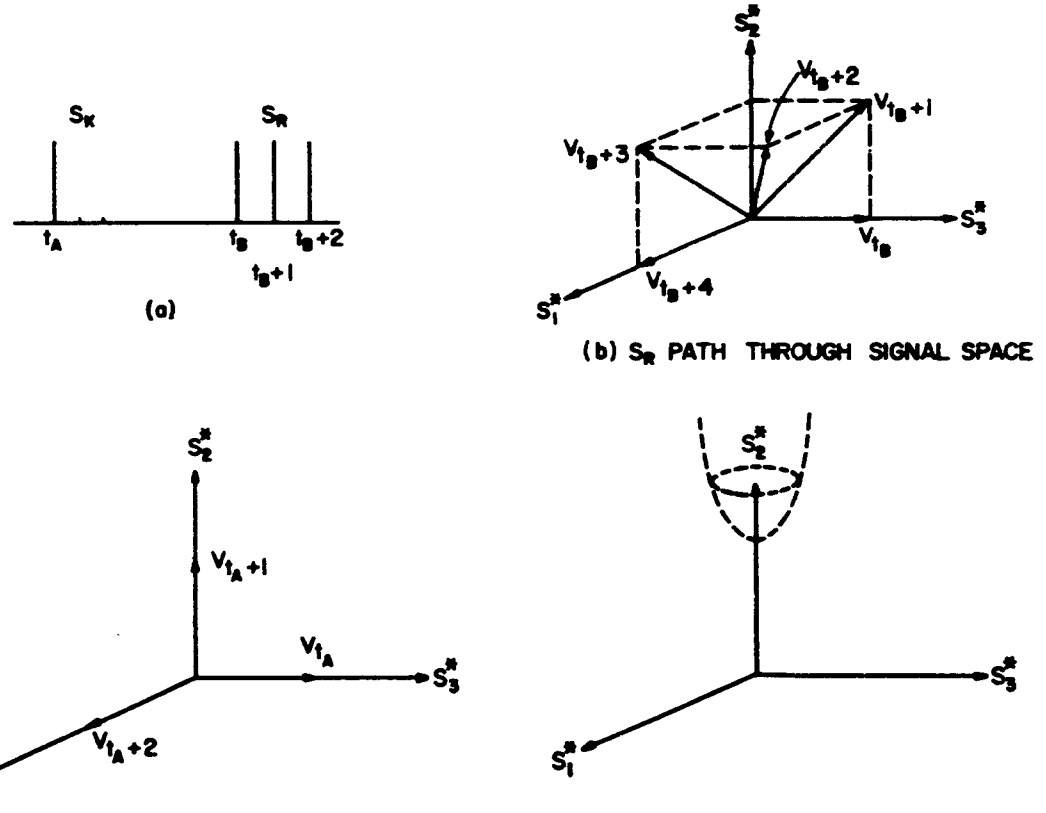

FIGURE B-1 DETECTION OF SIMILAR SIGNALS

The equation for the filter boundary may be written

$$V \cdot s_2^* = a\left\{ (V \cdot s_1^*)^2 + (V \cdot s_3^*)^2 \right\} + \Lambda$$

$$= a\left\{ (V \cdot s_1^*)^2 + (V \cdot s_2^*)^2 + (V \cdot s_3^*)^2 - (V \cdot s_2^*)^2 \right\} + \Lambda$$

$$= a\left\{ v_1^2 + v_2^2 + v_3^2 - (V \cdot s_2^*)^2 \right\} + \Lambda$$

$$\sum_{m=1}^{3} \frac{v_m s_m^*}{\sqrt{\sum_{1}^{3} s_m^{*2}}} = a\left\{ \sum_{m=1}^{3} v_m^2 - \left(\sum_{m=1}^{3} \frac{v_m s_m^*}{\sqrt{\sum_{1}^{3} s_m^{*2}}} \right)^2 \right\} + \Lambda$$

where

$$s_m^* = \{0, 1, 0\} \quad .$$

The form of the filter is identical to Equation (77). Now, however, the dimension of the energy measure is larger than the signal dimension in order to examine each side of the pulse for zero components (or small components if noise is present). The values of a and Λ may be selected such that only a signal of unit duration will be detected. The filter for detecting S_R would be a parabolic region in the $\{1, 1, 1\}$ direction. In this case, the energy measure and the signal have the same dimension so any rectangular pulse of more than three interval duration would be

detected as S_R. The addition of two more dimensions to the energy measure would provide a filter structure which could discriminate against longer pulses.

On the basis of the above discussion, a few experiments were performed using sampled, hand sent, Morse code as the input to the double filter system described in the paper. The space information was removed by placing the character pulses at fixed intervals of time. During the transmission the dot lengths varied between one and five intervals and the dashes between four and ten intervals. Initial estimates of the characters were used with

$$\text{dot estimate} = \left\{0, 0, 0, \frac{1}{\sqrt{3}}, \frac{1}{\sqrt{3}}, \frac{1}{\sqrt{3}}, 0, 0, 0, 0\right\}$$

$$\text{dash estimate} = \left\{\frac{1}{3}, \frac{1}{3}, \frac{1}{3}, \frac{1}{3}, \frac{1}{3}, \frac{1}{3}, \frac{1}{3}, \frac{1}{3}, \frac{1}{3}, 0\right\}$$

Trials were made with three choices of a and Λ. The results showed error rates of 7-8% in the character identification. Error rates of about 4% would have been obtained with slightly different parameter choices because half of the errors were due to a failure in detecting unit interval length pulses which are obviously dots. The filters followed the operator characteristics quite well, correctly detecting early dots of length five and later dashes of length four.

Final estimates were of the form

$$\text{dot estimate} = \{0, 0, .03, .68, .68, .27, 0, 0, 0, 0\}$$

$$\text{dash estimate} = \{.41, .41, .41, .41, .39, .33, .20, .10, .05, 0\}$$

One last trial was made with noise also present. The noise was of sufficient amplitude to prevent the measurement of pulse width by determining the interval that the threshold was exceeded. The filters missed about 35% of the pulses but incorrectly identified only 5%.

From the discussion and the experimental results, it is apparent that the basic filter structure can be used to separate pulses on the basis of pulse width, even in the presence of noise. The importance of extra dimensions in the detection of similar waveforms was also demonstrated but it leads to more missed signal errors. The filter also demonstrated the ability to track slowly varying patterns in a real situation.

REFERENCES

1. Minsky, M., "Steps Toward Artificial Intelligence," Proc. IRE, Vol. 49, No. 1, pp. 8-30, January 1961.

2. Glaser, E. M., "Signal Detection by Adaptive Filters," The Johns Hopkins University, Radiation Laboratory, Technical Report No. AF-75, April 1960.

3. Jakowatz, C. V., Shuey, R. L., and White, G. M., "Adaptive Waveform Recognition," General Electric Research Laboratory, Schenectady, New York, 60-RL-2435E, May 1960.

4. Braverman, D. J., "Machine Learning and Automatic Pattern Recognition," Stanford Electronics Laboratory, Stanford, California, Technical Report No. 2003-1, February 17, 1961.

5. Gold, B., "Machine Recognition of Hand-Sent Morse Code," Trans. IRE, Prof. Group on Information Theory, Vol. IT-5, No. 1, pp. 17-24, March 1959.

6. Turner, R. D., "The Generalized Search Process," Second Scientific Report, Operations Research on Recognition, ASCRL, AF(604)-6103, General Electric Advanced Electronics Center, Ithaca, New York, November 1961.

7. Brennan, E. J., "An Analysis of the Adaptive Filter," General Electric Electronics Laboratory, Syracuse, New York, R61ELS-20, 1961.

8. Brennan, E. J., "Adaptive Filter Simulation Study," General Electric Electronics Laboratory, Syracuse, New York, R61ELS-114, September 22, 1962.

9. Middleton, D., "The Effects of Variable Amounts of Prior Information on Detection and Discrimination of Partially Known Signals," The Johns Hopkins University, Radiation Laboratory, Internal Memorandum, RL/62/IMA-4, May 17, 1962.

10. Ogg, F. C., "The Use of Prior Information in Signal Detection," The Johns Hopkins University, Radiation Laboratory, Internal Memorandum, RL/61/IMA-20, October 31, 1961.

11. Helstrom, C. W., Statistical Theory of Signal Detection, Pergamon Press, New York, 1960.

12. Roe, G. M., and White, G. M., "Probability Density Functions for Correlators with Noisy Reference Signals," Trans. IRE, Prof. Group on Information Theory, Vol. IT-7, No. 1, pp. 13-18, January 1961.

13. Waters, W. M., "Pulse Separation by Amplitude Filters," The Johns Hopkins University, Radiation Laboratory, Technical Report No. AF-77, May 1960.

10 Defense Document Center
Arlington Hall Station
Arlington 12, Virginia

ASD
Wright-Patterson AFB, Ohio
1 Attn: ASAPRL
1 ASAPT
1 ASNC
1 ASND
1 ASNG
1 ASNPVD-1
1 ASNPVD-2
1 ASNR
1 ASNS
1 ASNSED
1 ASNY
1 ASORR (Mr. Catansarite)
1 ASRC
1 ASRE
1 ASRNET-3
1 ASRNGE
1 ASRNOO
1 ASRNC (Mr. Stimmel)
1 ASRNC (Mr. Portune)
2 ASRNCG-1
1 ASRNCG-2
1 ASRNET-1
2 ASRNCF-1
1 ASRNRS
1 ASRNRS-3
1 ASROO
1 ASRSSE-2
1 ASOQ (Gp. Capt. Fletcher)

1 ARL
Wright-Patterson AFB, Ohio
Attn: ARM (Mr. Wolaver)

RADC
Griffiss AFB, New York
1 Attn: RAAL
1 RAD (Dr. I. J. Gabelman)
1 RALC (J. E. Gruickshank)
1 RALSS (M. A. Diab)
1 RAUAA (John P. Huss)
1 RAUAT
1 RAUMA (C. R. Miller)
1 RAUMM
5 RAWE
1 RAWEC
1 RAWES
2 RAWI

AFSC
Andrews AFB
Washington 25, D.C.
1 Attn: SCTAN
1 SCRC (Lt. Col. Thompson)

HQ, USAF
Washington 25, D.C
1 Attn: AFRDR-IN (Lt. Col. Pinson)
1 AFOOR-SV-ES (Lt. Col. Smith)
1 AFORQ-SA (Lt. Col. Ragsdale)
1 AFMPP-EQ (Lt. Col. Manbeck)
1 AFORQ-AD

1 USAFSS (ODC-R)
San Antonio, Texas

1 RTD (RTHR, Col. Schulte)
Bolling AFB,
Washington, D.C.

2 PACAF (PFOOT-D)
APO 953
San Francisco, California

2 USAFE (DCS/Ops)
APO 633
New York, New York

1 35 35th NTW
Attn: Electronic Warfare Familiarisation Course
Mather AFB, Calif.

1 TAC (OA)
Langley AFB, Va.

1 DCAS (DCLMT/TDC)
AF Unit Post Office
Los Angeles 45, Calif.

SAC
Offutt AFB, Nebr.
1 Attn: DORQP
1 DOPLT

1 AFMDC (MDRRF-1)
Holloman AFB, N.M.

1 Air University Library (AUL-6234)
Maxwell AFB, Ala.

2 9th AF (DOTR-FR (Capt. O.E. McCain)
Shaw AFB, S. C.

1 ADC (ADOOA)
Ent AFB, Colorado

1 Director
Weapons Systems Evaluation Group
Room 1E-875, The Pentagon
Washington 25, D.C.

10 Scientific and Technical Information Facility
Attn: NASA Representative (Code: S-AK/DL)
P. O. Box 5700
Bethesda, Md.

1 Commanding Officer
U.S. Army Signal Res. and Dev. Lab.
Attn: SIGRA/SL-SE, Mr. I. O. Myers
Fort Monmouth, N.J.

1 Chief Signal Officer
Research and Development Div.
Avionics and Surveillance Branch
Washington 25, D.C.

1 Assistant Secretary of Defense
Research and Development Board
Attn: Technical Library
Department of Defense
Washington 25, D.C.

1 Director
National Security Agency
Attn: C3/TDL
Fort George G. Meade, Md.

1 Army Ordnance Missile Command
Attn: ORDXM-RR, Hallowes, Jr.
Redstone Arsenal, Alabama

2 Commanding General
Army Ordnance Missile Command
Attn: AMSMI/RNR - Re-entry Physics Branch
Redstone Arsenal, Alabama

1 Commanding Officer
U.S. Army Signal Res. and Dev. Lab.
Attn: SIGRA/SL-N-5, Dr. H. Bennett
Fort Monmouth, N.J.

1 Commanding General
White Sands Missile Range
Attn: ORDBS-OM-TL
New Mexico

2 Commanding Officer
Picatinny Arsenal
Attn: Tech. Information Section
ORDBB-VA6
Dover, N.J.

1 USA Signal Electronic Research Unit
P. O. Box 205
Mountain View, Calif.

1 US Army Signal Corps School
Attn: DST, USASCS (Mr. Henry Allem)
Fort Monmouth, N.J.

1 Chief of Naval Research
Attn: Code 427
Department of the Navy
Washington 25, D.C

1 Commander
U.S. Naval Ordnance Laboratory
Attn: Eva Liberman, Librarian
White Oak, Silver Spring, Md.

1 Director
Material Laboratory
New York Naval Shipyard
Brooklyn 1, N.Y.

1 Commander
U.S. Naval Missile Center
Attn: Technical Library, Code NO 3022
Point Mugu, California

1 Commanding Officer
U.S. Naval Air Dev. Center
Engineering Development Lab.
Attn: J. M. McGlone
Johnsville, Pa.

1 Commanding Officer
U. S. Naval Ordnance Laboratory
Attn: Code 74
Corona, California

1 Chief
Bureau of Naval Weapons
Department of the Navy
Attn: RRRE-2
Washington 25, D.C.

2 Director
U. S. Naval Research Lab.
Attn: Code 2027
Washington 25, D.C.

1 Chief, Bureau of Ships
Attn: Code 335
Room 1532, Main Navy Building
18th and Constitution Ave., N.W.
Washington 25, D.C.

1 Airborne Instruments Lab.
A Division of Cutler-Hammer Inc.
Attn: Library
Walt Whitman Road
Melville, Long Island, N.Y.

1 Analytic Services, Inc.
Attn: Library
1150 Leesburg Pike
Bailey's Crossroads, Va.

2 The Johns Hopkins University
Applied Physics Laboratory
Attn: Mr. George L. Seielstad
8621 Georgia Avenue
Silver Spring, Md.

1 Bjorksten Research Labs., Inc.
P. O. Box 265
Madison 1, Wisconsin

1 Cook Electric Company
Cook Technological Center Div.
6401 W. Oakton Street
Morton Grove, Ill.

1 Electronic Communications, Inc.
Research Division
1830 York Road
Timonium, Md.

1 General Dynamics/Fort Worth
A Div. of General Dynamics Corp.
Attn: Chief Librarian
P. O. Box 748
Fort Worth 1, Texas

1 General Electric Company
Advanced Electronics Center
Attn: Library
Cornell University Industrial Res. Park
Ithaca, N.Y.

1 Grumman Aircraft Engineering Corp.
Engineering Library, Plant 5
Attn: M.O. Friedlander, Head Librarian
Bethpage, Long Island, N.Y.

2 The Hallicrafters Company
Attn: Library
4401 West Fifth Avenue
Chicago 24, Illinois

1 HRB-Singer, Inc.
Attn: Library
Science Park Box 60
State College, Pa.

1 The University of Michigan
Institute of Science and Technology
Attn: IRIA
P. O. Box 618
Ann Arbor, Michigan

2 ITT Federal Laboratories
Div. International Telephone and
Telegraph Corp.
500 Washington Avenue
Nutley, N.J.

1 Jansky and Bailey
A Div. of Atlantic Research Corp.
1339 Wisconsin Ave., N.W.
Washington 7, D.C.

1 Massachusetts Institute of Technology
Lincoln Laboratory
Attn: Library
P. O. Box 73
Lexington 73, Mass.

1 Massachusetts Institute of Technology
Electronics Systems Laboratory
Attn: John E. Ward, Rm. 32-401
Cambridge 39, Mass.

1 Lockheed Georgia Company
Attn: Dept. 72-15
Marietta, Ga.

1 Martin-Marietta Corp.
Martin Company Division
Attn: Science-Technology Library
Baltimore 3, Md.

1 Mitre Corporation
Attn: Library
Bedford, Mass.

1 Motorola Inc.
Systems Research Lab.
3330 Indiana Avenue
Riverside, Calif.

2 North American Aviation, Inc.
Attn: Technical Library
International Airport
Los Angeles 9, California

1 Northrop Corporation
Norair Division
Attn: Technical Information, 3924-31
1001 E. Broadway
Hawthorne, Calif.

2 Radio Corporation of America
Defense Electronic Products, DSD
Attn: L. R. Hund, Librarian
8500 Balboa Blvd.
Van Nuys, Calif.

1 Raytheon Company
Attn: Librarian
P.O. Box 636
Santa Barbara, Calif

1 Revere Copper and Brass Inc.
Foil Division
Attn: Mr. Arthur Ferretti
196 Diamond Street
Brooklyn 22, N.Y.

1 Stanford University
Stanford Electronics Labs
Attn: Security Officer
Stanford, Calif.

1 Sylvania Electric Products Inc.
Technical Information Section
P. O. Box 188
Mountain View, Calif.

1 Sylvania Electric Products, Inc.
Sylvania Electronic Systems
Attn: Applied Research Lab. Library
40 Sylvan Road
Waltham 54, Mass.

1 The Ohio State University
Research Foundation
Attn: Dr. Curt A. Lewis
1314 Kinnear Road
Columbus 12, Ohio

1 The RAND Corporation
Attn: Library
1700 Main Street
Santa Monica, Calif.

1 The University of Michigan
University Research Security Office
Attn: Dr. B. F. Barton
Director, CEL
P. O. Box 622
Ann Arbor, Michigan

2 Thompson Ramo Wooldridge Inc.
Ramo-Wooldridge Division
Attn: Technical Library
8433 Fallbrook Avenue
Canoga Park, Calif.

1 Space Technology Labs, Inc
STL Technical Library
Attn: Document Acquisitions Group
One Space Park
Redondo Beach, Calif.

1 Unidynamics
Div. of Universal Match Corp.
Attn: Technical Library
4407 Cook Avenue
St. Louis, Missouri

1 Westinghouse Electric Corporation
Defense Center - Baltimore
Attn: Technical Information Center
P. O. Box 1693
Baltimore 3, Maryland